Doctoral Thesis

Regulation of TDP2 functions by SUMO interactions

Jenna Ariel Lieberman

Regulation of TDP2 functions by SUMO interactions

Realizado en CABIMER

Departamento de Biología del Genoma

Memoria presentada por

Jenna Ariel Lieberman

Para optar al grado de Doctor en
Biología Molecular y Biomedicina

29 September, 2017

Director

Felipe Cortés Ledesma

Tutor

Andrés Aguilera López

ABSTRACT

Topoisomerase 2 (TOP2) performs a vital enzymatic activity, solving DNA topological problems in fundamental metabolic processes. The enzyme is able to untangle DNA by passing an intact helix through a transient double-strand break (DSB). The intermediate of its catalytic cycle, TOP2 covalently bound to DNA, is usually short lived, and is known as the TOP2 cleavage complex (TOP2cc). However, TOP2cc can be stabilized upon collision with the transcription or replication machinery, or upon the addition of TOP2 poisons, such as etoposide, which prevent religation of the transiently cleaved DNA. Stabilized TOP2 trapped in these cleavage complexes is degraded by the proteasome, leaving a small peptide still covalently bound to the DNA. Tyrosyl-DNA phosphodiesterase 2 (TDP2) is a protein involved in the removal of proteasome degraded TOP2cc, thus important for the efficient repair of TOP2-induced DNA DSBs. Consequently, TDP2-deficient cells are sensitive to etoposide. We report an additional function of TDP2, able to remove full-length undegraded TOP2 from covalent complexes.

Sumoylation is an important modification involved in the DNA damage response (DDR). While TOP2 sumoylation is important in several cellular processes, it was not known whether TOP2 is sumoylated in the context of the cleavage complex and its possible physiological relevance. In this work, we describe for the first time SUMO1 and SUMO2/3 modification of TOP2cc, with TDP2 being able to remove such structures. We imply a role for the novel TDP2 split-SIM (SUMO interacting surface) in the preferential removal of SUMO modified TOP2cc. With a physical proximity screen, we identify the SUMO E3 ligase ZNF451 as a novel factor involved in TOP2cc metabolism, which together with TDP2 is involved in a novel pathway for the repair of TOP2cc independent of known proteasomal pathways.

TABLE OF CONTENTS

FIGURES INDEX

Figures Introduction

Tables Introduction

Figures Results

Figures Discussion

ABBREVIATIONS

AD	GAL4 activation domain
Asp	Aspartic acid
Asn	Asparagine
ATP	Adenosine triphosphate
BD	GAL4 DNA binding domain
BSA	Bovine serum albumin
cAE	C-terminal alanine, glutamic acid
cc	Cleavage complex
CCC	Covalently closed circular
cTDP2	*Caenorhabditis elegans* tyrosyl-DNA phosphodiesterase 2
DDR	DNA damage response
DNA	Deoxyribonucleic acid
DSB	Double-strand break
EAPII	ETS1-associated protein II
EDTA	Ethylenediaminetetraacetic acid
EEP	Exonuclease-endonuclease-phosphatase
EV	Empty vector
FBS	Fetal Bovine Serum
FC	Fold-change
G0	Gap 0 phase of cell cycle
G2	Gap 2 phase of cell cycle
GFP	Green fluorescent protein
G segment	Gate segment
Gy	Gray
His	Histidine
HR	Homologous recombination
ICE	*In vivo* complex of the enzyme
Ile	Isoleucine
IP	Immunoprecipitate
IR	Ionizing radiation
kDa	Kilodalton
Leu	Leucine
LB	Lysogeny broth
LTR	Long terminal repeat
M	Mitotic phase of cell cycle
MEFs	Mouse embryonic fibroblasts
MG132	Proteasome inhibitor
MGF	Methionine-Glycine-Phenylalanine motif

MLL	Mixed lineage leukemia
MRN	Mre11/Rad50/Nsb1 complex
mTDP2	*Mus musculus* tyrosyl-DNA phosphodiesterase 2
NB	Nuclear body
NFκB	Nuclear factor kappa-light-chain-enhancer of activated B cells
NHEJ	Non-homologous end joining
NLS	Nuclear localization signal
NSCLC	Non-small cell lung cancer
nt	Nucleotide
P	Phosphate
PCR	Polymerase chain reaction
PD	Parkinson disease
PLRP	Proline-Leucine-Arginine-Proline motif
RC	Relaxed circular
RT	Reverse transcriptase
SB	SUMO binding element
shRNA	Short hairpin RNA
SIM	SUMO-Interacting motif
SMC	Structural maintenance of chromosomes
SNP	Single nucleotide polymorphism
ss	Single stranded
SSB	Single strand break
SUMO	Small Ubiquitin-like modifier
t	Time
TAK1	TGF-β activated kinase 1
TDP	Tyrosyl-DNA phosphodiesterase
TDP1	Tyrosyl-DNA phosphodiesterase 1
TDP2	Tyrosyl-DNA phosphodiesterase 2
TF	Transcription factor
TIPIN	Timeless interacting protein
TNF	Tumor necrosis factor
TOP1	Topoisomerase 1
TOP1cc	Topoisomerase 1 cleavage complex
TOP1mt	Mitochondrial Topoisomerase 1
TOP2	Topoisomerase 2
TOP2α	Topoisomerase 2 alpha
TOPβ	Topoisomerase 2 beta
TOP2cc	Topoisomerase 2 cleavage complex
TOP3	Topoisomerase 3

TRAF	Tumor necrosis factor receptor-associated factors
Tryp	Tryptophan
T segment	Transfer segment
TSS	Transcription start site
TTRAP	TRAF- and TNF receptor-associated protein
Ub	Unbound
UBA	Ubiquitin associated-like domain
UIM	Ubiquitin-interacting motif
VP16	Etoposide
WCE	Whole cell extract
WRNIP1	Werner DNA helicase interacting protein
Y	Tyrosine
YFP	Yellow fluorescent protein
Y2H	Yeast two-hybrid
γH2AX	Phosphorylated histone H2AX (gamma H2AX)
3AT	3-Amino-1,2,4-Triazol (inhibitor of *HIS3* gene product)

I. INTRODUCTION

1. DNA Topoisomerases

"Since the two chains in our model are intertwined, it is essential for them to untwist if they are to separate […] Although it is difficult at the moment to see how these processes occur without everything getting tangled, we do not feel that this objection will be insuperable."

-J.D. Watson and F.H.C. Crick, 1953

The story of topoisomerases, the enzymes known as topological problem solvers, begins with the description of the necessity of their function, derived from the double-helical structure of DNA and its compaction inside the nucleus. At the very beginning of the discovery of the structure of DNA, *Watson and Crick* recognized that the cell certainly had to have mechanisms to allow accessing the information stored in DNA without it getting all tangled up in the process (Watson & Crick, 1953). It would take almost 20 more years for the first validation of this theory, and, to date, we are still learning more about the intricacy of topoisomerases and their involvement in an increasing number of cellular processes (Seol & Neuman, 2016; McKinnon, 2016; Ashour et al., 2015; Nitiss, 2009b; Deweese, 2009; Champoux, 2001).

James C. Wang, a pioneer in the field, proposed in 1971 that DNA topo-isomerization is catalyzed by an enzyme that forms bond with DNA, and purified the first known member of the topoisomerase family from *Escherichia coli* extracts, protein ω (omega) (later known to be topoisomerase 1 (TOP1)), able to relax negatively supercoiled DNA (Wang et al., 1971). Depew and Wang detected the formation of a complex between TOP1 and single-stranded DNA, and presented

evidence that the protein is able to create transient breaks in the DNA backbone (Depew et al., 1978). Wang proposed the term topoisomerase in 1979 (Liu & Wang, 1979).

TOP2 is involved in various processes in which access to the DNA is needed. Such processes that involve strand unwinding create a topological problem in the form of compensatory "overwinding" in a different location in the DNA molecule, which can't be solved by simple rotation due to the large size of the eukaryotic chromosome.

From bacteria to higher eukaryotes, all topoisomerases have a common mechanism of action, which involves creating a transient break in DNA to manage the topological state (Champoux, 2001). There are two main classes of topoisomerases, type I and type II, which differ in how many DNA strands of a duplex are cut during a catalytic cycle. Type I topoisomerases cleave only one DNA strand. Within type I are type IA, in which the protein links to a 5'phosphate of the DNA during its catalytic cycle, such as bacterial TOP1, and type IB, with the protein attaching to a 3'phosphate. All higher eukaryotes and yeast have TOP1, a type IB enzyme, which has important roles in aiding with replication fork movement and transcription-related supercoil resolution, and is indispensable in development (Lee et al., 1993) (see Table 1 for a list of human topoisomerases). Mitochondrial TOP1mt, a paralog of nuclear TOP1, is also a type IB enzyme, specific for the replication of mitochondrial DNA in vertebrates (Rosa et al., 2009). Two isoforms of topoisomerase 3 (TOP3) are also present in higher eukaryotes, TOP3α and TOP3β, which are type IA. Whereas type IA enzymes employ a single-stranded passage mechanism, type IB topoisomerases use a swivelase mechanism, involving DNA

end rotation (Koster et al., 2005).

While type I enzymes can modulate over- and underwinding, they have the limitation of not being able to remove knots and tangles from duplex DNA. On the other hand, type II enzymes, which cleave both DNA strands, are able to remove such structures. Type II topoisomerases also include type IIA and IIB, both with a strand passage mechanism. While eukaryotes lack type canonical IIB topoisomerases, a type IIB related enzyme necessary for meiotic recombination, Spo11, is present. One form of type IIA topoisomerase 2 (TOP2) is in present in lower eukaryotes and invertebrates, while higher eukaryotes have two TOP2 paralogs, which are 170 kDa topoisomerase 2α (TOP2α) and 180 kDa topoisomerase 2β (TOP2β) in mammals (Drake et al., 1989). They share around 77% sequence homology but differ in the C-terminal regions (Linka et al., 2007). Due to the C-terminal differences, TOP2α has a preference for relaxing positive supercoils, while TOP2β does not seem to have a supercoiling preference (McClendon et al., 2005). The C-terminal differences between TOP2α and TOP2β may correspond to differences in cellular function.

The TOP2α isoform is essential in all cells, and TOP2α protein levels peak at G_2/M phase of cell cycle (Woessner et al., 1991). TOP2α is essential for DNA decatenation, chromosome condensation and disjunction (Grue et al., 1998). Although required for normal mammalian development, in some cell lines TOP2β is not expressed, and is dispensable for proliferation and survival *in vitro* (Chen & Beck, 1995). However, it is the main topoisomerase 2 activity in differentiated cells. TOP2β was discovered to be involved in an early stage of granule cell differentiation (Tsutsui et al., 2001). During the process of replication, the two

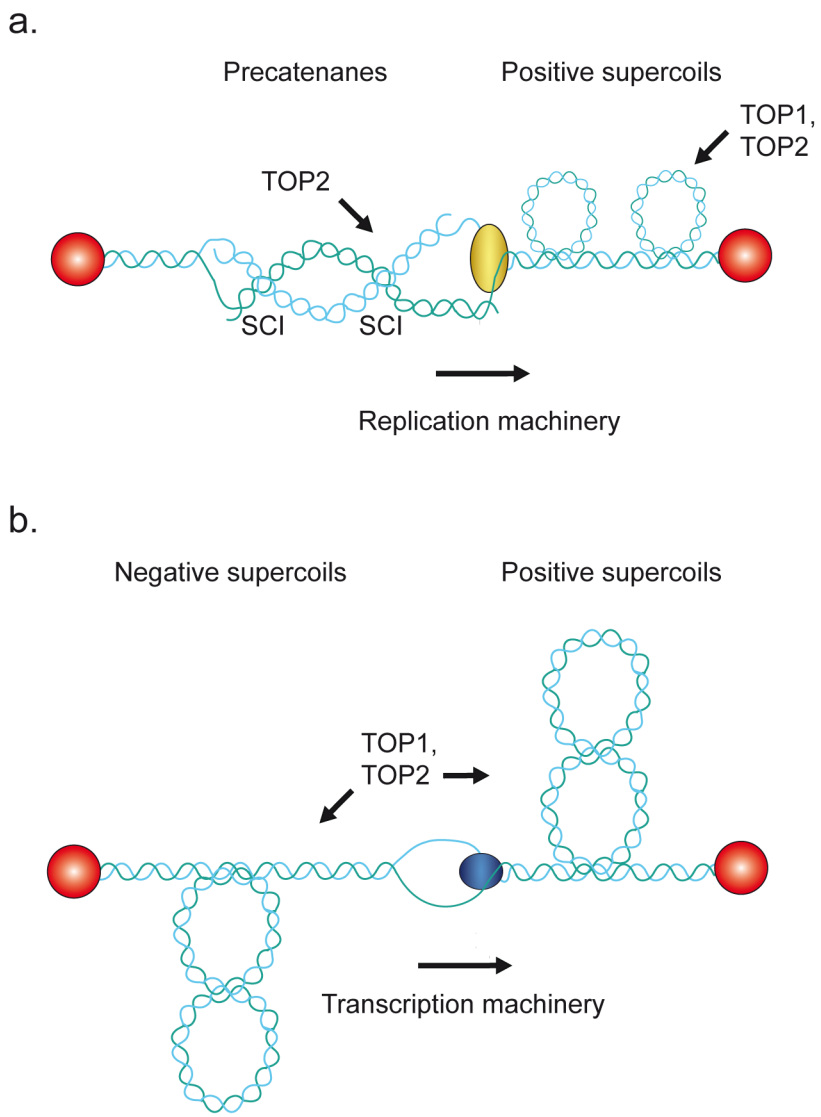

Figure I1. Nuclear processes affect DNA topology. DNA replication and transcription are used as examples. DNA ends are attached to a hypothetical immobile structure, represented by red ellipses, and are unable to rotate. **a.** As the replication machinery (yellow) advances, turns ahead of it are compressed and the DNA cannot rapidly rotate, creating positive superhelical stress which forms positive supercoils ahead of the advancing fork. When the fork occasionally rotates with the turn of the DNA helix, precatenanes can form. If not resolved by topoisomerase action, fork progression can be impeded and precatenanes can lead to the formation of sister chromatid intertwinings (SCI). **b.** During transcription, as RNA polymerase (blue) advances, the DNA becomes overwound and forms positive supercoils. The DNA behind the replication bubble is underwound, and forms negative supercoils. While both TOP1 and TOP2 can remove positive and negative supercoils, only TOP2 can resolve SCI. This figure is based on *Wang, 2002*, *Deweese & Osheroff, 2009*, and *Jeppsson et al., 2014*.

strands of the double helix are permanently separated. Eukaryotic TOP2, redundantly with TOP1, can remove overwinding causing positive supercoiling in front of the replication machinery (Figure I1a) (Brill et al., 1987; Deweese &

Osheroff, 2008). While replication fork rotation can alleviate some superhelical tension that builds up ahead of the progressing fork, it can bring about intertwinings of daughter duplexes (precatenanes) that rely solely on TOP2 to resolve them prior to separation and cell division (Pommier et al., 2016). Additionally, it has been observed that eukaryotic TOP2, along with TOP1, associates directly with specific replication origins to assist in activation (Abdurashidova et al., 2007).

Another process in which topoisomerase action is needed is transcription (Figure I1b). As transcription proceeds, DNA ahead of the RNA polymerase becomes positively supercoiled, while the DNA behind it becomes negatively supercoiled and the DNA must be relaxed, by either TOP2 or TOP1 redundantly (Wu et al., 1988). In yeast, transcription elongation of long genes is aided by TOP2 (Joshi et al., 2012). TOP2β seems to be the main mammalian TOP2 isoform responsible for removing torsional stress during transcription. Additionally, TOP2β cleavage has been implicated in the control of promoter activity during brain development, transcription of hormonally regulated genes, and activation of certain immediate early response genes (Ju et al., 2006; Pommier et al., 2016; Madahbushi et al., 2015). TOP2β has even been linked to expression of long genes related to synaptic function and autism spectrum disorders (King et al., 2013).

1.1. Topoisomerase 2 catalytic reaction

The basic reaction tactic for TOP2 is the creation of a transient DNA double strand break (DSB), with each subunit of the homodimeric enzyme breaking one strand. An unbroken duplex is passed through the break, which is then resealed. TOP2 has three regions of protein interfaces, referred to as gates, which are the N-

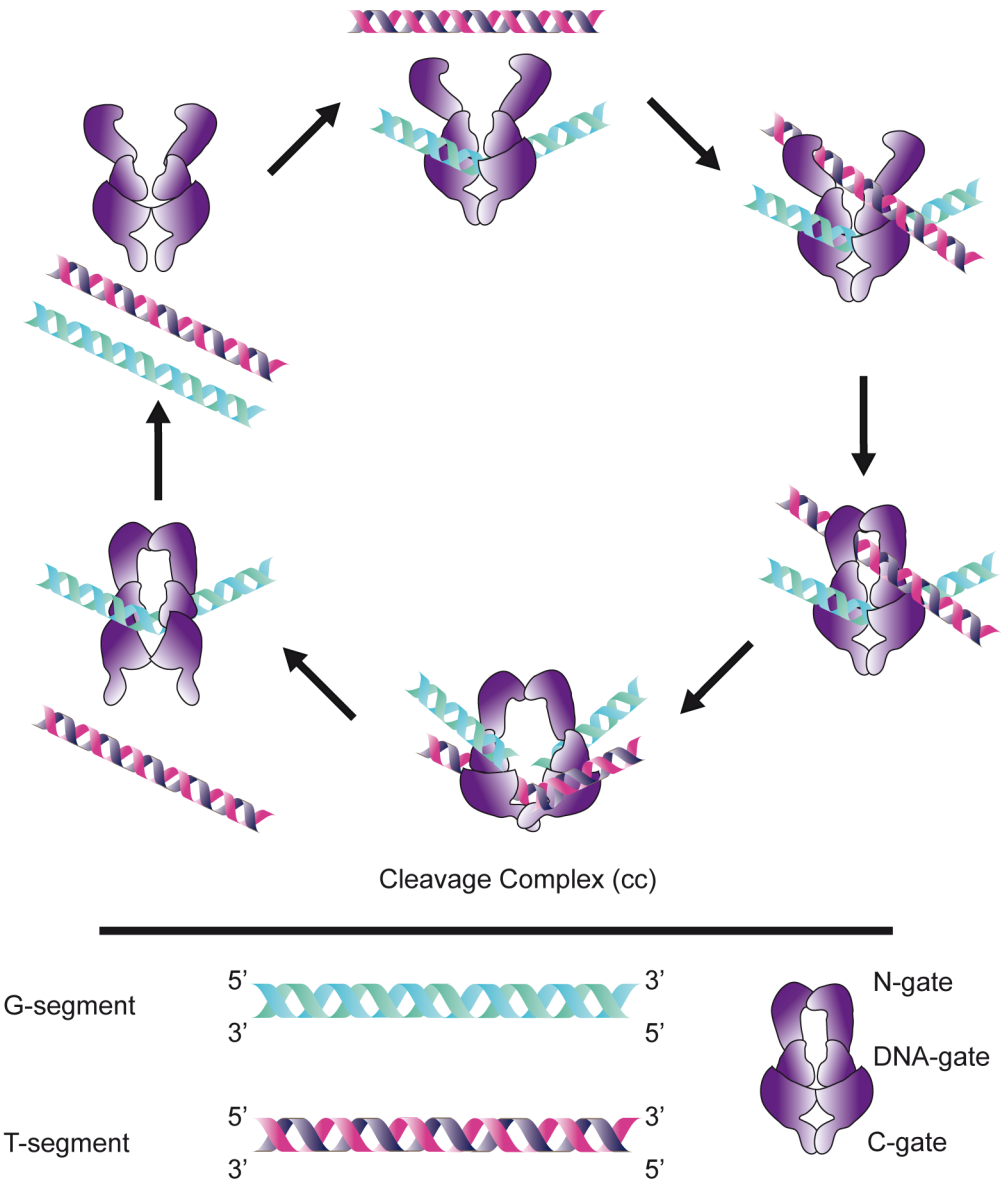

Figure I2. Type IIA topoisomerase action. Mechanism of action of type IIA topoisomerases, such as TOP2. TOP2 Binds the G segment (light blue and green), bending it. In the open clamp conformation, it waits for a second DNA segment. When the T segment (pink and purple) enters the N-gate, the clamp closes, the G segment is broken. The TOP2cc is formed with a phosphotyrosine bond between each strand and a tyrosine in each TOP2 subunit. The DNA-gate is opened and the T segment passes through to the central cavity. Then, the DNA-gate closes and the G segment is religated. The exit C-gate opens to release the T segment. The G segment can either be released, or undergo an additional catalytic cycle.

gate, DNA-gate, and C-gate (Figure I2, bottom right). Historically, TOP2 has been described as having a two-gate mechanism, as described by Wang and colleagues (Roca et al., 1996).

More specifically, as can be appreciated in (Figure I2, top middle), the TOP2 active site opens up and binds the segment of DNA that later will be broken, which is designated the G or "gate segment," which is then strongly bent. While in the open-clamp conformation, the enzyme waits for the second DNA segment, the T segment ("transfer segment"). Upon ATP binding, the enzyme undergoes a conformational change and forms a new protein-protein interface, the "N-gate," which is in a closed clamp conformation that closes the active site, which may capture the T segment. In the presence of Mg^{2+}, upon closure of the clamp, TOP2 induces a DSB in the G segment, catalyzed by an active site tyrosine in each subunit. A phosphotyrosine linkage is formed between each tyrosine and a single strand of DNA, forming the covalently linked TOP2-DNA cleavage complex (TOP2cc), also known as the cleavable/covalent complex. This triggers a conformational change that opens a gap in the G segment and opens the DNA-gate, through which the enzyme passes the T segment, which moves to the central TOP2 cavity. Once the DNA-gate closes, on religation of the G segment, the carboxyl terminus exit gate, "C-gate," can open, releasing the T segment on the opposite side. ATP hydrolysis may assist in the strand passage, and a second hydrolysis allows clamp re-opening. The G segment can either be released or another catalytic cycle can initiate with the same G segment (Vologodskii, 2016; Nitiss, 2009b).

The cleavage reaction is easily reversed because the energy is conserved in the form of the phosphotyrosyl bond, and ATP is not required for this reaction. The

ATP requirement of the TOP2 catalytic cycle is due to the unidirectional transfer of the T segment (Roca et al., 1996). *Maxwell and co-workers* suggest that the role of ATP hydrolysis could serve as protection against accidental DNA DSBs (Bates et al., 2011). *Berger and colleagues* stipulate that the ATPase domains pivot about each other to guarantee unidirectional strand passage (Schmidt et al., 2012).

1.2. Topoisomerase inhibitors and poisons

There are two categories of drugs that impact the catalytic activity of TOP2. The first, "catalytic inhibitors," decrease the overall activity of the enzyme and kill cells by eliminating the essential activity of TOP2 (Nitiss, 2009a). TOP2 catalytic inhibitors are mostly nonspecific, except for the bisdioxopiperazines, which include ICRF-187 and ICRF-193.

On the other hand, TOP2 "poisons" increase the number of TOP2cc and generate cytotoxic lesions. Many bind to the enzyme and stabilize TOP2cc, preventing religation of transiently cleaved DNA strands by trapping the enzyme in covalent complexes on the DNA. It has also been suggested that instead of blocking religation, many TOP2 poisons stimulate cleavage, generating high levels of TOP2cc that generate DNA damage (Robinson et al., 1991). Etoposide (VP16), the anthracyclines doxorubicin and danorubicin, and the anthracenedione mitoxantrone are some of the most widely clinically used TOP2 poisons. Etoposide is an epipodophyllotoxin derived from podophyllotoxin (found in the American Mayapple). Etoposide and other TOP2 poisons are used as tools in the laboratory to produce TOP2 induced DSBs.

As an increasingly aging population affects worldwide cancer incidence, so does the need for selective and effective cancer treatments. Chemotherapy is one of the most common treatments. Exogenous agents that specifically target TOP2 can take advantage of the necessity for topoisomerase activity and that they induce transient DNA breakage (Vos et al., 2015). Etoposide, for example, is widely used for the treatment of various malignancies. However, TOP2 poisons such as etoposide also affect healthy tissues, causing undesirable side effects such as secondary malignancies. An example of an etoposide rooted secondary malignancy is translocations of mixed lineage leukemia (MLL) gene causing acute myeloid leukemia (t-AML), that can be linked to trapping of TOP2cc in the *MLL* gene (Lovett et al., 2001).

Because of its expression in proliferating tissue, ideally TOP2 poisons would preferentially target TOP2α. Indeed, targeting of TOP2β leads to cardiotoxicity and highly contributes to secondary malignancies. While TOP2α and TOP2β share high amino acid sequence homology in the catalytic domains, it may be possible for the generation/identification of TOP2α-specific agents. For example, the compound NK314 has been observed to specifically target TOP2α (Toyoda et al., 2008).

1.3. Topoisomerase 2 induced DNA damage and repair

Topoisomerase activity has been described as a “double-edged sword,” referring to the essentiality of the enzymatic activity and the danger it poses to genomic integrity at the same time, due to the capacity to induce DSBs (Wang et al., 1990; Liu et al., 2001; Nitiss, 2009b). As so, there is a critical balance of the level of cleavage complexes in order for the cell to survive, with either too few or too many

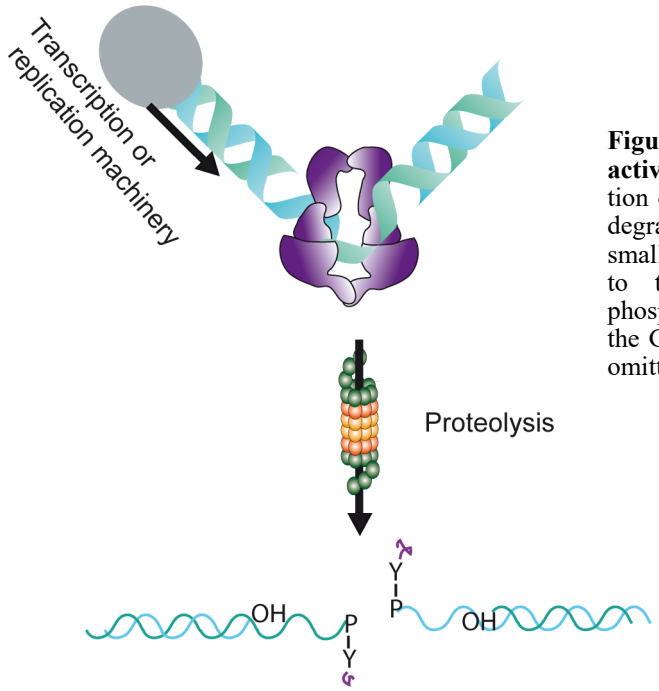

Figure I3. Abortive Topoisomerase 2 activity. Upon collision with transcription or replication machinery, TOP2cc are degraded by the 26S proteasome, leaving a small peptide adduct still covalently linked to the 5' DNA-terminus through a phosphotyrosyl bond. For simplicity, only the G-segment is shown and T-segment is omitted.

causing cell death. Inside the TOP2cc, the strand breaks with 4 nucleotide overhangs introduced by TOP2 are protected by the protein covalently bound to the 5' DNA end of the break, and as such are protected. However, the DNA cleavage action of TOP2 does have the ability to generate DSBs and elicit the DNA damage response (DDR) and any collision that can incite processing can potentially generate a DSB (Connelly & Leach, 2004).

For TOP2-mediated damage repair to occur, the first step involves recognition of the TOP2 complex as "trapped." Recognition of a trapped covalent complex as damage is probably consequence of blocking replication or transcription (Deweese & Osheroff, 2009). Drug-TOP2-DNA complexes might remain reversible until processing takes place, meaning that the TOP2cc can likely revert (reseal the broken DNA within the cleavage complex) if recognition and repair have yet to be initiated (Nitiss, 2009a). Upon collision with the transcription or replication machinery, accumulated TOP2cc intermediates are converted into permanent DSBs.

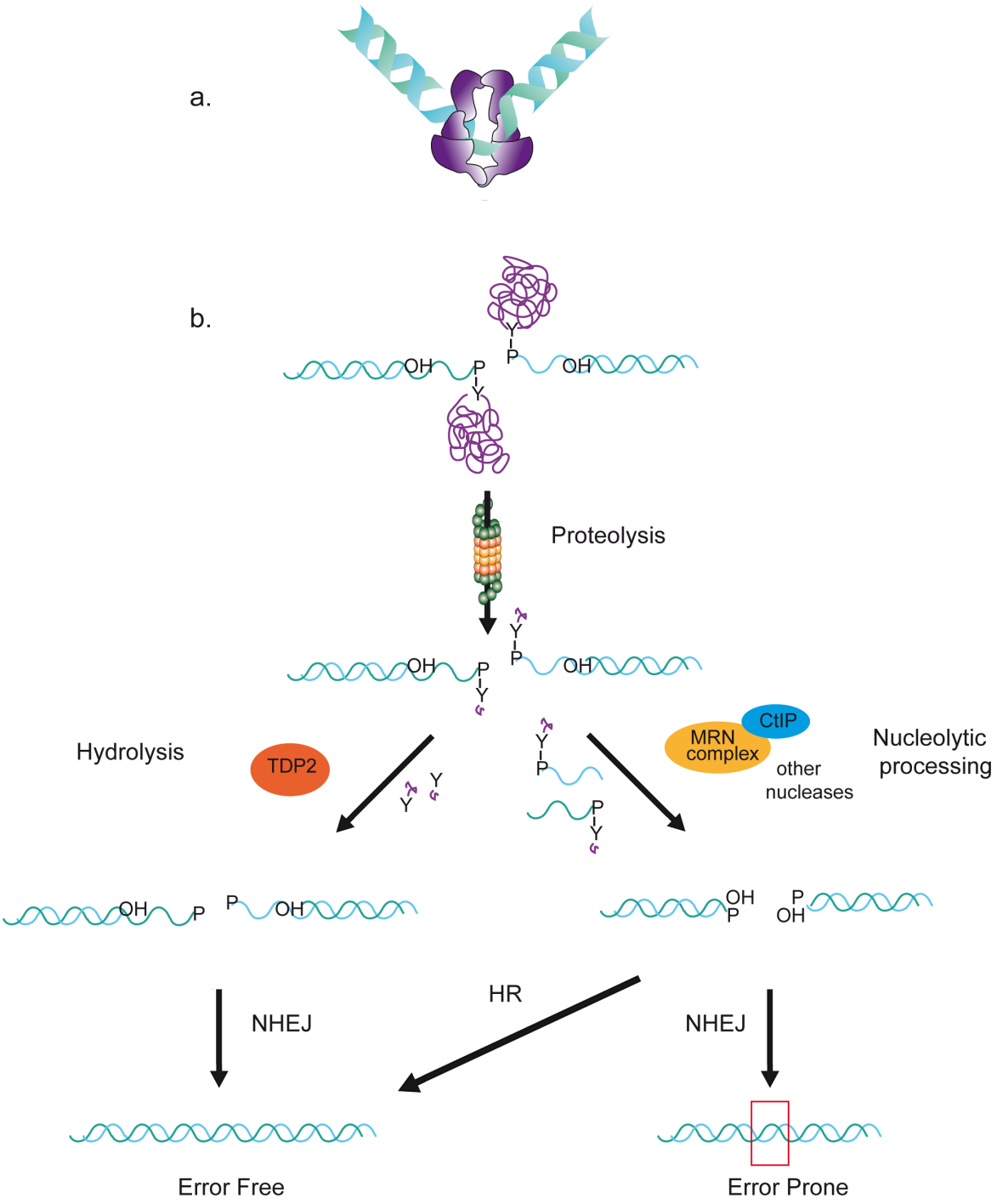

Figure I4. Resolution of abortive Topoisomerase 2 cleavage complexes. a. TOP2cc. For simplicity, only the G-segment is shown and T-segment is omitted. Simplified representation of "**a**" in **b.** and model for the removal of abortive TOP2cc (purple). TOP2 covalently linked to 5' termini by phosphotyrosyl bond between tyrosine in the protein and phosphate of DNA is partially degraded by the proteasome leaving peptide of unknown size. The peptide adduct is removed by either hydrolysis by TDP2 (left) or nucleolytic pathways (right). The DSB is repaired by HR (bottom right) or NHEJ (bottom left and right). Nuclease action can be error prone, creating single or multiple nucleotide deletions (red box) or error free, while TDP2 processing is error free. P- phosphate, Y- tyrosine, OH- hydroxide.

Following collision, proteasome degradation of the TOP2cc by the 26S proteasome leaves a residual peptide adduct attached to the DNA, which must be removed or processed in order for DNA DSB repair to occur (Figure I3) (Mao et al., 2001). This is because DSBs with a chemical modification at the ends cannot be directly ligated (Povirk, 2012). The important proteolysis step commits to repair of the TOP2-mediated damage, as once commenced, the enzyme probably can no longer continue its catalytic cycle. The major cellular protease, which is involved in this process, is the 26S proteasome, composed of the core 20S proteasome and 19S AAA ATPase regulatory complex.

Eukaryotic cells have two main types of enzymatic activities that can repair TOP2-mediated DNA damage (Figure I4). The enzymatic activity of tyrosyl-DNA phosphodiesterase 2 (TDP2) is one way to remove the TOP2-derived peptide adduct (Cortes-Ledesma et al., 2009). It is hypothesized that TDP2 processes TOP2-DNA oligopeptides following TOP2cc degradation, although in this thesis, we will propose an additional mechanism that is independent of TOP2cc degradation. Nonetheless, TDP2 converts the blocked DNA ends into ligatable ends by cleaving the 5`tyrosyl phosphodiester bond. A critical question in TOP2 biology is how does TDP2 access the TOP2 phosphotyrosyl chemical bond, which is buried within the TOP2 protein shell (Wu et al., 2011), and protected from TDP2 enzymatic activity (Figure I5), and how this activity may be regulated.

A second way to eliminate the residual TOP2 derived peptides in vertebrates is with endonucleases such as CTIP and MRE11, a component of the MRE11/ RAD50/NSB1 (MRN) complex. *Gautier and colleagues* used *Xenopus laevis* cell free extracts to identify MRN-CTIP-BRCA1 as an important pathway in processing

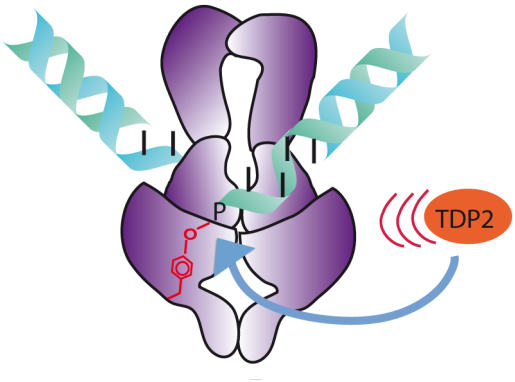

Figure I5. The TOP2 phosphotyrosyl chemical bond is buried within the TOP2 protein shell. The cellular mechanisms that regulate TDP2-catalyzed phosphotyrosyl bond hydrolysis in poisoned TOP2cc are unknown.

TOP2-DNA adducts in S-phase (Aparicio et al., 2016; Hoa et al., 2016). Paull and coworkers suggested an important role for CTIP and its nuclease activity for the resolution of TOP2-induced DSBs, a pathway possibly distinct from the MRN-CTIP -BRCA1 pathway due to the mechanism being independent of the MRN and CTIP-BRCA1 interaction (Makharashvili et al., 2014). Once the TOP2 block is removed, subsequent repair of the break can take place by one of the two main DSB repair pathways, further detailed below.

2. Tyrosyl-DNA phosphodiesterase 2

The laboratory of Howard Nash described the first enzyme capable of cleaving 3′-phosphotyrosyl bonds between proteins and DNA in *Saccharomyces cerevisiae*, and named it tyrosyl-DNA phosphodiesterase 1 (TDP1) (Pouliot et al., 1999). Found in all eukaryotes, TDP1 is implicated in the repair of TOP1 mediated single strand breaks (SSB), and can also repair indirectly induced double strand breaks. However, mammalian TDP1 lacks the 5′phosphotyrosyl activity weakly detected in *S. cerevisiae* TDP1 and has a main 3′-TDP activity. In a genetic screening, *Caldecott and colleagues* discovered TDP2 as the first specific 5′-tyrosyl DNA phosphodiesterase (Cortes-Ledesma et al., 2009). TDP2 represents the only

known 5′-TDP activity in vertebrate cells, therefore the only enzyme capable of removing TOP2-derived structures from DSBs without having to remove adjacent nucleotides (Zeng et al., 2011). While TDP2 is capable of removing 3′-phosphotyrosyl termini, it does so with at least 50-fold decreased activity compared to 5′-phosphotyrosyl termini (Gao et al., 2012). Nonetheless, *Zeng et al.* (2012) observed that TDP2 has a role in the repair of TOP1-mediated DNA damage in the absence of TDP1. However, they did not detect a role of TDP1 in the repair of TOP2-induced DNA damage.

TDP2 is a member of the metal-dependent ($Mg^{2+/}Mn^{2+}$) family of phospho-diesterases (Rodrigues-Lima et al., 2001). While not present in yeast, it is evolutionary conserved in metazoans. TDP2 is a pleiotropic protein with promiscuous interactions, not limited to DNA repair functions. The involvement of TDP2 in inhibition of cell growth and induction of apoptotic processes is reflected in the various names assigned to the protein as these functions were uncovered (Li et al., 2011).

The role in tumor necrosis factor (TNF) receptor signaling (apoptosis and inflammatory response), warranted appointing the protein name TRAF- and TNF receptor-associated protein (TTRAP) (Pype et al., 2000). TDP2 has functions in the NFκB pathway, playing a role in TGF-β induced apoptosis. Additionally, TDP2 inhibitory effects on ETS1, a transcription factor with roles in apoptosis, differentiation, tumorigenesis, and metastasis (Li et al., 1999; Pei et al., 2003), derived the alternate name, ETS1-associated protein II (EAPII).

TDP2 may also have a role in regulation of the cell cycle, as seen by *Zhou et al.* (2013). Interestingly, overexpression of TDP2 induces cell apoptosis in U2OS

cells (human osteosarcoma with low endogenous TDP2 expression), and cell cycle arrest in G2/M phase in Saos-2 cells (human osteosarcoma cells with deficient p53 expression). TDP2 inhibitory activity on cell growth was dependent on its catalytic phosphodiesterase activity, as was inhibition of cyclin B1 expression in both cell types, a key regulator in G2/M transition, causing cell cycle arrest, which may account for apoptosis in the cell lines. The authors conclude that the DNA repair activity of TDP2 is important for its ability to modulate cell growth in osteosarcoma cells. Despite these additional functions, the enzymatic functions of TDP2 and its role in repairing TOP2 induced DSBs was sufficient enough to warrant renaming of the protein in 2009 to its current name.

2.1. TDP2 structure

In 2012, two TDP2 structures were simultaneously published. *Aihara and colleagues* solved the crystal structure for full-length *Caenorhabditis elegans* TDP2 (cTDP2) (Shi et al., 2012) while Scott Williams' laboratory crystallized the catalytic portion of *Mus musculus* TDP2 (mTDP2) DNA complexes (Schellenberg et al., 2012).

TDP2 has a modular architecture, comprised of an unstructured N-terminal stretch, and a small N-terminal α-helical bundle forming the ubiquitin-associated (UBA) like domain, which is flexibly linked to the C-terminal catalytic "EEP domain" (exonuclease-endonuclease-phosphatase) (Cortes-Ledesma et al., 2009;

Figure I6. Domain organization of human TDP2. TDP2 is comprised of a UBA domain and a catalytic EEP domain. UBA- Ubiquitin associated-like domain.

Schellenberg et al., 2012) (Figure I6). TDP2 catalytically important residues, residing in the EEP domain, include Glu-152, Asp-262 (Cortes-Ledesma et al., 2009), Asn-120, and His-351 (Gao et al., 2012). The enzyme has no endo/ exonuclease activity, being highly specific for 5'Y terminus, preferring 5'single-stranded (ss) overhangs.

Contrary to the canonical tri-helix UBA domain structure, the cTDP2 N-terminal domain contains four short α-helixes (Shi et al., 2012), a unique pattern that is conserved across species (Rao et al., 2016). It is not essential for the 5'-tyrosyl DNA phosphodiesterase activity of TDP2 *in vitro*, but contains homology to known UBA domains, and is thus designated as a "UBA-like" domain. Aihara and coworkers suggest that the UBA domain is integral to the DNA repair function of TDP2 *in vivo* based on the fact that F62R mutation in the UBA-Ub interaction surface decreases viability in assays done with complementation of *TDP2*$^{-/-}$ DT40 cells (Rao et al., 2016).

2.2. TDP2 and human health

Given its multiple roles and importance in the DNA damage response, it is easily conceivable that *in vivo*, *TDP2* mutations can have serious consequences. Indeed, loss of TDP2 function can lead to neurological defects and TDP2 expression is altered in a subset of cancers (Li et al., 2011; Gómez-Herreros et al., 2014). Despite dramatic etoposide sensitivity, *Tdp2*$^{-/-}$ mice are phenotypically normal, although a large number of neuronal genes exhibit altered expression in developing brains and a mild loss of cerebellar interneurons was observed. *Caldecott and colleagues* identified a human homozygous *TDP2* splice site-mutation causing

intellectual disability, epilepsy, and ataxia in affected patients. Blood and lymphoblastoid cell extracts from affected individuals completely lacked a detectable 5′TDP activity. As such, patient lymphoblastoid cells were hyper-sensitive to etoposide and defective in repairing DSBs.

Additionally, TDP2 may be related to Parkinson disease (PD) pathogenesis, by association with DJ-1, a protein whose missense mutations are capable of causing early-onset recessive PD (Zucchelli et al., 2009). PD missense mutations of DJ-1 affect the ability of TDP2 to protect neuroblastoma cells from apoptosis induced by proteasome inhibition, causing cell death by JNK and P38 MAPK pathways.

Furthermore, in several studies, TDP2 has been linked to viral infection. It was observed that TDP2 interacts with HIV-1 integrase, and facilitates lentiviral integration (Zhang et al., 2009). However, it has yet to be determined whether this function depends on TDP2 phosphodiesterase activity. Also, TDP2 was proposed to have a role in Hepatitis B persistence, which depends on a nuclear episome, which is a covalently closed circular (CCC) DNA (Koniger et al., 2014). *In vitro*, TDP2 can cleave the tyrosyl-phosphodiesterase bond between the reverse transcriptase (RT) protein and the 5’ end of the minus strand of relaxed circular (RC) DNA, which must be removed in order to form CCC DNA. However, alternative work showed that TDP2 knockout had little effect on preventing formation of CCC-DNA *in vivo* and preventing Hepatitis B infection (Cui et al., 2015). Similarly, the picanovirus takes advantage of the ability of host TDP2 to remove the VPg cap covalently bound to RNA. The TDP2 VPg unlinkase activity removes this covalent linkage that stems from the replication of viral genomic RNA (Virgen-Slane et al.,

2012). This identifies TDP2 as a potential antiviral target for treating picanovirus diseases, which include rhinoviruses that cause the common cold.

3. DNA double strand break repair

As aforementioned, the DNA cleavage activity of TOP2 has the ability to provoke the DDR, once the irreversible break with a TOP2-protein adduct covalently linked to DNA results from proteasomal degradation of trapped TOP2cc (Figure I3). The most deleterious type of genomic DNA lesions is the DSB, the type of strand break that can be created by TOP2 activity, and its repair its critical for survival and the maintenance of genome integrity (Khanna & Jackson, 2001). This is orchestrated by a signal transduction pathway mentioned above: the DDR. Activation of the DDR induces the repair of the lesions, cell cycle arrest, an appropriate transcriptional program and, in cases of severe damage, senescence or apoptosis (Ciccia & Elledge, 2010). The DNA damage signaling cascades from the DDR are complex, coordinated events that require the actions of various proteins that can be classified in different groups depending on their function. DNA damage sensors are proteins specifically involved in recognizing the lesion, which activate transducers that in turn recruit mediators, which exponentially amplify the signal. Finally, effectors proteins are able to carry out DNA repair, activate cell cycle checkpoint, remodel the chromatin or interfere with other cellular processes involved (Polo & Jackson, 2011).

In the particular case of DSBs, the KU70–KU80 heterodimer and the MRN complex are earliest factors to bind to DSBs (Lisby 2004). After DSB recognition, three different phosphatidylinositol 3-kinase-related kinases (PIKKs) can be

recruited to sites of damage: DNA-PKcs (DNA-dependent protein kinase catalytic subunit), ATM (Ataxia Telangiestasia-Mutated) and ATR (ATM- and Rad3-Related); serving as a transducers of the signal by phosphorylating numerous proteins (Marechal & Zou, 2013). With the help of mediator proteins, ATM and ATR can activate the effector kinases CHK1 and CHK2, which then spread the signal throughout the nucleus to trigger cell cycle arrest. This prevents adverse consequences of DNA lesions and their transmission to daughter cells (Polo & Jackson, 2011). Eventually, if the DNA damage cannot be repaired, DDR participates in activating apoptosis, which is essential to remove potentially dangerous cells from the organism (Roos & Kaina, 2013).

One significant feature of DDR proteins is their local accumulation at damage sites (Polo & Jackson, 2011). Taking the advantage of this characteristic, it is possible to detect discrete foci by immunofluorescence techniques (Costes et al., 2010). Through this method, DSB induction and disappearance have been analyzed for last 20 years (Rogakou et al., 1999). It is worth noting that one of the earliest events in DSB signaling is the phosphorylation in Serine139 of histone variant H2AX (known as γH2AX), which can be carried out redundantly by ATM, ATR and DNA-PKcs. The number of nuclear γH2AX foci corresponds well with the number of DSBs, and when counted in immunofluorescence staining, serves as a good tool to estimate DSBs.

The two main pathways in cells for repairing DSBs are nonhomologous end-joining (NHEJ) and homologous recombination (HR). HR takes advantage of homologous DNA sequences as a template to perform error free DSB repair, therefore is limited to the S and G2 phases of the cell cycle due to the requirement

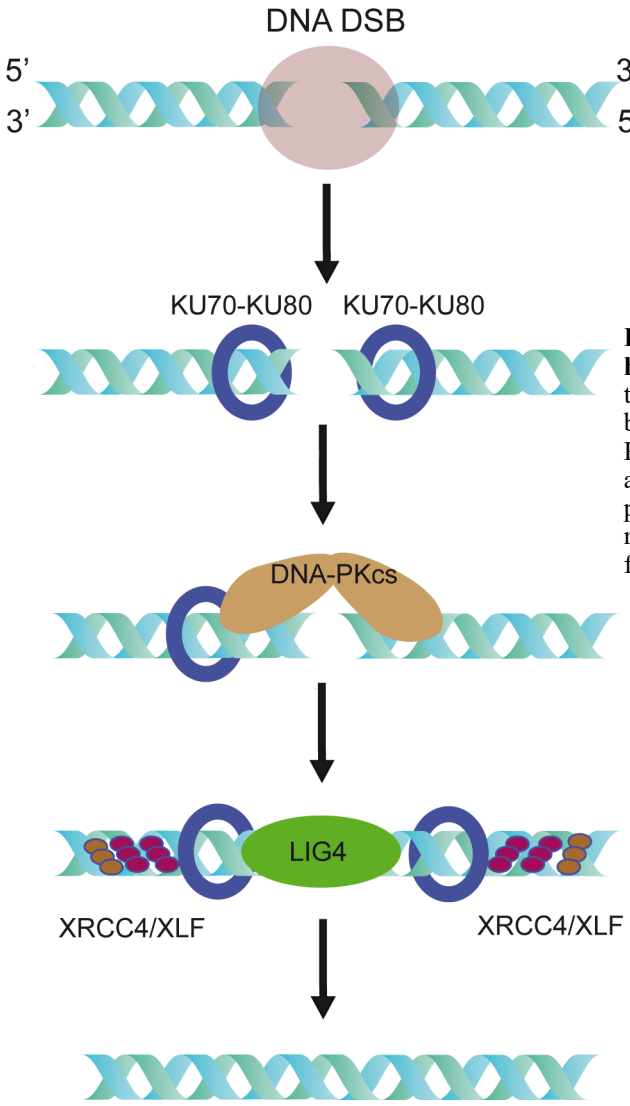

Figure I7. DNA DSB repair by non-homologous end joining. KU recognizes the DSB and binds the DNA ends, followed by DNA-PKcs recruitment to form the DNA-PK complex. DNA-PKcs is phosphorylated, and disassembled from the DNA. Accessory proteins XRCC4 and XLF form helical filaments bridging DNA ends, while LIG4 performs ligation of the broken DNA ends.

for the sister chromatid as a template (Rothkamm et al., 2003). NHEJ, the main DSB repair pathway in mammalian cells, is a faster repair process, and directly ligates broken DNA ends throughout most of the cell cycle (Figure I7).

NHEJ plays a dominant role in repairing etoposide-induced DSBs, which is the main pathway that follows TOP2-residual peptide removal by TDP2 (Gómez-Herreros et al., 2013). In the mammalian NHEJ pathway, the DSB is first recognized by the dimeric proteins KU70-KU80 (Ku), which binds DNA ends specifically and serves as a loading protein to which other NHEJ proteins can be

recruited. Ku translocates inwards allowing DNA-PKcs to bind DNA ends, together forming the DNA-PK complex, which bridges and stabilizes the ends (Meek et al., 2008). DNA-PKcs protein kinase activity is stimulated, and it is autophosphorylated, which prompts a conformational change that promotes its release from DNA ends (Lees-Miller & Meek, 2003). Accessibility of the DSB to other repair factors is regulated by this assembly and disassembly, and DNA-PKcs autophosphorylation seems to be required for the NHEJ pathway to proceed. DNA ligase IV (LIG4) is recruited and performs ligation of broken DNA ends. This is helped by cofactor X-Ray Cross Complementing Protein 4 (XRCC4), XRCC4-Like Factor (XLF), Aprataxin-and-PNK-Like Factor (APLF), and PAralog of XRCC4 and XLF (PAXX) (Mari et al., 2006; Uematsu et al., 2007; Ochi et al., 2015), which are accessory proteins that directly or indirectly favor end-bridging and ligation (Roy et al., 2015; Liu et al., 2017).

On the other hand, the mammalian MRE11/RAD50/NBS1 complex (MRN complex) initiates DSB repair by HR, recognizing and stabilizing broken chromosome ends (Lisby et al., 2004; Paull & Deshpande, 2014). CTIP promotes the process of extensive end resection, which is performed by MRE11 nuclease activity, committing the repair pathway to HR and inhibiting NHEJ. Importantly, while DSB induction strongly activates ATM and DNA-PKcs, ATR is recruited to DSBs specifically when DNA is resected (Shiotani & Zou, 2009b). The nuclease action creates 3'-single stranded ends, which are rapidly coated with Replication Protein A (RPA), protecting DNA ends (Alani et al., 1992; Mimitou & Symington, 2010). The MRN complex is important for controlling resection, and also has a role in recruiting and activating the kinase ATM. RPA is then replaced by the

recombinase RAD51 that forms a filament that aids in the search for the homologous DNA sequence and strand invasion. The invading strand serves as a template for DNA synthesis and allows the restoration of the disrupted genetic information.

4. Sumoylation

The human genome has a set of approximately 25,000 genes, which amazingly leads to a human proteome with over one million proteins. This variation comes at the transcriptional and mRNA level, from alternative promoters, differential transcription termination, and alternative mRNA splicing (Auoubi, 1996). Post-translational protein modifications (PTMs) are a clever way of further augmenting that complexity and diversity by adding small moieties, or even small proteins, to specific amino acid residues (Human Genome Sequencing Consortium, 2004). PTMs can affect activity, localization, and interaction with other molecules. They offer a quick and reversible way of changing substrate function without *de novo* protein synthesis (Ulrich, 2012b). The most common mechanism of action is the creation of interaction surfaces followed by recognition by downstream effector proteins through dedicated binding domains (Ulrich, 2012a). The updated UniProt database is a testament to the remarkable number of post-translational modifications that have been identified (The UniProt Consortium http://www.uniprot.org/docs/ptmlist).

A few well studied post-translational modifications include phosphorylation, acetylation, methylation, glycosylation, ubiquitination, and sumoylation. Different PTMs can even work together and influence each other (Ulrich, 2005). Covalent tagging of a protein by a second protein was first discovered with ubiquitin, which

links to a receptor lysine residue in a step-by-step conjugation cascade. Poly-ubiquitination occurs when further ubiquitin molecules are conjugated to each other by isopeptide bonds between the ubiquitin molecules and the lysine of the bound ubiquitin. Ubiquitination controls a myriad of processes, and as such, there are numerous downstream responses (Dikic et al., 2009). Histone ubiquitination, for example, is able to alter chromatin structure (Desterro et al., 1999) and poly-ubiquitination commonly signals for proteasomal degradation.

Sumoylation is another type of post-translational modification that involves covalent conjugation of a small protein, SUMO (Small Ubiquitin-like MOdifier) to a target lysine of a specific protein, in a manner similar to ubiquitin. While SUMO and ubiquitin share only 18% identity, the three dimensional structure is similar (Mahajan et al., 1997). Yeast and invertebrates have only one isoform (SMT3 in *S. cerevisiae*). The three main SUMO isoforms in mammalian cells are SUMO1, 2 and 3. SUMO1 shares about 48% sequence identity with SUMO2 and 46% identity with SUMO3. SUMO2 and 3 share 96% identity (Saitoh & Hinchey, 2000). SUMO2 and SUMO3 will be referred to as SUMO2/3 in this thesis when they are indistinguishable. A fourth isoform, SUMO4, is expressed in mammals, although it is not expressed in most tissues. Nonetheless, SUMO4 mRNA is expressed in kidney cells. On the other hand, SUMO modification can occur on the same lysine as ubiquitination, thereby inhibiting poly-ubiquitin mediated proteasomal degradation (Desterro et al., 1998).

SUMO1 was identified simultaneously by several groups (Okura et al., 1996, Shen et al, 1996; Boddy et al., 1996; Mahajan et al., 1997; Matunis et al., 1996). In a screening performed by *Okara and colleagues* (Okura et al., 1996),

SUMO was identified and named Sentrin, with TNF receptor 1 interactions detected. *Chen and coworkers* (Shen et al., 1996) also identified SUMO as a small protein with homology to ubiquitin that associates to human RAD51 and RAD52 DNA DSB repair proteins, noting high expression in many tissues, especially testis. They named it UBL1 for Ubiquitin-Like 1. At the same time, utilizing a human cDNA library, *Freemont and colleagues* (Boddy et al., 1996) screened for PML (ProMyelocytic Leukemia protein) interacting clones and identified SUMO1 (referred to as PIC1). This represented the first nuclear body (NB)-associated protein identified to interact with PML (PMB NBs are further detailed below).

One of the most important SUMO1 targets in the cell is RANGAP1, the GTPase-activating protein for RAN, which is linked to nuclear import. *Melchior and colleagues* discovered that a small ubiquitin-related peptide, which they named SUMO1, was required for RANGAP1 localization to the nuclear pore complex (NPC) (Mahajan et al., 1997). Simultaneously, *Blobel and colleagues* also identified SUMO1 as the covalent modification of RANGAP1, and designated it as GMP1 (Gap modifying protein 1) (Matunis et al., 1996).

4.1. SUMO conjugation

There are important distinctions between the SUMO1 and SUMO2/3 conjugation pathways. In mammalian cells, there is relatively little free SUMO1, with 90% being conjugated (Kamitani et al., 1997). In the cell, there is a larger pool of free SUMO2/3 than SUMO1. Protein damaging stimuli induces SUMO2/3 conjugation to high molecular weight proteins, indicating a role in cellular response

to environmental stress (Saitoh & Hinchey, 2000). SUMO2/3 has a N-terminal Ψ-K-X-E substrate consensus motif and can form polymeric chains on protein substrates. SUMO1 does not form chains, but can cap SUMO2/3 chains. The majority of SUMO modified proteins are in the nucleus, but also cytosolic targets have been identified.

60% of covalent SUMO modification occurs in sites that follow this modification consensus sequence, Ψ-K-X-E (Qi et al., 2014). The first amino acid, Ψ, is a large hydrophobic amino acid, such as A, I, L, M, P, F, V or W. The second amino acid is the lysine that receives the covalent SUMO conjugation, and the third, represented by X, can be any amino acid residue. The fourth amino acid is glutamic acid, which has a negative charged side chain.

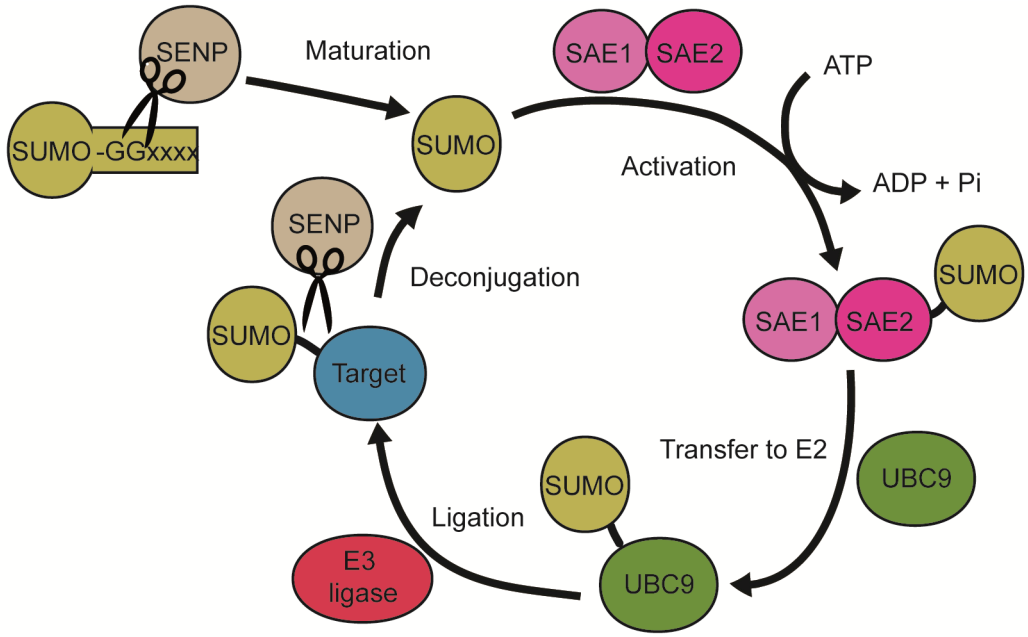

Figure I8. SUMO conjugation cycle. Inactive SUMO precursor is processed by a SENP to expose the C-terminal di-glycine motif during the maturation process. Mature SUMO (SUMO-GG represented as SUMO) is then activated by SUMO activating enzyme (E1). Next, it is transferred by transesterification to the E2, which is UBC9. Conjugation to the target lysine follows, which can be facilitated by an E3 SUMO ligase. Deconjugation from substrates is carried out by specific SENPs (SUMO-specific proteases).

SUMO conjugation is similar to that of Ubiquitin, with own specialized enzymes that help form the isopeptide bond between carboxyl terminus of SUMO and the designated lysine side chain of target protein (Figure I8). The C-terminal diglycine residue of SUMO is essential for conjugation to other proteins (Kamitani et al., 1997). SUMO is translated as a precursor, and the four amino acids of the C-terminus (His-Ser-Thr-Val in SUMO1) following the Gly-Gly residues must be removed post-translationally prior to conjugation. SUMO deconjugation is carried out by SUMO isopeptidases, SUMO-specific proteases/Sentrin proteases (SENPS). This 6-member family of cysteine proteases is responsible for maturation, deconjugation, and depolymerization of SUMOs (Nayak & Muller, 2014) and allows for the reserve of free SUMO.

The E1 SUMO activating enzyme, a heterodimeric protein of SAE1 and SAE2 in humans (SUMO Activating Enzyme) (Desterro et al., 1999), catalyzes ATP-dependent formation of thioester linkage between SUMO and SAE2. UBC9, the E2 conjugating enzyme for SUMO, transfers thioester-linked SUMO to itself in a transesterification process (Johnson et al., 1997). The last step of SUMO conjugation involves the formation of an isopeptide bond between SUMO and the target substrate, facilitated by the action of UBC9 and E3 protein ligases.

SUMO1 conjugation *in vitro* does not require E3 protein ligase activity equivalent to E3 ubiquitin protein ligase in ubiquitin conjugation (Desterro et al., 1999). Additionally, the E1 and E2 enzymes do not discriminate among SUMO isoforms 1-3 (Tatham et al., 2003). The E3 enzyme can act to add specificity to targets. Some examples of known SUMO E3 ligases are RanBP2, Polycomb Protein PC2 (CBX4) and the PIAS family.

Additionally, the sumoylation pathway has a noteworthy role in the DDR, with SUMO being necessary to maintain genome stability. DNA damage induces a sumoylation wave of various proteins at multiple sites, mediated by the E3 SUMO-ligases PIAS1 and PIAS4, in order to foster protein-protein interactions and increase repair rate. As a matter of fact, SUMO, UBC9, PIAS1 and PIAS 4, and two of their substrates, BRCA1 and 53BP1, are relocated to γH2AX foci upon DNA damage.

Because of the relevance of sumoylation in the cell, there is a continued search for additional proteins that can serve as components of the sumoylation machinery. Recently, the novel protein Zinc Finger Protein 451 (ZNF451) was identified as a possible novel class of SUMO E3 ligases.

4.2. SUMO-interacting motifs

When covalent SUMO modification of a protein serves to provide a binding site for other proteins, this is likely due to a SUMO interacting motif (SIM), also known as SUMO binding amino acid sequence motif (SBM), on interacting proteins, creating sumoylation-dependent protein-protein interactions (Song et al., 2004). SIMs have been identified in numerous types of proteins including SUMO ligases, transcription factors, and transcription repressors. Not all predicted SIMs are functionally relevant, as a given SIM may not be functionally exposed in a protein structure. Additionally, there is no one “universal SIM.”

With screening using human cDNA, a general SIM motif consisting of a hydrophobic core sequence flanked by an acidic region has been described, h-h-X-S -X-S/T-a-a-a (see Table 2) (Minty et al., 2000). The motif was found in PIASx and is conserved in the PIAS and PKY gene families. The SIM consists of a serine

doublet separated by an amino acid (S-X-S/T), with a possible substitution of the second serine for threonine. The N-terminal side is composed of hydrophobic amino acids (h), while the C-terminus has acidic amino acids (a) such as aspartic acid (D) or glutamic acid (E).

In 2004, *Song and colleagues* described V/I-X-V/I-V/I as a SIM able to bind to the main SUMO paralogues in mammalian cells (SUMO1, SUMO2, and SUMO3 were tested) albeit with different affinities. Valine and isoleucine are exchangeable in the SIM sequence, as both are similar and have branched aliphatic side chains. The publication of this SIM refuted the dominant role of the serine residues as published by *Minty et al.* (2000). The V/I-X-V/I-V/I SIM is important, for example, for the sumoylation-mediated protein-protein interaction between RANGAP1 and RANBP2 (Song et al., 2004). The hydrophobic core, often adjacent to a negatively charged acidic cluster of amino acids, is an essential component of SUMO-interacting motifs.

Hannich and coworkers (2005) derived a yeast SIM from data of clones (FIR1, RIS1, SAP1, and NIS1) that bound a non-conjugatable form of yeast SUMO (SMT3): K-X_{3-5}-I/V-I/L-I/L-X_3-D/E/Q/N-D/E-D/E. Similar to the SIM described by *Minty and colleagues* (2000), there is both an N-terminal hydrophobic cluster and C -terminal acidic cluster.

Hecker et al. (2006) highlight the importance of hydrophobic residues, analyzing previously published SIMS and, in combination with their results, they proposed a universal SIM with hydrophobic core sequence with stretches of three or four hydrophobic isoleucine, leucine, or valine residues [V/I/L] plus one acidic/ polar residue at position 2 or 3. Surrounding this core domain is a disordered

sequence of acidic amino acid residues with a net negative charge. The majority of SIMs contained serines or threonines, separating the acidic and hydrophobic parts of the SIM, which can serve as possible phosphorylation sites (Hecker et al., 2006). In fact, the phosphorylation of serine in the SIM of PIASxα may contribute to the spatial orientation of binding to sumoylated targets.

Ouyang and colleagues identified a non-consensus SIM required for SUMO2 specific binding, I/V/L-D/E-I/V/L-D/E-I/V/L (Ouyang et al., 2009). Their results indicated that interaction between the SIM of CoREST1 (part of the LSD1/ CoREST1/HDAC co-repressor complex) and SUMO2 mediates changes in chromatin structure and transcription, relevant for cell type-specific gene expression. Additionally, *Vogt and Hofmann* published three SIMS in 2012 (Vogt & Hofmann, 2012).

Interestingly, *Hecker and colleagues* identified a potential SIM in human TDP2, ^{280}IVDV^{283}, an inversion of the predicted SIM V/I-X-V/I-V/I (Hecker et al., 2006). *Song and coworkers* showed that both parallel and antiparallel binding to SUMO could occur, indicating the possibility of these amino acids serving as a SUMO-binding domain (Song et al., 2005). The potential SIM of TDP2 lacked the characteristic acidic track (SIM with surrounding sequence: RCGGLPNN**IVDV**-WEFLGKPKH), which influences general SIM binding to SUMO1 but not SUMO2 (Hecker et al., 2006). Mutating the four amino acids of TDP2 ^{280}IVDV^{283} to alanines, Hecker and colleagues observed that binding to SUMO isoforms is abolished. To test the contribution of negatively charged residues in isoform specific binding, Leucine^{286}, Glycine^{287}, and Lysine^{288} were mutated to glutamine, aspartic acid, and glutamine. SUMO1 binding was increased, while SUMO2 binding

decreased. The N-terminal domain of TDP2 UBA-like domain is specific for ubiquitin binding, and does not bind SUMO (Rao et al., 2016).

4.3. ZNF451 is a novel SUMO E3 ligase

ZNF451 is a 121 kDa multi-zinc finger SUMO E3 ligase specific to SUMO2/3 that acts as a transcriptional coregulator through its interactions with both PML bodies and the SUMO machinery (Cappadocia et al., 2015; Eisenhardt et al., 2015). Of the three alternatively spliced isoforms of the protein, isoform 1 (121 kDa protein) is the most expressed (Figure I9). Isoform 1 and 2 are almost identical, with isoform 3 only sharing the catalytic N terminal, pointing towards different substrate specificity and/or function.

ZNF451 integrates the function of SIMs and E3 activity to constitute a novel way of performing sumoylation. ZNF451 itself is autosumoylated in an atypical manner, in that the sumoylation at several non-consensus sites actually depends on a SIM within the protein (Eisenhardt et al., 2015). It is interesting that the covalent SUMO binding depends on a non-covalent SUMO interaction. Two N-terminal SIMs with an intervening proline-leucine-arginine-proline (PLRP) motif are responsible for the SUMO E3 ligase activity (Cappadocia et al., 2015). ZNF451 has the ability to elongate SUMO2/3 chains, an activity that has been proposed as an

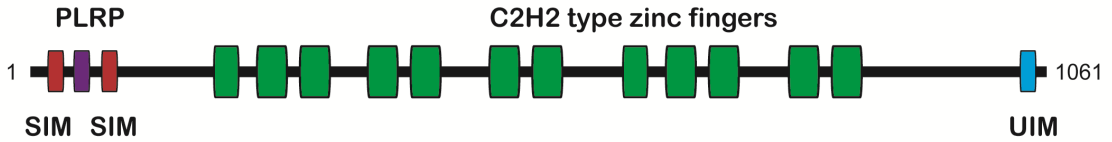

Figure I9. Domain organization of ZNF451. Colored boxes represent domains/motifs of ZNF451. The N-terminus of ZNF451 contains two SIMs with an intervening PLRP domain. ZNF451 also contains twelve C_2H_2 type zinc fingers, and a C-terminal UIM. SIM-Sumo Interacting Motif (red); PLRP- Proline-Leucine-Arginine-Proline motif (purple); UIM- ubiquitin interacting motif (blue); C_2H_2 type zinc fingers (green). This figure is based on *Cappadocia et al., 2015*.

"E4 elongase activity." The zinc finger region of the protein mediates substrate specificity while SUMO modifications are important for nuclear localization of ZNF451 (Karvonen et al., 2008). ZNF451 interacts weakly with androgen receptor (AR) in a SUMO1 enhanced manner.

Additionally, ZNF451 partially colocalizes to PML NBs, and while PML is a SUMO substrate of ZNF451, ZNF451 also regulates PML stability (Koidl et al., 2016). PML NBs are a functional promiscuous proteinaceous sub-nuclear compartments that are organized by the PML protein, and are implicated in diverse cell functions, such as stress response, DNA repair, apoptosis, and anti-viral immunity (Bernardi & Pandolfi, 2007; Sahin et al., 2014b). PML nuclear bodies may play an important role in integrating the sumoylation and ubiquitination pathways with SUMO1 and ubiquitin co-localizing in PML bodies upon inhibition of the proteasome (Bailey & O'Hare, 2005). Interestingly, like ZNF451, TDP2 is also a PML NB component (Xu et al., 2008).

4.4. Sumoylation of Topoisomerase 2

SUMO modification of topoisomerases was first discovered with TOP1, before being discovered in TOP2. Trapped TOP1 activates the ubiquitin/26S proteasome and results in its degradation (Mao et al., 2000b). Given these results, *Liu and colleagues* investigated if TOP2-induced damage induces sumoylation and/ or degradation of TOP2. TOP2 damage does, in fact, induce sumoylation. For example, both the TOP2 poison teniposide (VM-26) and bisdioxopiperazine inhibitor ICRF-193 cause rapid SUMO1 modification of TOP2α and TOP2β in HeLa cells (Mao et al., 2000a). Sumoylation can be an early signal for TOP2β

selective degradation by the nuclear proteasome following exposure to ICRF-193. When SUMO and UBC9 are conditionally knocked out, ICRF-193 induced degradation of TOP2β doesn't occur. ICRF-193 catalytic inhibitor traps TOP2 in the closed clamp conformation, not inducing TOP2-mediated DNA damage, which suggests that the conformational change of TOP2 may be the signal that triggers SUMO1 conjugation. The structure of TOP2 protein clamp on DNA induced by the drug can also be an obstacle for processes, therefore one could expect accelerated degradation (Isik et al., 2003). The pathway for degradation of TOP2cc was further elucidated, when *Ban and colleagues* observed that TOP2βccs arrest RNAPII transcription elongation and induce proteasomal degradation of TOP2β by a ubiquitin-free pathway that involves 20S proteasome and 19S AAA ATPases, components of the 26S proteasome (Ban et al., 2013).

In addition to the response to damage, sumoylation of TOP2 plays an important role in mitosis. TOP2α is sumoylated in two distinct regions, at several sites in the C-terminal domain (CTD) and at lysine 660 (in *Xenopus laevis*) in the catalytic core of the enzyme where cleavage and relegation of DNA occur (Ryu et al., 2010). As previously mentioned, in order for correct chromosome segregation to occur, sister chromatid cohesion must resolve properly, with TOP2α decatenating centromeric DNA (Lee & Bachant, 2009). Although TOP2α can be found bound throughout the chromosome, the majority of the sumoylated form is found clustered at the mitotic centromere in early mitosis (Ryu et al., 2010). It has been suggested that this sumoylation is important for the localization of the histone H3 kinase Haspin and histone H3 phosphorylation at the centromere,

which are important for the recruitment of other mitotic factors (Yoshida et al., 2016a).

There is evidence that different E3 SUMO ligases are involved in TOP2 sumoylation. In vertebrates, *Dasso and colleagues* used *X. laevis* egg extracts to demonstrate that PIASy is responsible for SUMO2/3 modification of TOP2α, important for the remodeling of TOP2 on mitotic chromosomes at the metaphase-anaphase transition (Azuma et al., 2003; Azuma et al., 2005). However, a different SUMO ligase has also been implicated in TOP2α sumoylation through SUMO1 modifications. The RANBP2 SUMO E3 ligase domain binds to TOP2α in mitosis and regulates its sumoylation and localization to inner centromeres, to mediate sister-chromatid segregation. (Joseph et al., 2004; Dawlaty et al., 2008).

While TOP2 sumoylation has an important role in both the DDR and mitosis, until now it has remained unknown whether or not TOP2 is sumoylated in the context of the cleavage complex. Additionally, if TOP2cc are SUMO modified, the E3 SUMO ligase responsible has not been identified and may or may not be one of the known TOP2 E3 SUMO ligases mentioned above.

5. INTRODUCTION TABLES

	Classification	DNA end	Cofactors	Supercoiled substrates	Other substrates
TOP1	Type IB	3’	None	+, -	
TOP1mt	Type IB	3’	None	+, -	
TOP2α	Type IIA	5’	Mg^{2+} and ATP	+, -	knots, catenanes
TOP2β	Type IIA	5’	Mg^{2+} and ATP	+, -	knots, catenanes
TOP3α	Type IA	5’	Mg^{2+}	-	Hemicatenanes, Double Holiday Junctions, D
TOP3β	Type IA	5’	Mg^{2+}	-	RNA knots, R loops

Table I1. Human Topoisomerases. There are six topoisomerases present in *Homo sapiens*, including type IA, type IB, and type IIA. Adapted from *Pommier et al., 2016*.

Select SIMs	Reference
h-h-X-S-X-S/T-a-a-a	*Minty et al., 2000*
V/I-X-V/I-V/I	*Song et al., 2004*
K-X_{3-5}-I/V-I/L-I/L-X_3-D/E/Q/N-D/E-D/E	*Hannich et al., 2005*
V/I/L/M/F/W/A-V/I/L/M/F/W/A-X-S-X-S/T-D/E-D/E-D/E	*Hecker et al., 2006*
I/V/L-D/E-I/V/L-D/E-I/V/L	*Ouyang et al., 2009*
P/I/L/V/M-I/L/V/M-X-I/L/V/M-[D/S/E/>]$_3$	*Vogt et al., 2012*
P/I/L/V/M-I/L/V/M-D/L/T	*Vogt et al., 2012*
[D/S/E]$_3$-I/L/V/M-X-[I/L/V/M/F]$_2$	*Vogt et al., 2012*

Table I2. Selected identified SIMs. Hydrophobic and acidic amino acids are important in published general and specific SIMs.

II. OBJECTIVES

II. Objectives

Because TOP2 is sumoylated in several physiological processes and in response to etoposide, and TDP2 has been reported to interact with SUMO through a published SIM, we aimed to uncover novel functions of TDP2 in the resolution of TOP2cc, the possible role of SUMO, and novel factors involved in the process, therefore updating the current model for the removal of TOP2cc. Hence, the objectives of this thesis are as follows:

1. Characterization of non-covalent TDP2-SUMO interactions.
    1.1. Verify SUMO isoform specific interactions with TDP2.
    1.2. Define and characterize the SIM of TDP2.
    1.3. Determine the physiological relevance of TDP2 interaction with SUMO.
2. Role of TOP2 sumoylation and effect of TDP2.
    2.1. Address TOP2 sumoylation in the context of the cleavage complex.
    2.2. Determine a possible role of TDP2 on sumoylated TOP2cc.

III. RESULTS

1. TDP2 is a SUMO binding protein

TDP2 is a pleiotropic protein involved in various cellular processes. Upon the discovery of its unique 5'phosphodiesterase activity (Cortes-Ledesma et al., 2009), and in order to further characterize the protein, Felipe Cortés-Ledesma and Maria C. Zuma (in the laboratory of Keith Caldecott) performed a yeast two-hybrid (Y2H) screening utilizing TDP2 as bait (*TDP2* cDNA cloned into the pGBKT7 vector) with a pACT human cDNA library.

To perform a Y2H, a gene of interest is cloned into an expression vector to express the protein (designated as the 'bait') as a fusion to the DNA binding domain (BD) of a transcription factor (TF). In this case, TDP2 was used as a C-terminal bait protein fused to amino acids 1-147 of the GAL4 DNA BD. A second hybrid is con-

a.

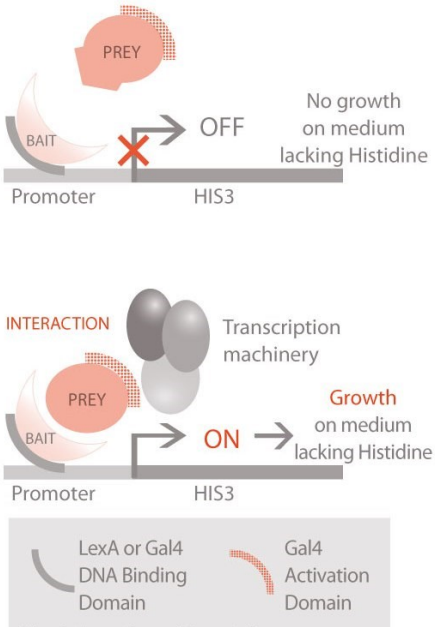

b.

Y2H Hits
Sumo 1
Sumo 2
UBC2I
PIAS1
PIAS3
Ubiquitin B
RYBP
BTBD6
RIOK1
PCBP1
SCRN1
TPT1
RPL13
C5orf15
PRMT1
RPS3A
PHB2
HNRNPA2B1
PABPC1
PCNA
CYBASC3

Figure 1. Yeast two-hybrid principle and potential TDP2-interacting factors. a. Yeast two-hybrid principle. A fusion 'hybrid' is constructed between a protein of interest, the 'bait', and the DNA Bind-ing Domain (DNA BD) of the transcription factor (TF). A second hybrid is constructed between the 'prey' protein and the Activation Domain (AD) of the TF. Interaction between the bait and the prey brings the DNA BD and AD in close proximity and a functional TF is reconstituted upstream of the reporter gene. From www.hybrigenics-services.com. **b.** List of potential TDP2-interacting factors identified in a yeast two-hybrid screening against a cDNA library. Courtesy of Maria C. Zuma, Felipe Cortés-Ledesma, and Keith Caldecott.

structed between a prey protein and the activation domain (AD) of the GAL4 TF. As depicted in Figure 1a, interaction between the bait and prey indirectly connects the AD and BD of the transcription factor, the AD is brought into proximity of the transcription start site (TSS), allowing transcription of the reporter gene *HIS3*, permitting growth in histidine-lacking media. Since *HIS3* has leaky expression in many yeast strains, including Y190, a competitive inhibitor of the *HIS3* gene product, 3-Amino-1,2,4-Triazol (3AT), was added to -His plates at a concentration previously determined by titer to remove background. pGBKT7 contains the *TRP1* nutritional marker while the pACT vector contains the *LEU2* marker, allowing yeast auxotrophs to grow on the corresponding limiting synthetic media.

Surprisingly, of 62 isolated candidates of the Y2H screening, 14 corresponded to SUMO1, 12 to SUMO2, and 10 to UBC2I, homolog of the SUMO conjugating enzyme UBC9 (Figure 1b). Additional members of the SUMO conjugation machinery were identified such as the E3 SUMO ligases PIAS1 and PIAS3. Ubiquitin was also detected in the screening. The interactions detected with SUMO and the sumoylation machinery through the Y2H opened the possibility of TDP2 having a physiologically relevant interaction with SUMO.

TDP2 interactions with SUMO were confirmed with directed Y2H studies and the SUMO isoform specificity was tested, checking which (if any) interacts more strongly with TDP2. pGBKT7-TDP2, the vector utilized for the Y2H screening, was used. *SUMO1* and *SUMO2* were cloned into the pACT vector to express the corresponding prey proteins fused C-terminally to the GAL4 activation domain (AD). After transformation of these vectors into the Y190 strain (see methods table 1 for genotype) and selection on –Leu –Tryp plates, individual yeast colonies con-

taining both plasmids were selected and 5X drop dilutions were performed on -Leu -Tryp plates to represent growth, serving as a loading control (left panel of Figure 2). Interaction was represented in the right panel, by growth on -Leu -Tryp -His plates.

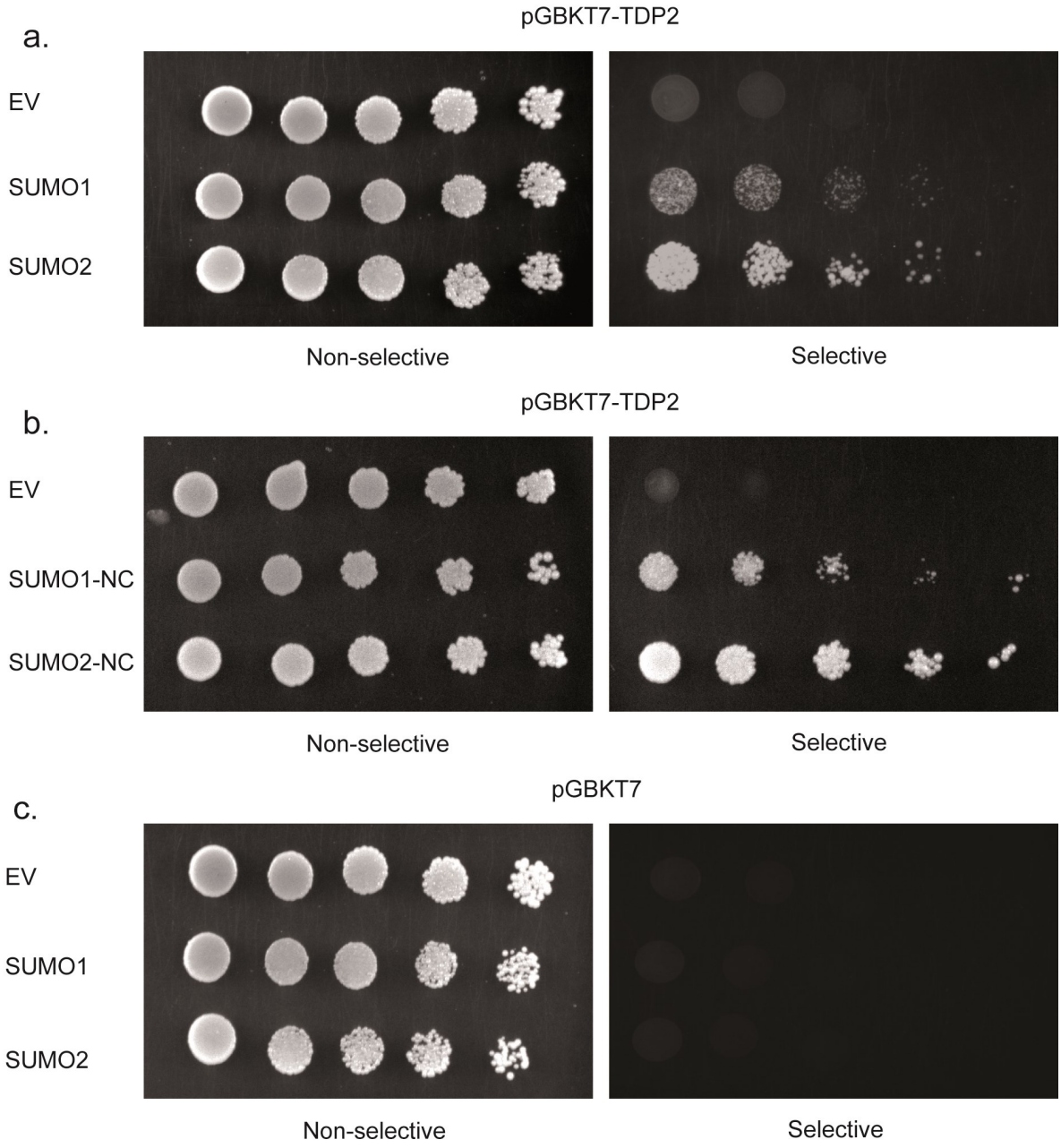

Figure 2. Yeast two-hybrid interactions of SUMO with TDP2. Yeast two-hybrid interactions of SUMO with TDP2. 5X drop dilutions plated on (-Leu -Tryp) plates (left) or (-Leu -Tryp -His) plates with the addition of 3AT (right). **a.** TDP2 bait in combination with prey of empty vector (EV) control pACT (BD alone), SUMO1, or SUMO2. **b.** TDP2 bait in combination with prey of control pGBKT7 (AD alone), non-conjugatable SUMO 1 (SUMO1-NC), or non-conjugatable SUMO2 (SUMO2-NC). **c.** pGBKT7(AD alone) with EV, SUMO1, or SUMO2.

Growth on -Leu -Tryp -His plates was observed for yeast cotransformed with pGBKT7-TDP2 and both pACT-SUMO1 and pACT-SUMO2, indicative of interaction (right panel of Figure 2). More growth was observed for pGBKT7-TDP2 + SUMO2 than for pGBKT7-TDP2 + SUMO1, indicating a stronger interaction with SUMO2 as compared to SUMO1 (Figure 2a). As expected, there was no growth of yeast transformed with pGBKT7-TDP2 and the empty pACT vector containing only the AD on -Leu -Tryp -His plates, indicating that the SUMO interactions are specific. Additionally, the empty pGBKT7 vector containing only the BD did not interact with the AD (pACT) nor with SUMO (Figure 2c).

The TDP2 and SUMO interaction could be representative of either a non-covalent SUMO interaction through a TDP2 SIM or covalent conjugation of SUMO to the TDP2 protein. In order to check this, we made use of non-conjugatable SUMO1 and SUMO2 lacking the C-terminal diglycine motif important for covalent SUMO conjugation, a gift from Mario García (CABIMER), in the pLexA vector containing the LexA DNA binding domain and the *TRP1* nutritional marker. *TDP2* was cloned into the pACT vector. TDP2 interaction did not decrease for either isoform when the non-conjugatable forms of SUMO were used, indicating that covalent sumoylation was not necessary for the observed interaction (Figure 2b).

Our results were consistent with the observations of *Dikic and colleagues* (Hecker et al., 2006), who used non-conjugatable SUMO1 or SUMO2 as bait to perform a large scale Y2H screening with human cDNA libraries to identify SUMO interacting partners. They identified several proteins, one of which was TTRAP (TDP2), with a stronger interaction detected with SUMO2 as compared to SUMO1 in both yeast and cells.

Using the program GPS-SUMO 1.0 (Qi et al., 2014) with a medium threshold, there was a predicted SUMO-interacting motif (SIM) in human TDP2 at ^{280}IVDV^{283} (isoleucine, valine, aspartic acid, isoleucine) with a score of 59.475 (Figure 3b). Only the aspartic acid residue is conserved in the mouse protein (Figure 3a), although it is surrounded by different hydrophobic residues, ^{290}VFDA^{293}. *Hecker et al.* (2006) also identified the same SIM in human TDP2 as the prediction software.

^{280}IVDV^{283} is an inversion of the predicted SIM V/I-X-V/I-V/I (Hecker et al., 2006). *Song and colleagues* showed that both parallel and antiparallel binding to

a.

```
Human      MELGSCLE-------GGR----EAAEEEGEPEVKKRRLLCVEFASVASCDAAVAQCFLAE 49
Mouse      MASGSSSDAAEPAGPAGRAASAPEAAQAEEDRVKRRRLQCLGFALVGGCDPTMVPSVLRE 60
           *  **. :       .**      * :  * .**:*** *: ** *..** ::. ..* *

Human      NDWEMERALNSYFEPPVEESALERRPETISEPKTYVDLTNEETTDSTTSKISPSEDTQQE 109
Mouse      NDWQTQKALSAYFELPENDQGWPRQPPTSFKSEAYVDLTNEDANDTTILEASPSGT-PLE 119
           ***: ::**.:*** * ::..  *:* *  : ::*******::.*:*  : ***     *

Human      NGSMFSLITWNIDGLDLNNLSERARGVCSYLALYSPDVIFLQEVIPPYYSYLKKRSSNYE 169
Mouse      DSSTISFITWNIDGLDGCNLPERARGVCSCLALYSPDVVFLQEVIPPYCAYLKKRAASYT 179
           :.* :*:*********  ** ******** ********:********* :*****::.*

Human      IITGHEEGYFTAIMLKKSRVKLKSQEIIPFPSTKMMRNLLCVHVNVSGNELCLMTSHLES 229
Mouse      IITGNEEGYFTAILLKKGRVKFKSQEIIPFPNTKMMRNLLCVNVSLGGNEFCLMTSHLES 239
           ****:********:***.***:*********.**********:*.:.***:*********

Human      TRGHAAERMNQLKMVLKKMQEAPESATVIFAGDTNLRDREVTRCGGLPNNIVDVWEFLGK 289
Mouse      TREHSAERIRQLKTVLGKMQEAPDSTTVIFAGDTNLRDQEVIKCGGLPDNVFDAWEFLGK 299
           ** *:***:.*** ** ******:*:************:** :*****:*:.*.******

Human      PKHCQYTWDTQMNSNLGITAACKLRFDRIFFRAAAEEGHIIPRSLDLLGLEKLDCGRFPS 349
Mouse      PKHCQYTWDTKANNNLRIPAAYKHRFDRIFFRA--EEGHLIPQSLDLVGLEKLDCGRFPS 357
           **********: *.** * ** * *********  ****:**:****:************

Human      DHWGLLCNLDIIL      362
Mouse      DHWGLLCTLNVVL      370
           *******.*:::*
```

b.

ID	Position	Peptide	Score	Cutoff	Type
hTDP2	280 - 284	CGGLPNN **IVDVW** EFLGKPK	59.475	55.31	SUMO Interaction

Figure 3. Alignment of mouse and human TDP2 with predicted SIM. a. TDP2 amino acid sequence alignment of *Homo sapiens* (human) and *Mus musculus* (mouse). Amino acids conserved between the two species are marked with an asterisk, and amino acids with high homology are marked with two dots, and with less homology marked with one dot. Predicted SIM and homologous sequence is marked in blue. **b.** SUMO prediction: Predicted Sumo-Interacting Motifs (SIMs) in *Homo sapiens* TDP2.

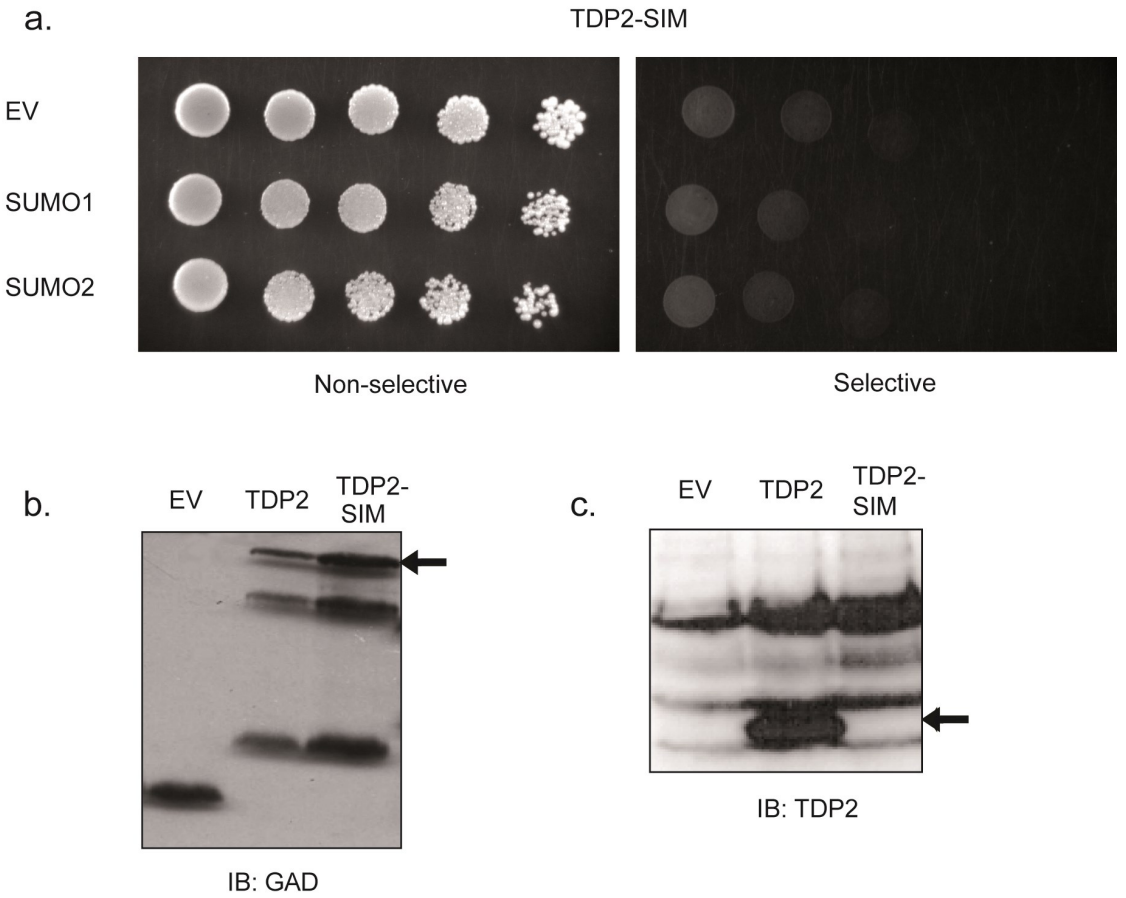

Figure 4. Yeast two-hybrid interactions of TDP2 with SUMO are abolished by SIM mutation. Yeast two-hybrid interactions with TDP2-SIM. **a.** 5X drop dilutions (left) plated on (-Leu -Tryp) and (right) (-Leu -Tryp -His). TDP2 bait in combination with prey of control (EV), SUMO1, or SUMO2. **b.** Immunoblot of yeast transformed with transfected with pGBKT7 empty vector (EV) containing GAD, TDP2 fused to GAD, or TDP2-SIM fused to GAD with GAD antibody. **c.** Immunoblot of HEK 293T cells transfected with empty pcDNA3.1 vector (EV), TDP2, or TDP2-SIM with TDP2 antibody. Arrows indicate the expected size of GAD-TDP2 or TDP2.

SUMO could occur, indicating the possibility of these amino acids serving as a SUMO-binding domain (Song et al., 2005). The potential SIM of TDP2 lacked the characteristic acidic track (SIM with surrounding sequence: GLPNN**IVDV**-WEFLG), which influences general SIM binding to SUMO1 but not SUMO2 (Hecker et al., 2006). Mutating the four amino acids of TDP2 ^{280}IVDV^{283} to alanines, *Hecker and colleagues* observed that binding of the TDP2-SIM mutant to SUMO isoforms is abolished. We then wanted to perform complementation experiments in mammalian cells to see the physiological relevance of the TDP2-SUMO

interaction, so we complemented *Tdp2*$^{-/-}$ MEFs, which have several known DSB repair phenotypes, with wild-type TDP2 and TDP2 that no longer interacted with SUMO. In order to do this, similar to the construct used by the Dikic laboratory (Hecker et al., 2006), we recreated the construct TDP2-SIM and cloned it into the pGBKT7 vector. With Y2H, we confirmed that TDP2-SIM loses the ability to interact with both SUMO1 and SUMO2 (Figure 4a). We checked expression in yeast, and confirmed that the transformed yeast properly express TDP2-SIM, even more so than wild-type TDP2 (Figure 4b). However, when we attempted to express TDP2-SIM in mammalian cells, we were unable to detect it through Western blotting of transfected cells (Figure 4c). This is specific to the SIM mutation, as wild-type TDP2 is expressed and properly detected. Lack of TDP2-SIM expression would make it unsuitable for complementation experiments.

To fully characterize the TDP2 SUMO interaction, we entered into collaboration with the group of R. Scott Williams, at the NIEHS/NIH in Research Triangle Park, North Carolina (USA). The group has crystallized and published several structures of TDP2.

Our collaborators solved the crystal structure of the catalytic portion of mouse TDP2 (mTDP2^{cat}, amino acids 108-362) interacting with SUMO2 (Figure 5). TDP2 has a novel sumo interacting surface that has been named split-SIM. Instead of having the described format of four or more adjacent hydrophobic amino acids, (see introduction: SUMO-interacting motifs) the TDP2 SIM is comprised of five SUMO-binding elements (SBs) in different parts of the protein (denoted as SB1-5) that form a novel SUMO interacting surface due to the 3D conformational of the protein. Two short β strands (β0 from region SB1, β14 from SB5) form the split-

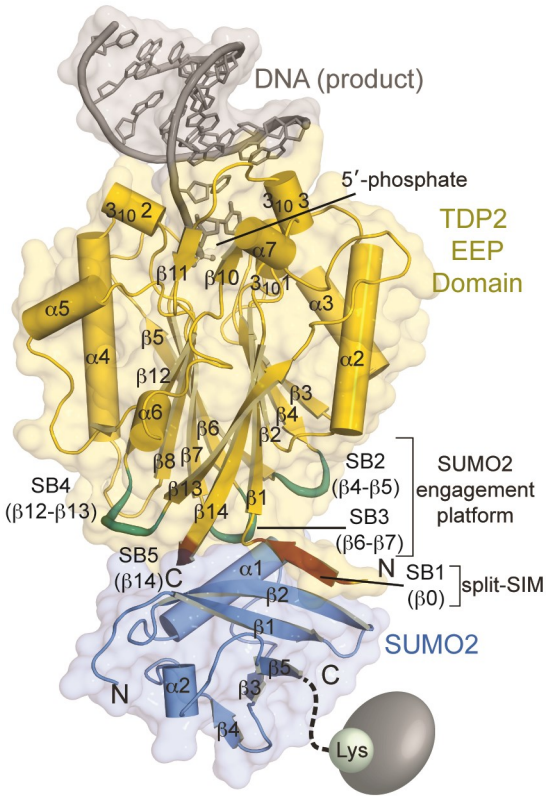

Figure 5. Overall structure of DNA/ mTDP2cat/SUMO2 complex. A split–SIM (burgundy) and three loops (turquoise) position a putatively sumoylated protein 40–70Å away from the 5′–phosphate of a substrate DNA (gray). Courtesy of Matt Schellenberg and R. Scott Williams (NIEHS/NIH).

SIM, with the C-terminal Leu370 from β14 inserting into the SUMO2 hydrophobic binding pocket. Three loops, SB2 (between β4-β5), SB3 (β6-β7), and SB4 (β12-β13) contribute to the split-SIM core, together forming a relatively large SUMO-SIM surface. Interestingly, the predicted SIM (^{290}VFDA^{293} in mouse) is not part of the split-SIM.

2. TOP2 is sumoylated in the context of the cleavage complex

Because both TOP2α and TOP2β are SUMO modified (see introduction: topoisomerases) and TDP2 has a novel split-SIM, we checked if TOP2 is sumoylated in the context of TOP2ccs. Additionally, there is the possibility that TOP2cc sumoylation could have a cross-talk with TDP2 and in some way regulate its function. To quantify covalent protein-DNA complexes in cells, we used the *in vivo* complex of the enzyme (ICE) assay (Nitiss et al., 2012).

The ICE assay is commonly used as a way to quantify TOP2 covalently bound to DNA. This assay uses a cesium chloride gradient to separate free proteins from proteins covalently bound to DNA, which are pelleted along with free DNA (Figure 6). The DNA pellet is resuspended, and equal amounts slot blotted to be probed with antibodies specific to either the α or β isoform of TOP2. Since TOP2α expression varies during the cell cycle, we removed artifacts due to cell cycle differences by arresting cells in G0/G1 by confluency and serum starvation.

We first analyzed the accumulation of TOP2 isoforms in wild-type primary MEFs. TOP2βcc were detected upon etoposide treatment (Figure 7). When the proteasome inhibitor MG132 was used to prevent degradation, there was not a significant increase in signal as compared to without MG132. Etoposide induced TOP2αcc were detected to a lesser extent as compared to TOP2βcc, and also do not have a significant increase upon inhibition of the proteasome.

We reasoned that since sumoylation is a covalent modification, we would be able to apply the assay in a novel approach to detect SUMO modified forms of

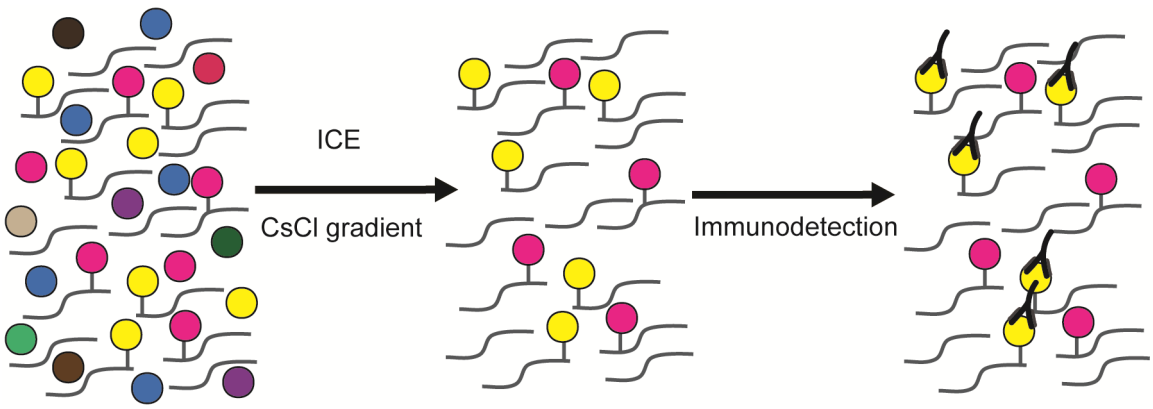

Figure 6: Schematic of *in vitro* complexes of the enzyme assay (ICE). (left) Nuclei contain proteins and DNA. Some of the DNA contains covalently bound proteins such as TOP2. Cells are lysed and passed through a cesium chloride gradient. (middle) DNA and DNA with covalently bound protein is isolated and immunoblotted, (right) and detected with specific antibodies.

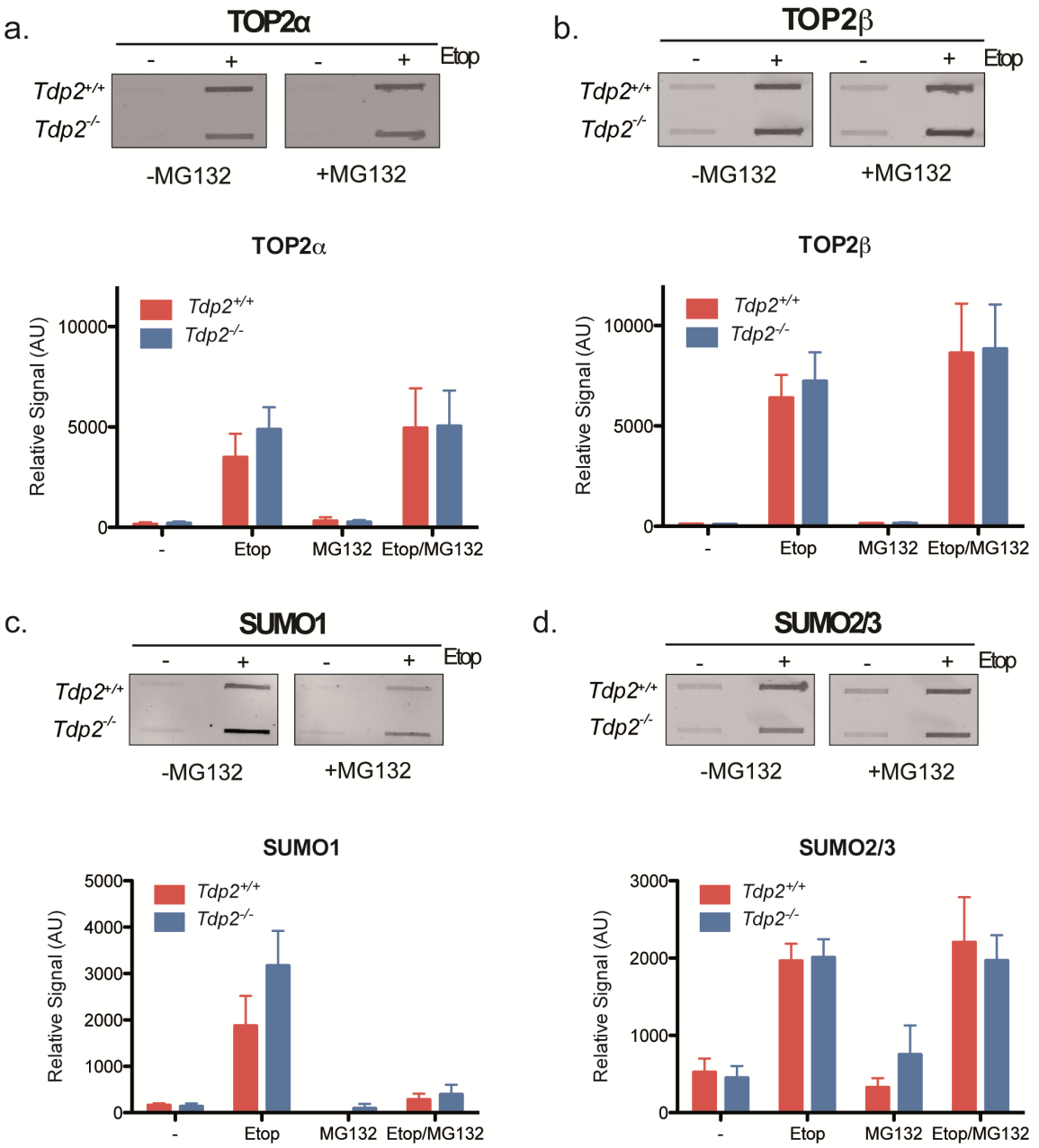

Figure 7. TOP2cc induced by etoposide are SUMO modified. Representative image and quantification of **a.** TOP2α; **b.** TOP2β; **c.** SUMO1; or **d.** SUMO2/3 covalently bound to genomic DNA isolated by ICE in *Tdp2*$^{+/+}$ and *Tdp2*$^{-/-}$ confluency-arrested primary MEFs with or without prior treatment with 100 μM etoposide for 1 h in the presence or absence of 20 μM MG132. Average ± s.e.m.; n≥7

TOP2cc. The presence of possible SUMO isoforms is confirmed by probing with antibodies specific to either SUMO1 or SUMO2/3 (the SUMO2/3 antibody recognizes both SUMO2 and SUMO3 isoforms). With the ICE assay, we were, in fact,

able to see both etoposide induced SUMO1 and SUMO2/3 signal. Etoposide induced SUMO1 signals decrease dramatically upon inhibition of the proteasome, consistent with the observations of Bailey and O'Hare (2005) that upon treatment with the proteasome inhibitor MG132, the free SUMO1 pool is depleted. SUMO2/3 signal does not change upon inhibition of the proteasome.

Our approach of detecting SUMO signal in TOP2ccs could raise the question of whether or not the signal actually corresponds to SUMO modified TOP2, or if it could correspond to modification of some other covalently bound protein. The first evidence that the SUMO signal corresponds to modified TOP2cc was that the signal was etoposide induced. Secondly, we performed Western blots of the ICE material, given that slot blotting has the limitation of not being able to resolve proteins by size. Cleavage complexes were micrococcal nuclease digested to remove them from DNA and allow separation by SDS-PAGE. Covalent complexes isolated from wild-type cells were analyzed and showed that etoposide treatment leads to a preferential accumulation of TOP2β and SUMO2/3 signals (Figure 8a). TOP2β migrated at its expected size forming a solid band and a higher molecular weight smear. SUMO2/3 signals appeared as a high molecular weight smear colocalizing with the smear of TOP2β, suggesting that the SUMO2/3 signal detected in the ICE assay corresponds to modification of TOP2β. TOP2α signal was also detected as a thin faint concrete band right below TOP2β, but to a much lesser degree than TOP2β. SUMO1 was detected as a high molecular weight smear to a lesser extent than SUMO2/3. However, the slot blot quantification indicates that the SUMO1 signal is not weaker than SUMO2. The observation of the presence of unmodified TOP2α and TOP2β indicates that only a fraction of TOP2cc are SUMO modified.

a.

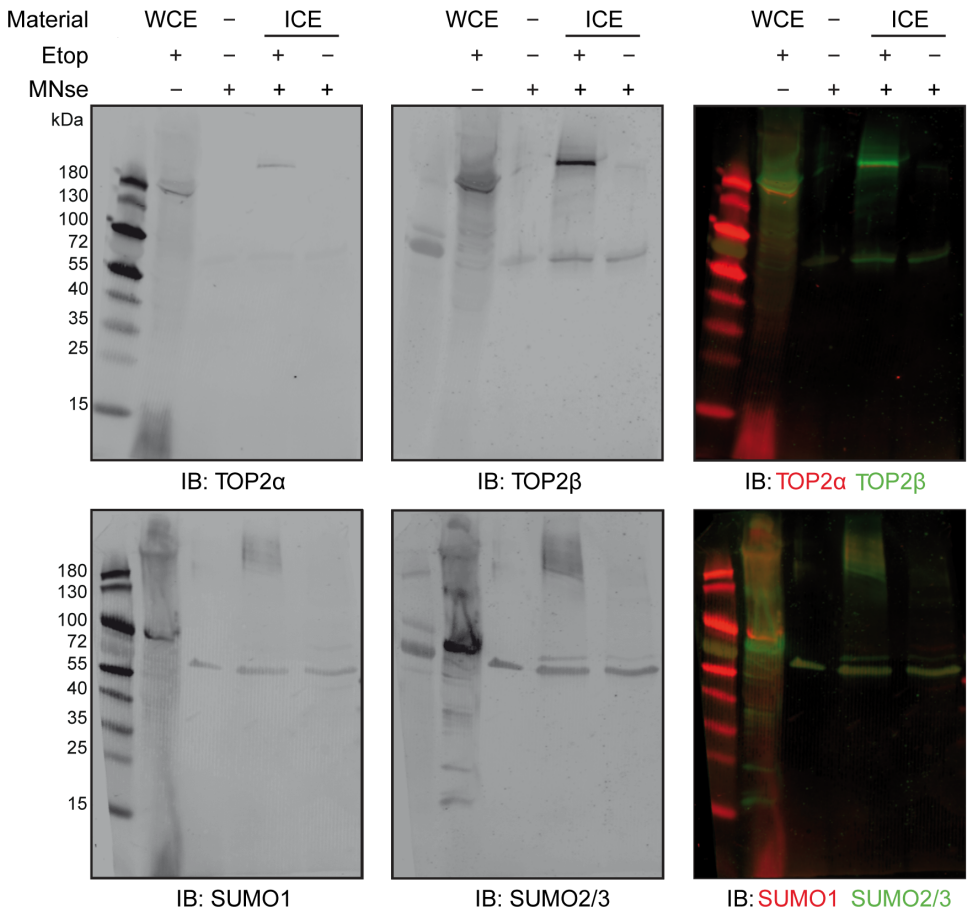

b.

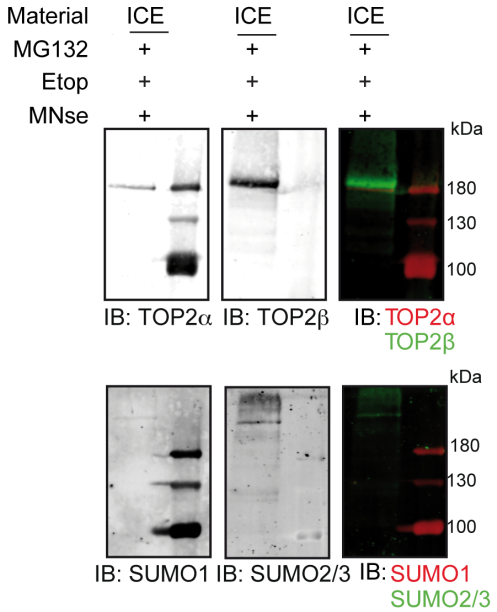

Figure 8. Full-length TOP2 in TOP2cc is SUMO modified. a. Immunoblot of TOP2α, TOP2β, SUMO1 and SUMO2/3 in whole cell extract (WCE) and covalently bound to genomic DNA in confluency-arrested primary MEFs following 1 h 100 μM etoposide treatment (Etop). Samples were treated by micrococcal nuclease prior to SDS-PAGE to remove covalently linked DNA. **b.** Same is in "**a.**", except sample was treated with MG132.

TOP2α, TOP2β, SUMO1 and SUMO2/3 are all detected in the whole cell extract (WCE). The lower molecular weight band that appears below the 55 kDa marker corresponds to the micrococcal nuclease digestion buffer which contains BSA. Western blot was then performed upon proteasome inhibition (Figure 8b) to confirm a lack of SUMO1 upon addition of MG132 that was seen in Figure 7. Only a very faint band was seen of SUMO1 that appeared similar in size to the band detected by the SUMO2/3 antibody. Finally, we designed an assay to measure TDP2 activity on the ICE substrate, and observed that the removal of this signal was dependent on TDP2 phosphodiesterase activity, which will be later discussed (Figure 14).

We then analyzed the accumulation of etoposide induced TOP2αcc and TOP2βcc in *Tdp2*$^{-/-}$ MEFs to see whether or not TDP2 has a role in the metabolism of cleavage complexes. Upon treatment with etoposide, TOP2αcc and TOP2βcc were detected with similar signal regardless of *Tdp2* background. Additionally, upon inhibition of the proteasome, levels in *Tdp2*$^{-/-}$ cells were similar to wild-type cells. We then checked if TDP2 has an effect on the sumoylation of TOP2cc. SUMO2 signal was induced equally in wild-type and *Tdp2*$^{-/-}$ cells, and did not differ when the proteasome was inhibited. However, we detected more SUMO1 modification of covalent complexes in *Tdp2*$^{-/-}$ background as compared to wild-type.

3. TDP2 binds sumoylated TOP2

The observation of SUMO modified TOP2cc together with the novel TDP2 split SIM lead us to wonder if TDP2 is able to interact with sumoylated TOP2. In collaboration, the R. Scott Williams laboratory purified TDP2 containing complexes by immunoprecipitating YFP-TDP2. Western blotting with corresponding antibodies confirmed TOP2α, TOP2β, and high molecular weight SUMO2/3, revealing that

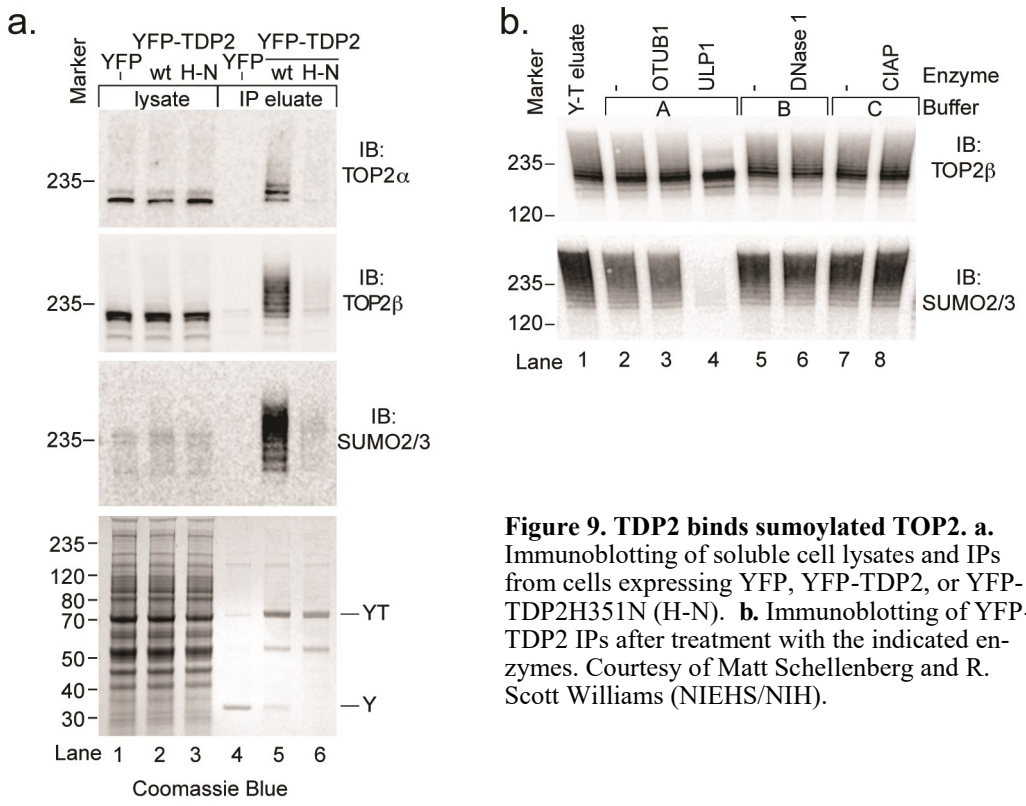

Figure 9. TDP2 binds sumoylated TOP2. a. Immunoblotting of soluble cell lysates and IPs from cells expressing YFP, YFP-TDP2, or YFP-TDP2H351N (H-N). **b.** Immunoblotting of YFP-TDP2 IPs after treatment with the indicated enzymes. Courtesy of Matt Schellenberg and R. Scott Williams (NIEHS/NIH).

TDP2 associates with covalently modified forms of intact (non-proteolyzed) TOP2 isoforms (Figure 9a, lanes 4,5).

Treatment of YFP-TDP2 immunopreciptated (IP) samples with the SUMO isopeptidase Ulp1 collapsed TDP2-bound TOP2 protein ladders to a uniformly migrating species, while the OTUB1 deubiquitinase, DNAse I, or alkaline phosphatase did not, indicating that TDP2 preferentially interacts with SUMO modified TOP2.

Intriguingly, IP conducted with an active site variant of TDP2 (H351N) that ablates catalytic activity (Schellenberg et al., 2012) was nearly devoid of SUMO2-TOP2 (Figure 9a, lane 6), indicating that TDP2-bound TOP2-SUMO2 complexes derive from TDP2 catalysis that liberates full-length sumoylated TOP2 from the insoluble chromatin fraction. Overall, these observations suggested that in addition to processing proetolyzed TOP2 fragments (Caldecott et al., 2012; Gao et al., 2014),

TDP2 can engage post-translationally marked intact TOP2 molecules. This prompted us to evaluate the role of TDP2 on non-proteolyzed TOP2cc.

4. TDP2 removes sumoylated TOP2cc

To confirm the novel function of TDP2 in TOP2cc removal, we first tested how proteasome inhibition influences TDP2 function in the repair of chromosomal DSBs, by monitoring the resolution of γH2AX foci following etoposide treatment. As explained in the introduction, upon induction of a DSB, the highly conserved histone variant H2AX is phosphorylated on serine 139, making γH2AX foci a good estimate of DSBs. γH2AX foci are induced by etoposide, and upon etoposide removal, we can measure DSB repair by scoring the remaining foci in different conditions or genotypes. Cells were arrested in G0/G1 by confluency and serum starvation. Since the proteasome facilitates conversion of TOP2cc into irreversible DSBs, higher doses of etoposide were required to induce quantifiable γH2AX foci in the presence of MG132, but they were induced in a dose-dependent manner (Figure 10a). γH2AX foci were induced in a similar manner in both wild-type and *Tdp2*$^{-/-}$ cells and were similar in appearance to those without proteasome inhibition (compare Figure 10b to Figure 10c).

As previously reported, *Tdp2*$^{-/-}$ MEFs show reduced efficiency of etoposide-induced γH2AX foci resolution when compared to wild-type cells, but alternative TDP2-independent mechanisms can also operate, leading to a slower repair rate (Figure 11ba, Figure 12a). At 3 and 6 hours post-etoposide removal, this difference is statistically significant when analyzed by two-way ANOVA with Bonferroni posttests with p-values of $p<0.001$ and $p<0.01$ respectively.

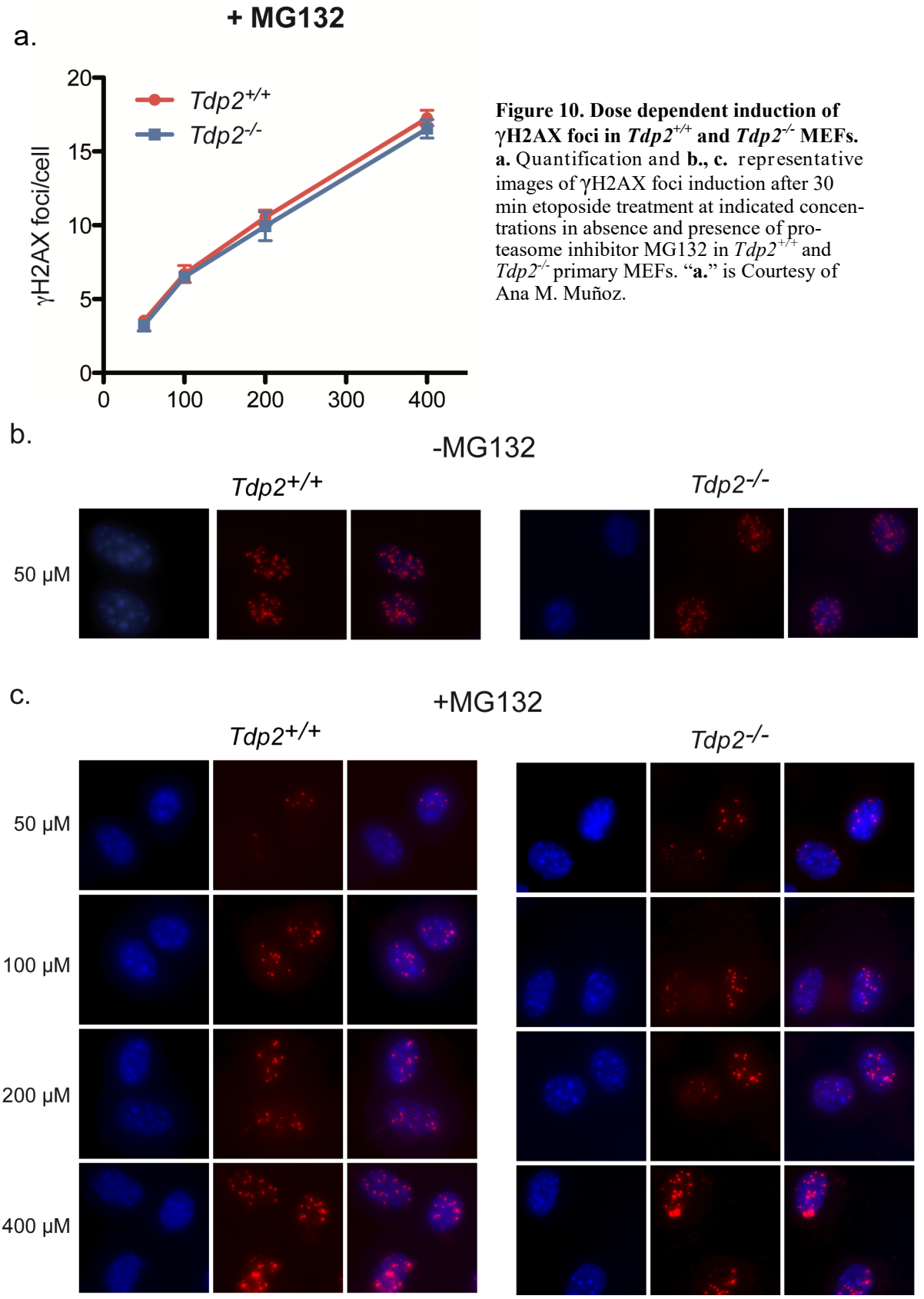

Figure 10. Dose dependent induction of γH2AX foci in *Tdp2*$^{+/+}$ and *Tdp2*$^{-/-}$ MEFs. **a.** Quantification and **b., c.** representative images of γH2AX foci induction after 30 min etoposide treatment at indicated concentrations in absence and presence of proteasome inhibitor MG132 in *Tdp2*$^{+/+}$ and *Tdp2*$^{-/-}$ primary MEFs. "**a.**" is Courtesy of Ana M. Muñoz.

In stark contrast, MG132 treatment completely abolished the repair capacity of *Tdp2*$^{-/-}$ cells (Figure 11b, Figure 12b). Since γH2AX foci can be induced post-etoposide removal, there was even an increase in foci between the time of etoposide removal (t = 0) and the repair time points, which have roughly double the number of foci. This increase was not seen in wild-type cells, which after 1 hour have the same number of foci as t = 0, because the cells had the ability to repair foci even while new foci were being induced, and foci were rapidly resolved after that, almost disappearing at 3 hours of repair. *Tdp2*$^{-/-}$ cells had absolutely no repair even after 6 hours. This suggests that chromosomal repair of etoposide induced DNA damage can still occur in the absence of proteosomal TOP2 degradation in a pathway that uniquely requires TDP2 function. The lack of γH2AX foci repair in TDP2-deficient background upon proteasome impairment was specific to TOP2 induced damage, as *Tdp2*$^{-/-}$ cells treated with ionizing radiation, which generates heterogeneous DNA damage, did not display the same severe repair defect as etoposide (see Figure 32).

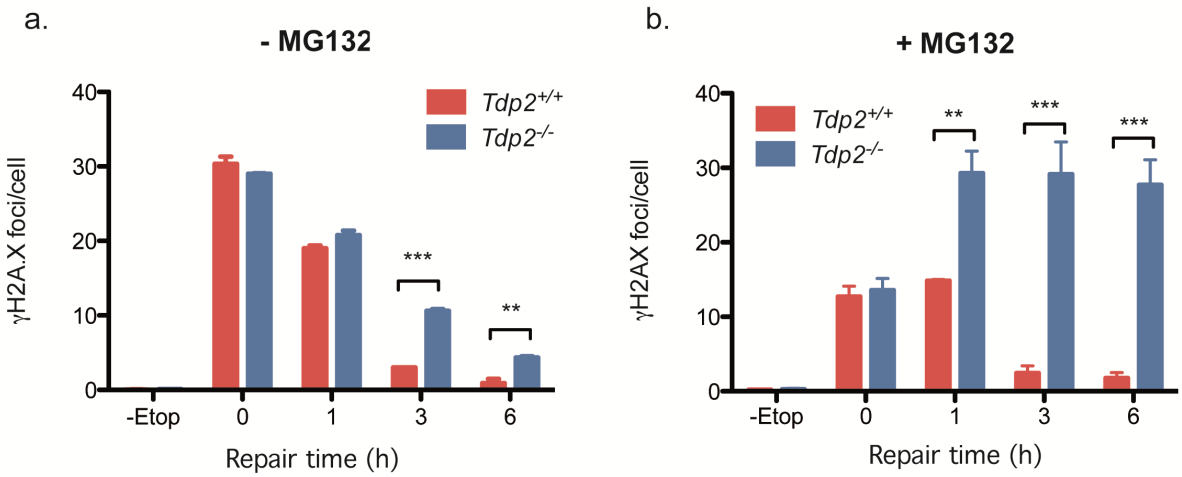

Figure 11. *Tdp2*$^{-/-}$ MEFs are unable to repair etoposide induced γH2AX foci when the proteasome is inhibited. a. Resolution of γH2AX foci in MEFs at the indicated time post 30 μM etoposide exposure. **b.** As "**a.**" except with 20 μM MG132 treatment and 200 μM etoposide. Average ±s.e.m.; n=3; ** p<0.01, *** p<0.001 (two-way ANOVA with Bonferroni post-test).

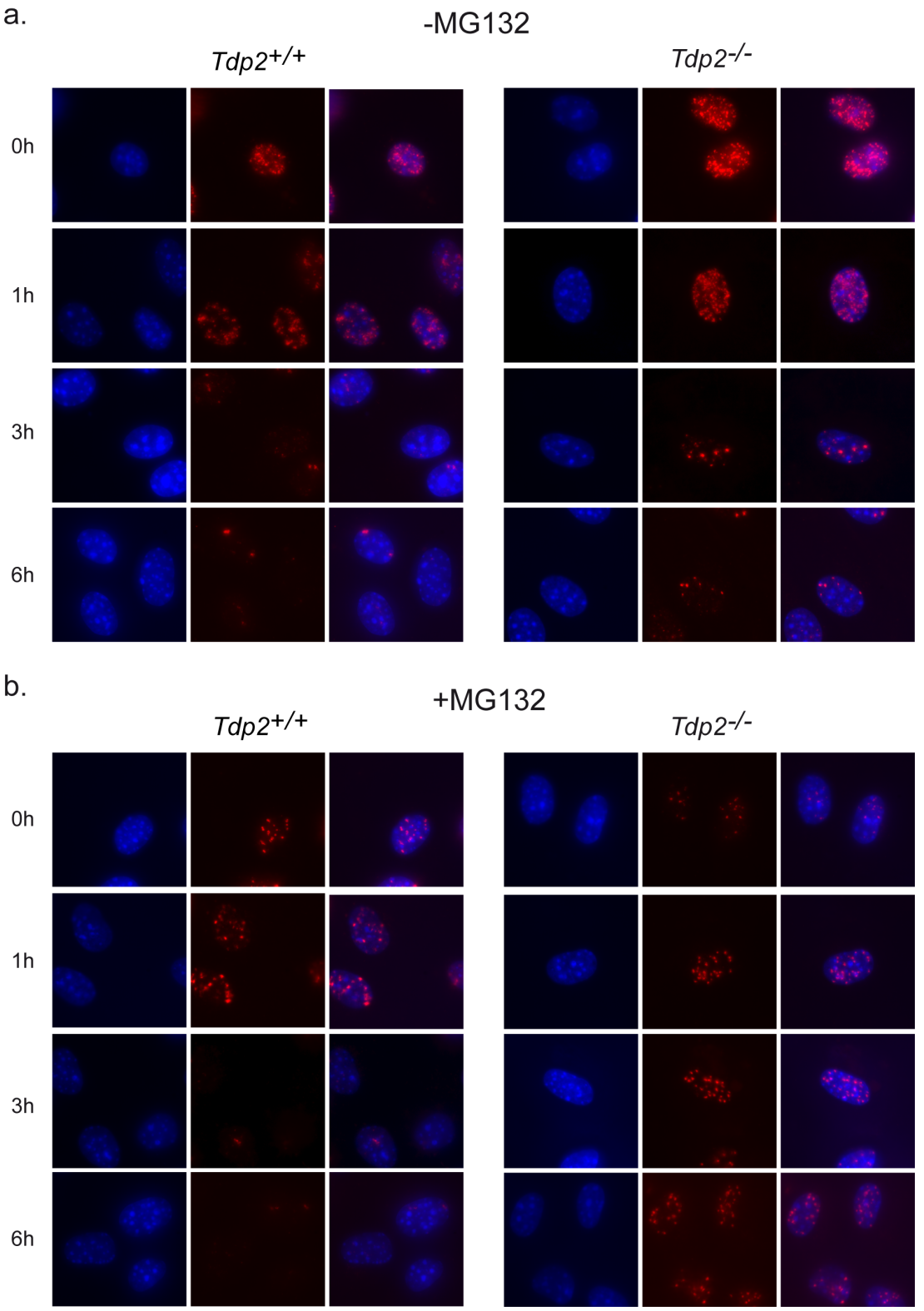

Figure 12. *Tdp2*$^{-/-}$ MEFs are unable to repair etoposide induced γH2AX foci when the proteasome is inhibited. a. Representative images of resolution of γH2AX foci in MEFs at the indicated time post- etoposide exposure. **b.** Same as "**a.**" except with MG132 treatment.

We then monitored the effect of TDP2 on the disappearance of cleavage complexes following etoposide removal with the ICE assay. Time points were taken at t = 0 (lysis after 1 hour of etoposide treatment), and 15 and 30 minutes post-etoposide removal. We monitored not only the disappearance of TOP2 signal, but also SUMO signal, which corresponded to sumoylated TOP2.

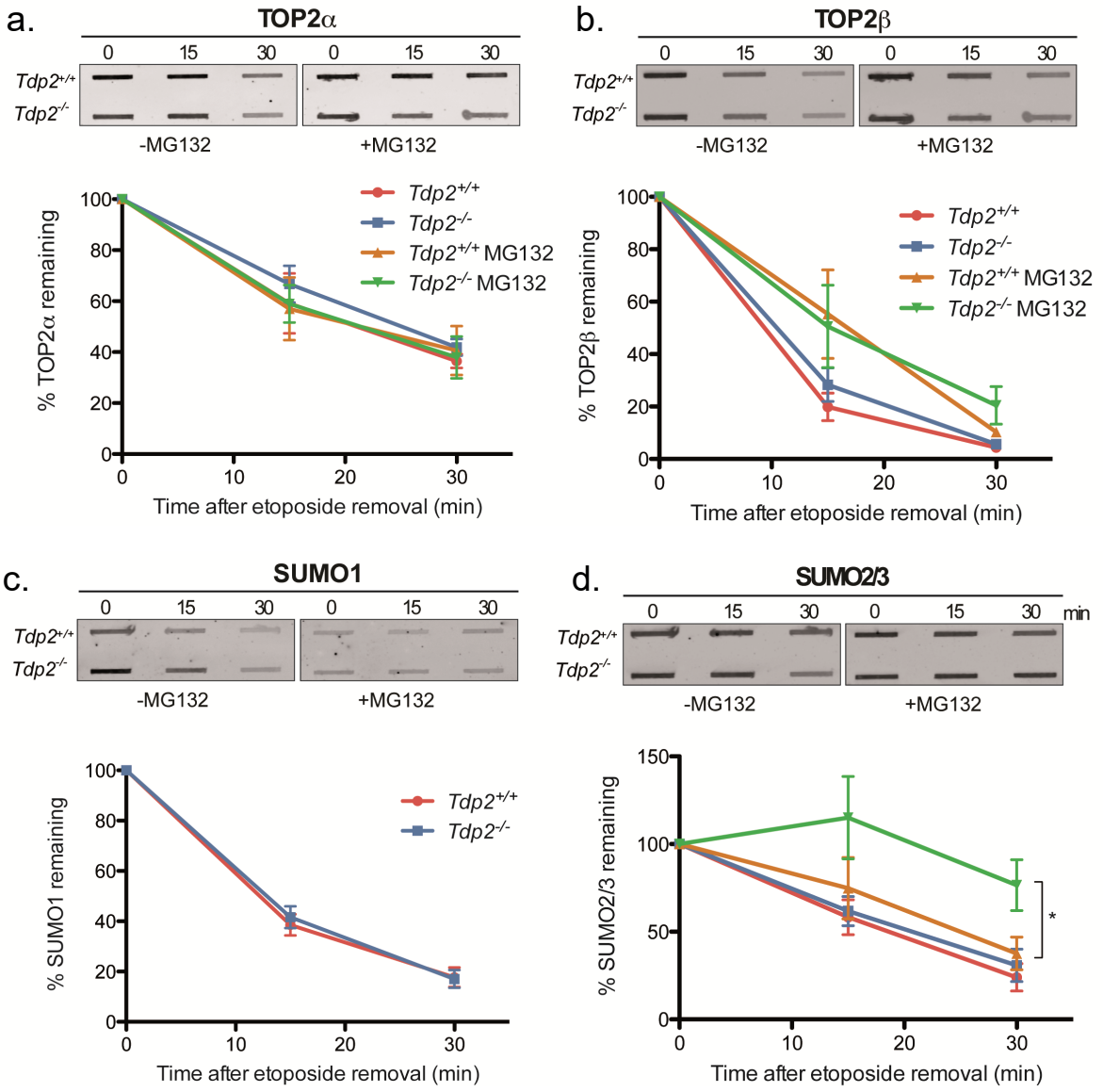

Figure 13. Disappearance of TOP2cc and SUMO in *Tdp2*$^{+/+}$ and *Tdp2*$^{-/-}$ MEFs. Representative image (top) and quantification (bottom) of **a.** TOP2α; **b.** TOP2β; **c.** SUMO1; or **d.** SUMO2/3 covalently bound to genomic DNA in MEFs following 1 h etoposide treatment and recovery for the indicated time at 37 °C in the presence or absence of 20 μM MG132. Average ± s.e.m.; n≥7; *p<0.05 (two-way ANOVA with Bonferroni post-test).

TOP2α signal disappeared at the same rate in both wild-type and *Tdp2*$^{-/-}$ cells, even when the proteasome was inhibited (Figure 13). TOP2β disappearance was also independent of *Tdp2* background, and the slower disappearance upon inhibition of the proteasome did not reach statistical significance. SUMO2 signal was lost at a slower rate in *Tdp2*$^{-/-}$ cells, but only when the proteasome was inhibited. This suggests a function of TDP2 in TOP2cc removal that is independent of the proteasome and facilitated by sumoylation. Interestingly, upon etoposide removal, SUMO1 signal, which is induced higher in *Tdp2*$^{-/-}$ cells, disappeared at the same rate regardless of background. A representative image of SUMO1 disappearance upon proteasome inhibition is included, but not quantified because of the lack of induction at t = 0. The lack of an effect in the disappearance of TOP2β is explained by a majority of non-modified cleavage complexes that retain the capacity to directly revert upon etoposide removal.

a.

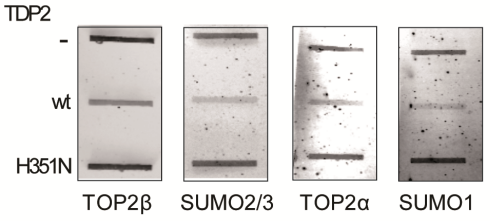

Figure 14. TDP2 removes TOP2 and SUMO from cleavage complexes *in vitro*. a. Representative image of covalently-linked TOP2α, TOP2β, SUMO1, and SUMO2/3 removal from DNA following treatment with 10 nM recombinant TDP2. **b.** Quantification of removal of both TOP2β and SUMO2/3 following treatment with indicated concentrations of TDP2. **c.** Same as "**b.**" except with TOP2β and SUMO2/3. Average ± s.e.m.; n≥3; p=0.0027 (F-test, exponential decay regression).

b.

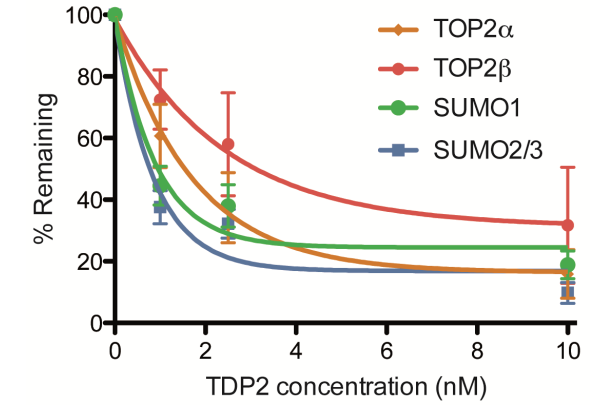

c.

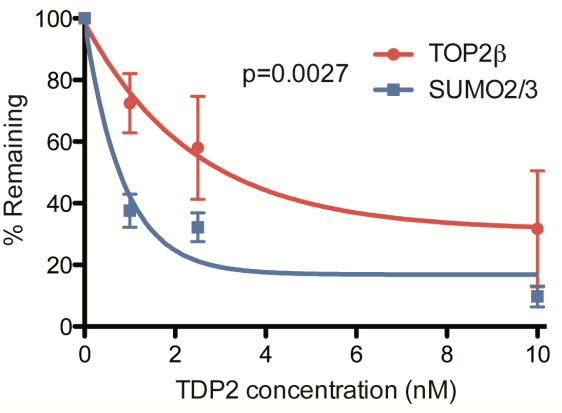

If TDP2 has an *in vivo* role in the removal of sumoylated covalent complexes, we surmised that we could design an *in vitro* approach to quantify and confirm this removal. To do so, we directly addressed TDP2 *in vitro* activity on material isolated by the ICE assay, specifically from etoposide treated wild-type primary MEFs. Incubation of the ICE material (DNA and covalently bound proteins) with purified wild-type TDP2 protein, but not with the TDP2-H135N catalytic mutant, lead to a loss in the amount of TOP2α, TOP2β, SUMO1, and SUMO2/3 that remains covalently linked to DNA (Figure 14). The lack of removal with the TDP2-H135N mutant indicated that it was dependent on TDP2 phosphodiesterase activity and ruled out the action of contaminant proteases or phosphodiesterases in the protein preparations. As mentioned above, specific removal of TOP2 and SUMO covalently bound to DNA dependent on TDP2 phosphodiesterase activity confirmed that both the SUMO1 and SUMO2/3 signals detected in the ICE assay correspond to sumoylated TOP2. The removal was dependent on TDP2 concentration, as adding more recombinant protein lead to a decreasing remaining signal. Interestingly, and consistent with the results observed in cells, TDP2 was more efficient in the removal of SUMO2/3 than of TOP2β, confirming that TDP2 can directly remove non-degraded TOP2 from cleavage complexes and that this can be facilitated by sumoylation by SUMO2.

These observations were unanticipated, as it has been presumed that TDP2 functionally engages only minimal TOP2 peptides resulting from proteasomal degradation, rather than full-length, post-translationally marked intact TOP2 molecules (Caldecott, 2012; Gao et al., 2014).

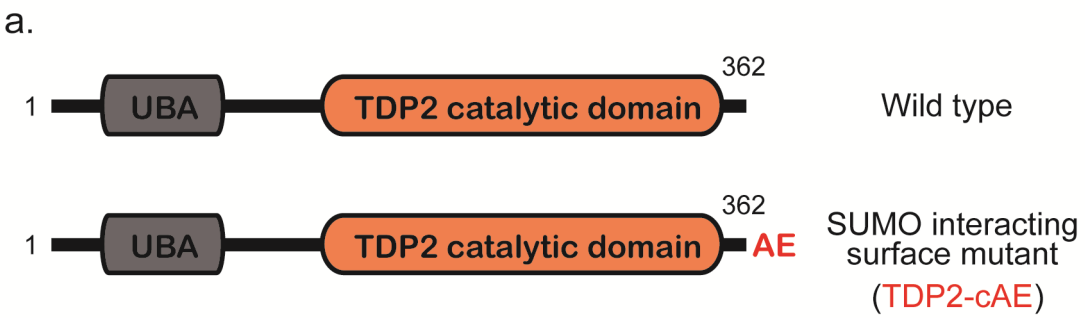

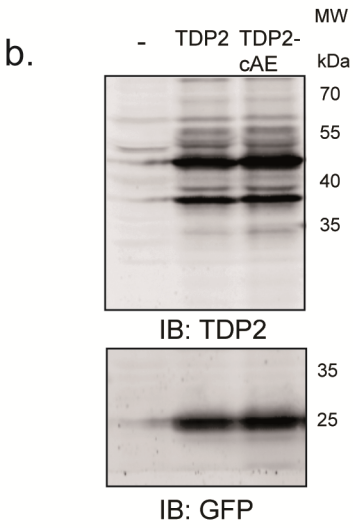

Figure 15. Schematic and expression of constructs used in experiments. a. Constructs with wild-type full-length TDP2 and TDP2-cAE, a SUMO-interacting mutant with a C-terminal AE extension were used. **b.** Immunoblotting of primary *Tdp2*$^{-/-}$ MEFs infected with lentivirus containing indicated constructs. Lane 1 is uninfected cells. GFP signal represents infection.

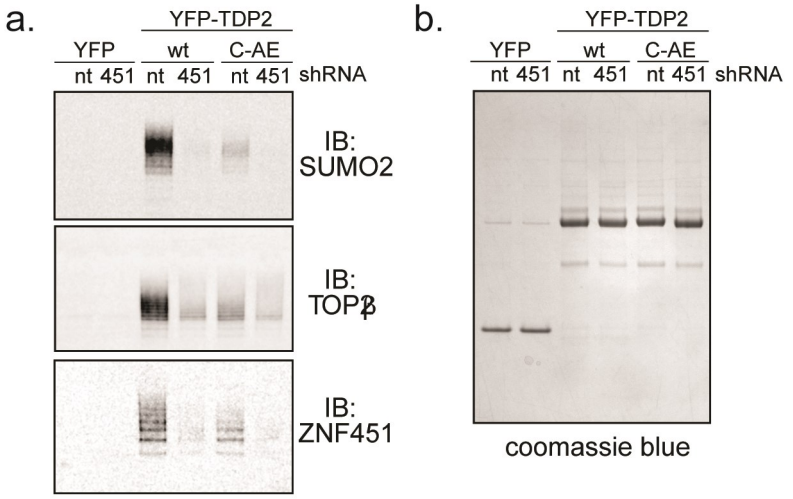

Figure 16. TDP2 binds sumoylated TOP2. a. Immunoblotting of anti-GFP immunoprecipitates from cells co-expressing YFP, YFP-TDP2 (wt), or YFP-TDP2-cAE (C-AE) and either non-targeting shRNA (nt) or shRNA against ZNF451 (451). **b.** Coomassie blue stain of "**a.**" Courtesy of Matt Schellenberg and R. Scott Williams (NIEHS/NIH).

5. SUMO interaction is not essential for sumoylated TOP2cc removal

In order to characterize the role of the Split-SIM, a mutant form of TDP2 that did not interact with SUMO and that was suitable for complementation assays was generated (Figure 15a, TDP2-cAE). By simply adding a C-terminal AE (alanine, glutamic acid) extension to the protein, a steric block was created and the C-terminal Leu370 could no longer form part of the split-SIM. TDP2-cAE was soluble and expressed in mammalian cells with expression levels similar to TDP2, as seen by Western blotting of *Tdp2*$^{-/-}$ primary MEFs (Figure 15b, lanes 2 and 3). Indeed, we observed that TDP2-cAE had a diminished interaction with SUMO2 as compared to TDP2 (Figure 16a, lanes 1, 3, and 5).

We first checked if TDP2 interaction with SUMO was important for the removal of TOP2cc. We performed the same *in vitro* activity assay as previously mentioned, but using recombinant TDP2 and TDP2-cAE. TDP2-cAE showed delayed kinetics in removing the sumoylated fraction of TOP2 from ICE purified TOP2cc, as detected by the slower disappearance of SUMO2/3 signal as compared to wild-type TDP2. TDP2-cAE had no effect on removal of bulk TOP2β (Figure 17), as analyzed with a nonlinear fit. The TDP2-cAE defect in SUMO removal was specific to SUMO2, as SUMO1 signal was removed at the same rate by TDP2-cAE as by TDP2. Similar to TOP2β, removal of TOP2α signal was also not affected with the TDP2-cAE mutant.

As a control, we checked TDP2-cAE activity on the removal of tyrosine from oligonucleotides in *in vitro* reactions, to make sure that the differences measured were not due to an overall difference in 5′tyrosyl DNA phosphodiesterase activity. Removal of a covalently bound tyrosine from a 20 nucleotide oligo was rep-

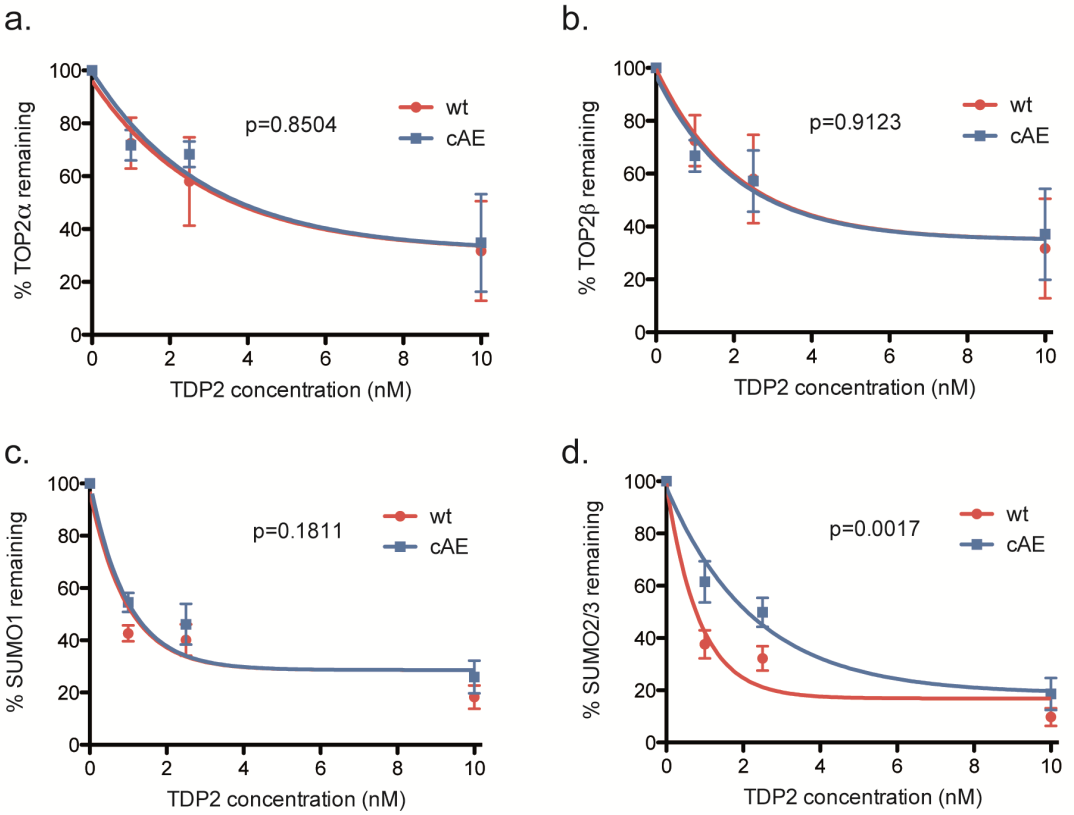

Figure 17. TDP2-cAE has diminished removal of SUMO modified TOP2. a. TOP2α, **b.** TOP2β, **c.** SUMO1 and **d.** SUMO2/3 covalently bound to genomic DNA following in vitro treatment with the indicated concentrations of recombinant wild-type (wt) or mutant TDP2 (TDP2-cAE). Average ± s.e.m.; n≥3; TOP2α p=0.850, TOP2β p=0.912, SUMO1 p=0.181, SUMO2/3 p=0.002 (F-test, exponential decay regression).

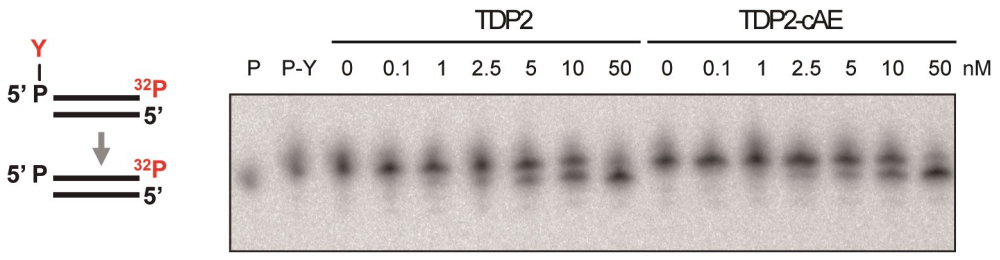

Figure 18. TDP2-cAE has similar 5'TDP activity as compared to TDP2. 5′–TDP activity following 1 h incubation of duplex oligonucleotide harboring a terminal 5′–phosphotyrosine moiety with the indicated TDP2. Reactions were run on a 20% TBE-urea gel.

resented by an increase in electrophoretic mobility on denaturing polyacrylamide gels. Comparing size markers (lanes 2 and 1), the higher molecular weight 5′Y (oligo with 5′-tryosine) migrates slower than lower molecular weight 5′P (oligo with 5′-phosphate) (Figure 18). TDP2-cAE had a similar activity on the oligonucleotides as wild-type TDP2 protein. This could be seen by partial conversion of 5′Y into 5′P with 10 nM protein (lanes 8 and 15) and almost complete conversion at 50 nM (lanes 9 and 16). This result indicated that the effect seen on removal of SUMO2 from ICE material was not due to an overall difference in activity of the proteins.

We then checked the cellular repair phenotypes of TDP2 losing its interaction with SUMO. We performed clonogenic survival assays in *Tdp2*$^{-/-}$ transformed MEFs infected with lentivirus overexpressing TDP2 or TDP2-cAE to see if TDP2-cAE mutant can complement the defect of *Tdp2*$^{-/-}$ MEFs in clonogenic survival following etoposide treatment, at least under conditions where TDP2 is overexpressed (Figure 19a). TDP2 expression lentiviruses were used to infect at a MOI 2.5, and etoposide treatment was performed continuously at the indicated concentrations. TDP2-cAE was able to fully complement the *Tdp2*$^{-/-}$ defect, to the same degree as complementation with wild-type TDP2.

We then performed γH2AX repair assays in *Tdp2*$^{-/-}$ primary MEFs infected with the lentiviruses mentioned above. Overexpression of TDP2 caused a significant decrease in the number of etoposide induced γH2AX foci as compared to the empty vector control (Figure 19b). For this reason, a decreased etoposide dose was used for cells infected with the empty vector, and in addition to raw values, repair of foci was represented normalized to the induction. TDP2 deletion itself displayed a repair defect (Figure 19c, d), and overexpression of TDP2 in *Tdp2*$^{-/-}$ cells was able to sup-

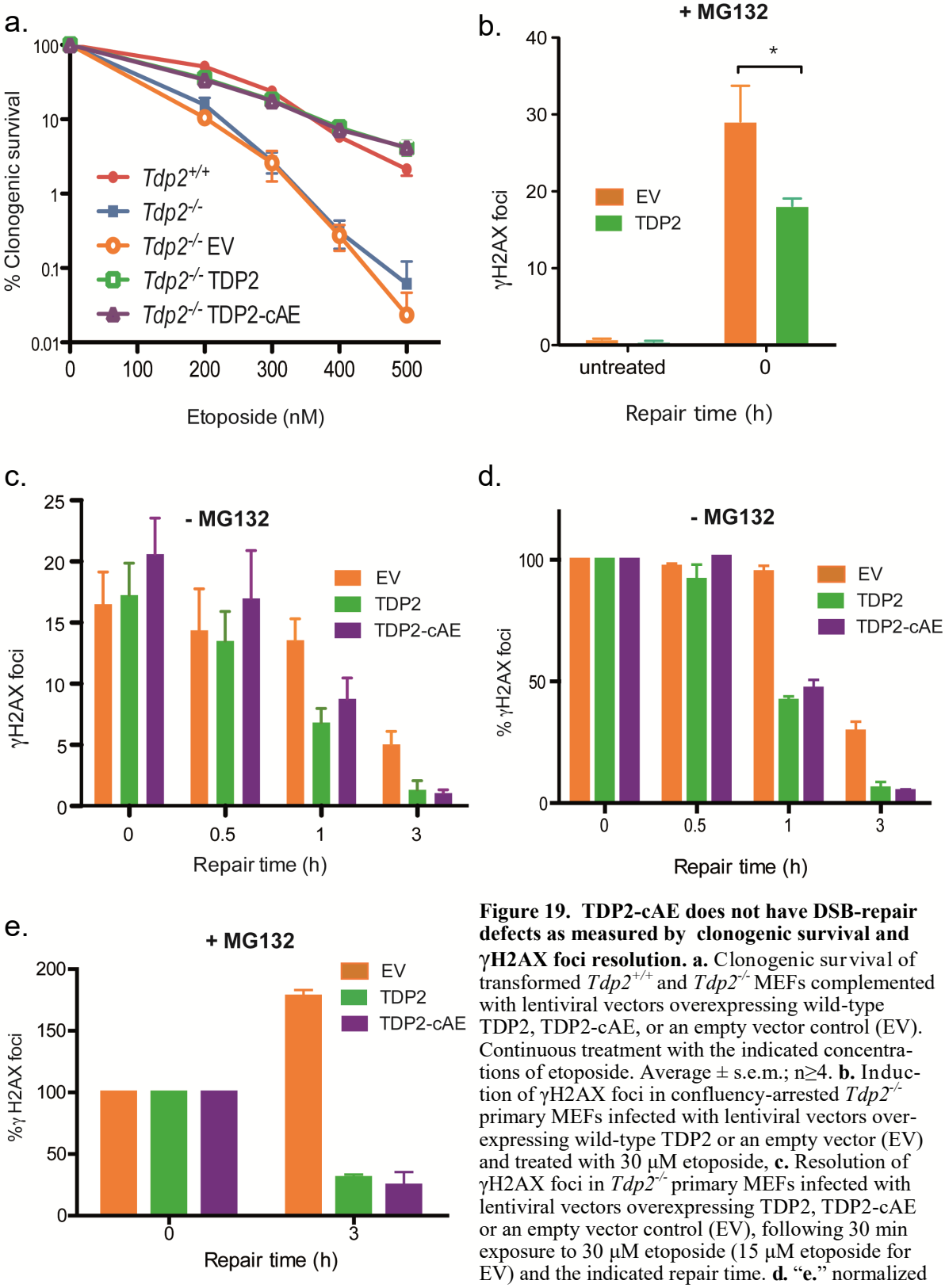

Figure 19. TDP2-cAE does not have DSB-repair defects as measured by clonogenic survival and γH2AX foci resolution. a. Clonogenic survival of transformed *Tdp2*$^{+/+}$ and *Tdp2*$^{-/-}$ MEFs complemented with lentiviral vectors overexpressing wild-type TDP2, TDP2-cAE, or an empty vector control (EV). Continuous treatment with the indicated concentrations of etoposide. Average ± s.e.m.; n≥4. **b.** Induction of γH2AX foci in confluency-arrested *Tdp2*$^{-/-}$ primary MEFs infected with lentiviral vectors overexpressing wild-type TDP2 or an empty vector (EV) and treated with 30 μM etoposide, **c.** Resolution of γH2AX foci in *Tdp2*$^{-/-}$ primary MEFs infected with lentiviral vectors overexpressing TDP2, TDP2-cAE or an empty vector control (EV), following 30 min exposure to 30 μM etoposide (15 μM etoposide for EV) and the indicated repair time. **d.** "**e.**" normalized to induction (t = 0). **e.** same as "**d.**" except 100 μM etoposide and 20 μM MG132. Average ± s.e.m.; n=3.

press the defect, as measured by a decrease in γH2AX foci at t = 1 and 3 hours as compared to the empty vector. TDP2-cAE was able to complement to the same degree as TDP2 and equally suppress the repair defect of *Tdp2*$^{-/-}$ MEFs. We then checked what would happen in conditions where the proteasome was inhibited with the only option for repair being a pathway depending exclusively on TDP2. After 1 hour of repair, both TDP2 and TDP2-cAE complement the *Tdp2*$^{-/-}$ cells allowing for repair to occur (Figure 19e).

7. Role of ZNF451 in cellular response to TOP2 damage

Additional factors of the cellular sumoylation machinery may be involved in regulating the TOP2-SUMO2-TDP2 interaction and TDP2–dependent TOP2cc repair. Performing the BioID screening has opened the door for further analysis of the interactions seen with TDP2. One potential candidate is ZNF451.

Because the BioID protocol identifies even transient proximity-based interactions, we first checked if the interaction detected between TDP2 with ZNF451 could be confirmed. We pulled down GFP-tagged TDP2 and successfully coimmunoprecipitated ZNF451 in HEK293T cells (Figure 29). In both the inputs and GFP-TDP2 elution, laddering was detected by the ZNF451 antibody, of which the upper bands could represent sumoylated forms. This laddering was also seen in MEFs and responds to shRNA ZFP451 knockdown, the mouse orthologs of ZNF451 (see Figure 31a).

We checked if ZNF451, like DNA repair proteins, localizes to chromatin upon DNA damage, and specifically TOP2 damage. Etoposide treatment in RPE-1 cells triggered an enrichment of ZNF451 in the chromatin cellular fraction that is visible upon proteasome inhibition (Figure 30). Proteasome inhibited etoposide treated cells accumulated both unmodified and higher molecular weight forms of ZNF451 in the chromatin fraction, likely corresponding to SUMO modified forms. Samples were normalized relative to the signal of the untreated sample without MG132. ZNF451 mobilization to chromatin was specific to TOP2 damage, and not observed following ionizing radiation induced DSBs (Figure 30b).

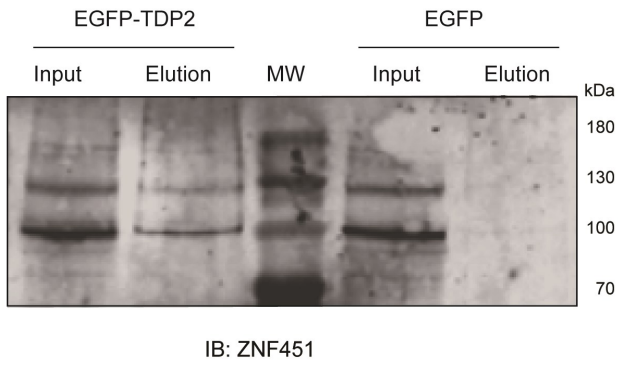

Figure 29. TDP2 interacts with ZNF451. Immunoprecipitation of GFP-tagged human TDP2 and GFP with GFP-Trap. Immunoblotting against ZNF451. MW- molecular weight marker.

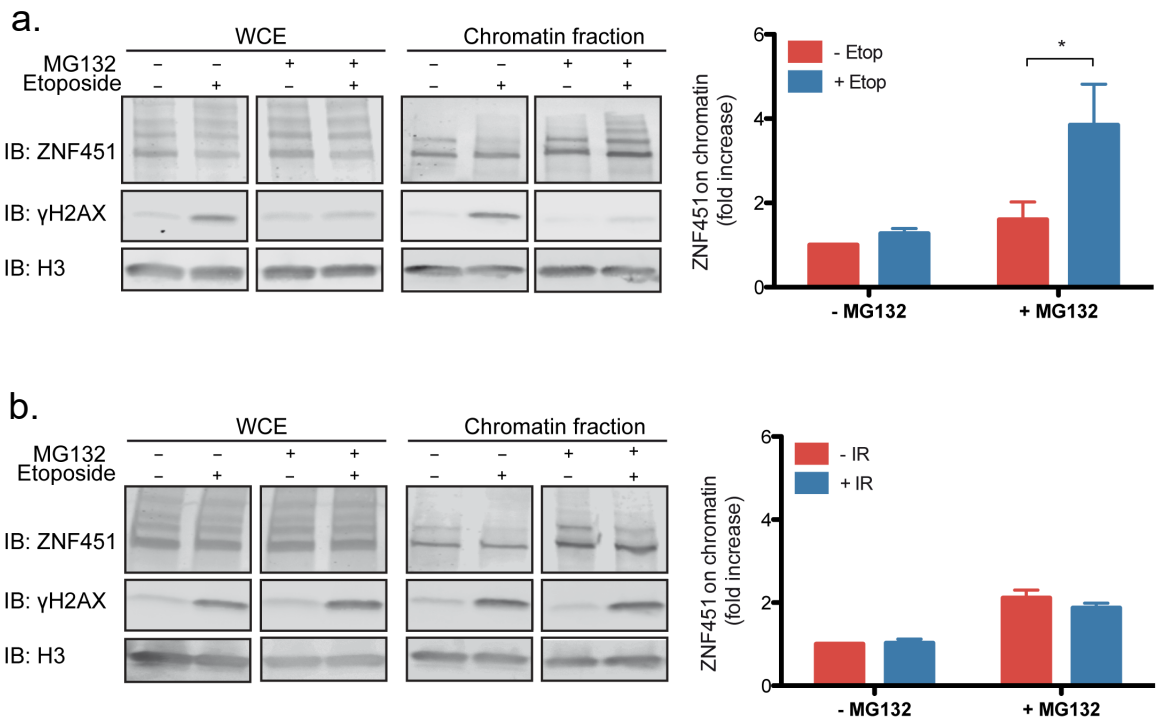

Figure 30. ZNF451 is recruited to chromatin upon TOP2 damage and proteasome inhibition. a. Representative image of immunoblots (left panel) against ZNF451 in whole-cell extracts (WCE) or chromatin fraction of RPE-1 cells upon treatment with and without etoposide and/or MG132. Quantification (right panel) of ZNF451 levels normalized to the corresponding H3 signal and expressed as fold increase compared to the untreated sample. Average ± s.e.m.; n=3; *p<0.05 (two-way ANOVA with Bonferroni post-test). **b.** Same as "**a.**", except cells were treated with or without 10 Gy ionizing irradiation (IR) in the presence or absence of MG132. Average ± s.e.m.; n=3.

We then checked the effect of ZNF451 on clonogenic survival following continuous etoposide treatment in wild-type cells (Figure 31). As mentioned above, ZFP451 knockdown was checked with Western blot, with tubulin as a loading control (Figure 31a). ZFP451 knockdown did, in fact, decrease cell survival following etoposide treatment in wild-type cells (Figure 31b). The shRNA used (ZFP451#2) was checked for off target effects by repetition of the clonogenic survival assay with a different shRNA (ZFP451 #1). The defect seen in wild-type cells upon ZFP451 knockdown was reproduced when shRNA ZFP451#1 was used. We then checked the effect of ZNF451 in *Tdp2*$^{-/-}$ cells, and observed that not only did *Tdp2*$^{-/-}$ itself have a strong defect, but upon ZNF451 knockdown, the clonogenic survival defect was exacerbated (Figure 31c). Clonogenic survival of both *Tdp2*$^{+/+}$ and *Tdp2*$^{-/-}$ cells is represented in Figure 31d.

Next, we explored the role of ZFP451 in DSB repair, scored by γH2AX foci resolution. ZFP451 depletion alone in MEFs did not confer a significant defect in γH2AX foci resolution in wild-type cells (Figure 32a). However, in cells with TDP2 deletion (*Tdp2*$^{-/-}$), ZFP451 knockdown caused a significant repair defect. Also, ZFP451 depletion caused a delay in the repair kinetics when combined with the proteasome inhibitor MG132 in wild-type cells (Figure 32b). However, *Tdp2* deletion is epistatic over ZFP451 knockdown when combined with proteasome inhibition, conditions where we already had no repair, suggesting that one function of ZFP451 is to modulate TDP2 dependent TOP2cc repair. Both TDP2 and ZNF451 have a role in DSB repair specific to TOP2 damage, as neither TDP2 knockout nor ZNF451 knockdown had an effect on the resolution of ionizing radiation (IR) induced γH2AX foci (Figure 32 c, d).

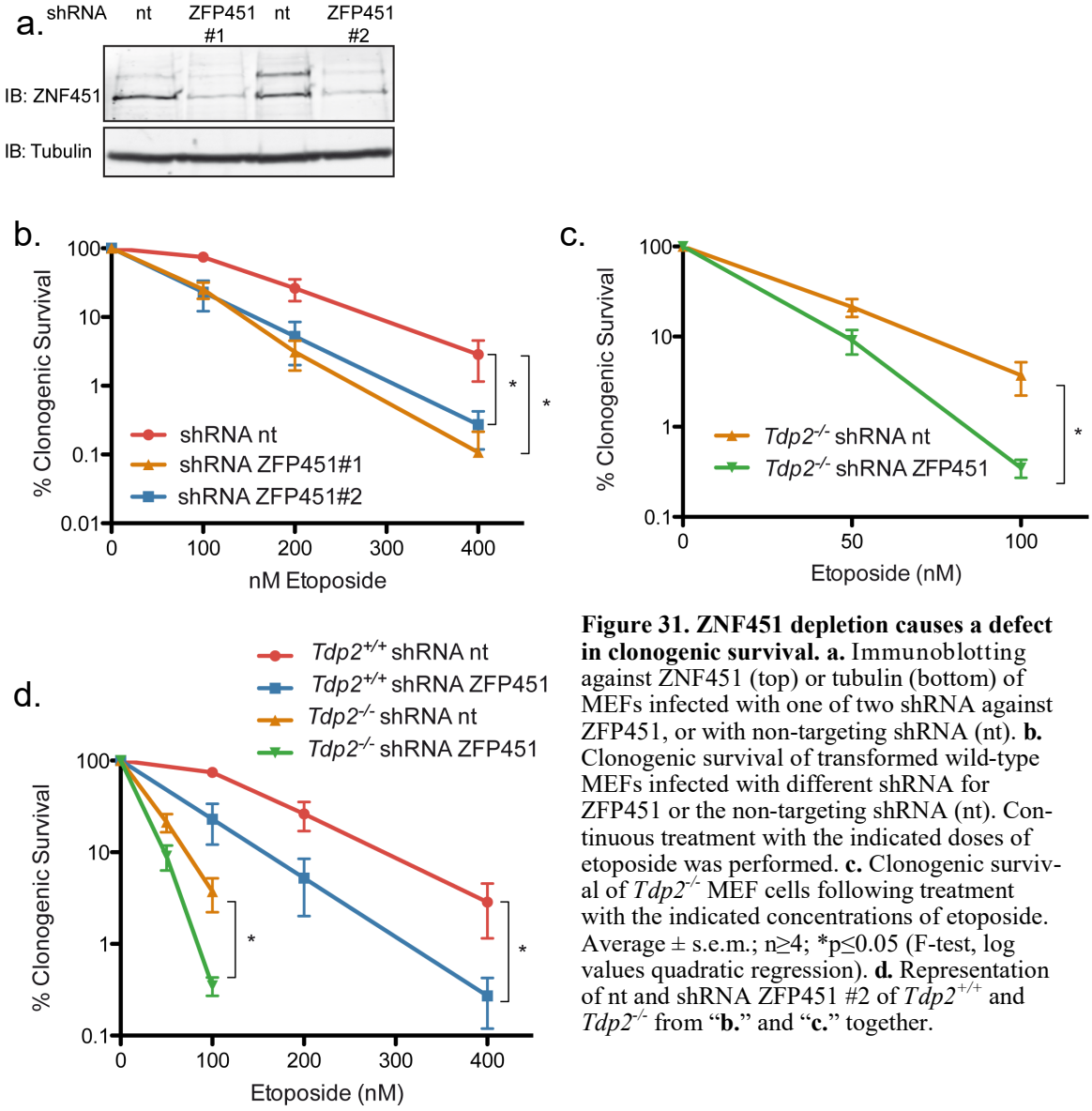

Figure 31. ZNF451 depletion causes a defect in clonogenic survival. a. Immunoblotting against ZNF451 (top) or tubulin (bottom) of MEFs infected with one of two shRNA against ZFP451, or with non-targeting shRNA (nt). **b.** Clonogenic survival of transformed wild-type MEFs infected with different shRNA for ZFP451 or the non-targeting shRNA (nt). Continuous treatment with the indicated doses of etoposide was performed. **c.** Clonogenic survival of *Tdp2*$^{-/-}$ MEF cells following treatment with the indicated concentrations of etoposide. Average ± s.e.m.; n≥4; *p≤0.05 (F-test, log values quadratic regression). **d.** Representation of nt and shRNA ZFP451 #2 of *Tdp2*$^{+/+}$ and *Tdp2*$^{-/-}$ from "**b.**" and "**c.**" together.

Overall, these results identify ZNF451 as a novel component in the cellular response to TOP2-induced damage that operates through both proteasome-dependent and -independent TOP2cc metabolism, with the latter being dependent on TDP2.

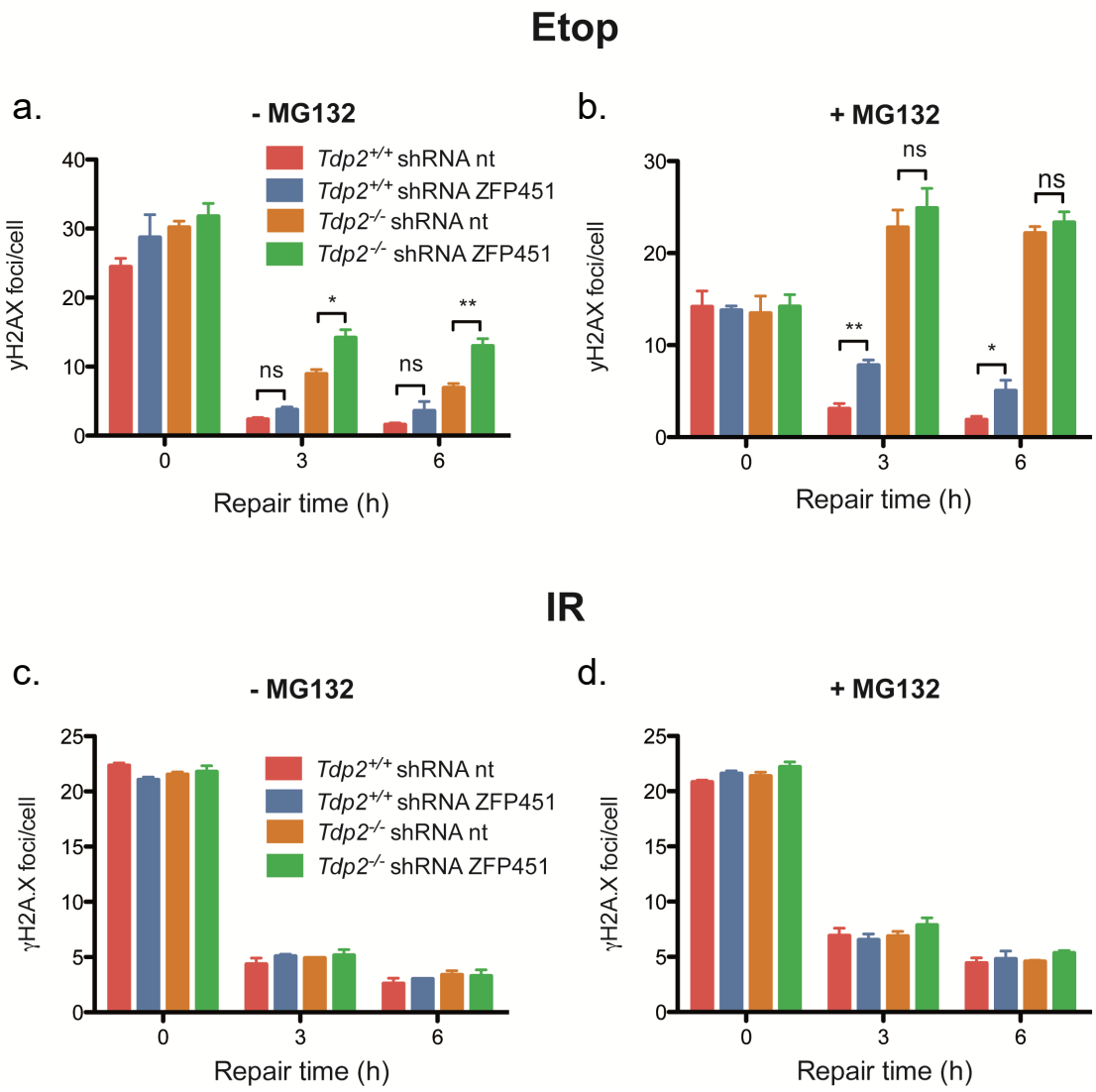

Figure 32. ZNF451 depletion causes a defect in the repair of γH2AX foci induced by etoposide. **a.** Resolution of DSBs marked by γH2AX foci in MEF cells post-etoposide exposure at the indicated repair time in the absence or **b.** presence of MG132. Average ±s.e.m.; n=3; ns $p \geq 0.05$, *$p < 0.05$, ** $p < 0.01$ (two-way ANOVA with Bonferroni post-test). **c., d.** Same as "**a.**" and "**b.**" respectively, except with ionizing radiaton (IR) treatment.

IV. DISCUSSION

IV. DISCUSSION

TOP2 is necessary for normal cellular processes, such as DNA replication, transcription, and cell division, but it can pose a threat to genome integrity, as the intermediate of its catalytic cycle, the enzyme covalently linked to 5'-phosphoryl end of a four-base staggered DSB, can interfere with cellular processes and needs to be removed in order to allow repair. Therefore, a thorough understanding of how TOP2cc are removed is imperative for advancing our understanding of processes and functions of TOP2, and furthering possible therapeutic avenues. The identification of TDP2 as the enzyme that specifically removes TOP2 from DNA by cleaving the 5'-phosphotyrosyl bond was an important advance in the DNA repair field (Cortes-Ledesma et al., 2009). TOP2cc in suicidal substrates had to undergo either proteolytic processing or denaturation to allow removal by TDP2 (Gao et al., 2014). However, whether or not TDP2 would be able to remove full-length TOP2 *in vivo* has remained unknown, and if so, how it would able to access the phosphotyrosyl bond between the topoisomerase and the DNA.

There have been numerous advances in the field of DNA topoisomerases since the discovery of *E. coli* TOP1 by James C. Wang, starting with biochemical studies aiming to elucidate the role in managing DNA topology. The discovery that topoisomerases are the targets of medications such as etoposide has been important not only in the laboratory, but also for applications such as antimicrobials and cancer chemotherapies. Also, the publication of topoisomerase crystal structures has aided in understanding of the mechanism. In addition, the resolution of several TDP2 crystal structures, such as full-length *C. elegans*, the catalytic portion of human TDP2, and the catalytic portion of mouse TDP2-DNA complexes, has provided

detailed information on TDP2 catalytic activity (Shi et al., 2012; Hornyak et al., 2016; Schellenberg et al., 2012). Structural and biochemical work by the Williams laboratory provided insight on structural mechanisms of the TDP2 active site (Schellenberg et al., 2016).

To shed light on the pathways involved in TDP2-mediate removal of TOP2cc and its possible regulation, this work has addressed the roles of both sumoylation and the novel SUMO E3 ligase ZNF451. A BioID screening opened the door for the identification of novel TDP2 interactors that may be involved in this process, or indicate additional roles of TDP2.

1. SUMO-modified TOP2cc

Upon etoposide treatment, both TOP2αcc and TOP2βcc accumulate in wild-type and *Tdp2*$^{-/-}$ MEFs. TOP2α signal being detected to a lesser degree than TOP2β is consistent with the prominent role of the TOP2β isoform in non-proliferating cells. Interestingly, etoposide induced TOP2cc are modified by both SUMO1 and SUMO2/3.

We have several indications that the SUMO2/3 signal corresponds primarily to modified TOP2β. Western blotting of micrococcal nuclease digested etoposide treated TOP2ccs indicates a high molecular weight smear of TOP2β signal of similar size to the SUMO2/3 smear, while TOP2α is only present as a non-modified band. Additional work done in the Cortés-Ledesma laboratory, such as pulling down SUMO2 and detecting TOP2β, indicates that this isoform is preferentially SUMO2/3 modified over TOP2α (Schellenberg & Lieberman et al., Science pending publication).

SUMO2/3 modification of TOP2cc was induced in a similar manner in both wild-type and TDP2-defficient cells. However, SUMO1 was induced more-so in etoposide treated *Tdp2*$^{-/-}$ cells than in wild-type cells. One possibility is that TDP2 is responsible for the removal of SUMO1 modified full-length TOP2cc. If that were the case, we would expect the disappearance of SUMO1 signal to be slower in TDP2 deficient cells upon etoposide removal as compared to wild-type cells. This is not the case, as the disappearance of SUMO1 signal is no different in wild-type and *Tdp2*$^{-/-}$ cells. Also, while we have observed that TDP2 is responsible for the preferential removal of SUMO2/3 modified TOP2cc, we do not see an accumulation of SUMO2/3-TOP2cc in *Tdp2*$^{-/-}$ cells, so it is reasonable that an alternative mechanism is at play.

One attractive scenario is that SUMO1 modification still remains on the peptide resulting from proteasomal degradation of TOP2cc. That would explain why there is an accumulation of SUMO1 signal in the absence of TDP2, which would be important for the removal of this residual peptide. An increase in proteasome degraded TOP2-DNA adducts in *Tdp2*$^{-/-}$ cells would likely not be able to be measured by neither the TOP2α nor TOPβ antibodies, which are specific to the C-terminus. The exact identity of the proteasomal product is unknown, although it undoubtedly contains the catalytic tyrosine (for example, Tyr805 in *H. sapiens* TOP2α, Try825 in TOP2β).

It would be interesting to uncover the identity of the degraded peptide adduct, whether it be a peptide with a specific sequence or a heterogeneous population of proteasomal degraded products. When Western blotting micrococcal nuclease digested etoposide-induced TOP2cc, the only detectable SUMO1 signal corresponds

to high molecular weight TOP2, which would be consistent with it being conjugated to full-length or minimally degraded forms. If there is, in fact, a SUMO1 modified lower molecular weight degraded TOP2 peptide that we are not detecting, it could be that the peptide is heterogeneous in size and/or lowly abundant, below detection levels. If that were the case, once again we could expect to see a delayed kinetic in the disappearance of SUMO1 signal in the absence of TDP2, which we do not see. Another explanation is that SUMO1 signal corresponds to modification of full-length TOP2cc and for some reason, in the absence of TDP2, there is either increased modification or accumulation of modified forms. In the future, it would be interesting to compare the SUMO1 signal in wild-type cells with *Tdp2*$^{-/-}$ cells by Western blot to see if there are additional lower molecular weight SUMO1 conjugates in *Tdp2*$^{-/-}$ cells, although with Western blot the level of detection may not be sufficient to discern a difference.

We do observe disappearance of SUMO1 signal upon inhibition of the proteasome with MG132 in both genotypes. This is most likely due to depletion of the cellular pool of SUMO1, which has been observed to deplete upon MG132 treatment (Bailey & O'Hare, 2005). An alternative possibility is that, in line with the discussion above, is that SUMO1 modification occurs on the peptide after proteasomal degradation. As such, upon inhibiting the proteasome, that signal would disappear. However, this is again not consistent with the results observed in the Western blots.

The dynamics of SUMO2/3 disappearance in proteasome inhibited *Tdp2*$^{-/-}$ MEFs were the first indication of the role of TOP2cc sumoylation in promoting proteasome-independent TDP2 catalyzed TOP2cc removal. While SUMO2/3 signal disappears more slowly in the absence of TDP2, TOP2 does not. There are several

plausible explanations for this. We are working with a pools of cells in which not all TOP2cc are SUMO modified. This is also explained by the reversion of reversible covalent complexes once the etoposide is removed, which could present a majority of TOP2cc. To clarify, when etoposide is removed from TOP2, the enzyme can re-seal the broken DNA within the cleavage complex, a phenomenon termed "reversal" (Tewey et al., 1994).

However, even when the proteasome is inhibited, there is still not a significant increase in the accumulation of neither etoposide induced TOP2αcc nor TOP2βcc, even in TDP2-deficient background. This is consistent with the observations of *Austin and colleagues*, who reported that proteasome inhibition in K562 cell line, human chronic myelogeneous leukemia, did not affect etoposide induced accumulation of TOP2cc (Lee et al., 2016). They used the same dose of etoposide as our experiments, although with two hour treatments, and measured TOP2cc with the cell-based TARDIS microscopy assay. However, with their conditions, they observed that MG132 treatment reduces the rate of removal of etoposide stabilized TOP2cc from DNA. We do indeed see a slower rate of removal of TOP2βcc when the proteasome is inhibited in both wild-type and *Tdp2*$^{-/-}$ cells, although this difference does not arrive to statistical significance when comparing to conditions without MG132.

Given the novel role of TDP2 in removing TOP2cc independent from the proteasome, one could reason that in *Tdp2*$^{-/-}$ cells, we could expect a greater accumulation, or at least a slower disappearance of these structures. There are several plausible explanations for the lack of such an observation. The high dose and long exposure of etoposide could be saturating the number of TOP2cc, preventing the

measurement of an increase in TDP2-deficient cells. Also, if only a small portion of TOP2cc are sumoylated, and this seems to be the case since in Western blots most TOP2 migrates with its expected size, and those could be preferentially targeted by TDP2, we would not see a measurable difference in TOP2cc removal when TDP2 is not present because the majority are not sumoylated.

It would be interesting in the future to address whether or not sumoylation itself could affect reversibility of TOP2cc. If SUMO2/3 modified TOP2cc are less likely to revert upon etoposide removal, then they would be more dependent on the pathways that remove trapped TOP2, such as that involving TDP2, especially when the proteasome is inhibited, which is in line with our observations.

2. TDP2 interaction with SUMO

The current understanding of what constitutes a SIM will be updated upon the identification of a nonconventional novel SUMO-interacting surface by our collaborators in the R. Scott Williams laboratory. Instead of four or five consecutive amino acids, the TDP2 split-SIM is comprised of SUMO binding loops. The SIM-SUMO interface is relatively large, giving TDP2 strong SUMO2 binding.

While the ^{280}IVDV^{283} sequence of human TDP2 is not contained within the newly identified split-SIM, phenotypes of mutating this putative SIM identified by *Hecker et al.* (2006) have been reported. For example, nucleolar localization of TDP2 was described as requiring binding to PML-NBs through the ^{280}IVDV^{283} SIM (Vilotti et al., 2011). Silencing TDP2 expression during proteasome impairment causes alterations in rRNA biogenesis, namely a decrease in pre-rRNA and an accu-

mulation of processing intermediates. The TDP2 SIM motif, but not TDP2 catalytic activity, has an important for role in ribosome biogenesis.

TDP2 ^{280}IVDV^{283} is likely not a bona fide SIM, although when mutated, it abolishes SUMO interactions. One possibility is that the mutation of ^{280}IVDV^{283} to alanines could alter the conformation of the protein and affect the interactions with at least SUMO. Notably, we were unable to express TDP2-SIM, our version of ^{280}AAAA^{283}, in human cells.

Another possibility is that ^{280}IVDV^{283} acts as an additional SIM. However, this was not observed by crystallization of TDP2 interacting with SUMO2. It would be interesting to take another look at the phenotypes of ^{280}AAAA^{283}, such as ribosome biogenesis, to see if they are recapitulated with split-SIM mutant TDP2-cAE. If they are not, it could be possible that role of TDP2 in ribosome biogenesis is related to interaction with protein(s) other than SUMO, that were abolished upon mutating ^{280}IVDV^{283}.

3. TDP2 removal of TOP2cc mediated by ZNF451

One of the most impacting results of this thesis is the discovery of a role of TDP2 in a novel proteasome-independent pathway for the removal of TOP2cc. There are several convincing evidences for the existence of such a pathway. First is the inability of alternative pathways to repair etoposide-induced DSBs upon proteasome inhibition in *Tdp2*$^{-/-}$ cells. This indicates that TDP2 is uniquely important to remove undegraded TOP2. Perhaps in this proteasome-independent pathway, DNA repair factors such as KU are unable to bind the break region of the DNA due to steric interference with TOP2 until this is removed by TDP2. This would not occur when TOP2 is degraded by the proteasome.

Second, the interaction of TDP2 with SUMO-TOP2 is completely dependent on its phosphodiesterase activity, suggesting that it arises as a result of TDP2 action on sumoylated cleavage complexes. Third, as mentioned above, in *Tdp2*$^{-/-}$ cells SUMO2/3 signal disappears slower. Finally, TDP2 has an *in vitro* activity on TOP2cc, showing a preference for SUMO-modified TOP2cc. Denaturing of covalent complexes on DNA has been reported to be sufficient to allow hydrolysis by TDP2, and the cleavage complexes on DNA isolated in the ICE protocol were denaturated by the initial cellular lysis with *N*-Lauroylsarcosine sodium salt (sarkosyl).

While TDP2 removes TOP2cc *in vitro*, a mechanism that would allow TDP2 to access the phosphotyrosyl bond of full-length TOP2 in cleavage complexes *in vivo* has not been previously reported. In the pending manuscript, the Scott Williams laboratory detected very little TDP2 activity on non-denatured reconstituted TOP2cc *in vitro* (Schellenberg & Lieberman et al., Science accepted). However, we do see a role *in vivo*, suggesting mechanisms that make covalent complexes accessible for TDP2. There are several evidences that the novel E3 SUMO2 ligase ZNF451 might regulate proteasome-independent mechanisms for TOP2 removal, which are addressed in this thesis and pending manuscript. First, we observed that TDP2 and ZNF451 interact and ZNF451 is mobilized to chromatin upon TOP2 damage. It was then observed that TDP2 has novel split-SIM that interacts strongly with SUMO2, and both TDP2 and ZNF451 are bound to sumoylated TOP2. It was observed that recombinant ZNF451 forms a stable complex with purified TOP2α and TOP2β, by analytical gel filtration chromatography in the accepted manuscript (Schellenberg & Lieberman et al., Science pending publication). Additionally, upon addition of

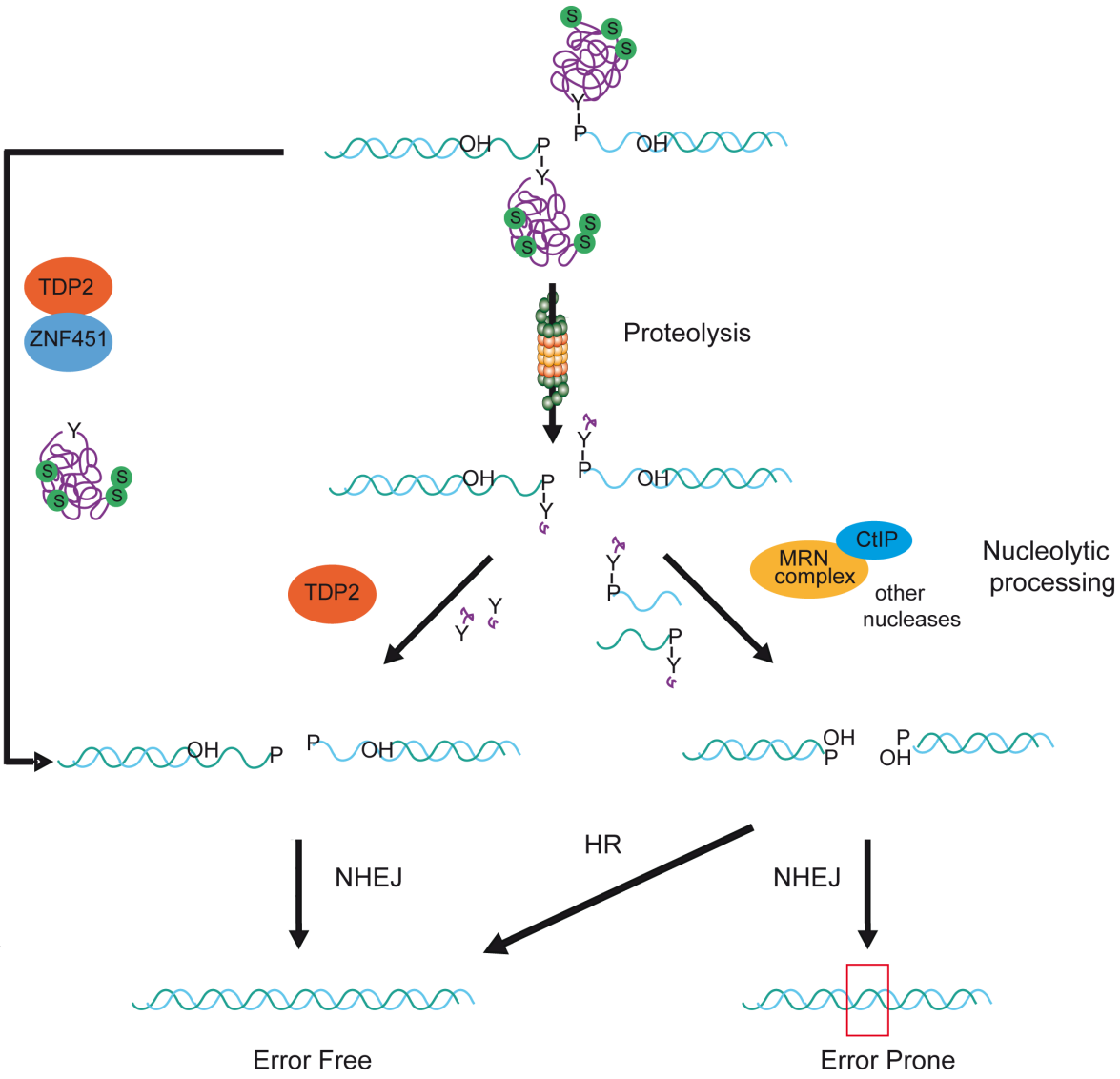

Figure D1. Proposed Model for resolution of abortive TOP2cc. For simplicity, only G-segment is shown. Proposed model for TDP2 removal of abortive TOP2cc (purple) comprised of full-length TOP2. TOP2 covalently linked to 5' termini by phosphotyrosyl bond between tyrosine in the protein and phosphate of DNA is SUMO modified (green) and is either partially degraded by the proteasome leaving a peptide of unknown size, or is removed in a proteasome independent pathway which involves TDP2 and ZNF451 acting on full-length TOP2 and can be modulated by the sumoylation of TOP2. Nucleolytic pathways are not shown for simplicity. P- phosphate, Y- tyrosine, OH- hydroxide, S-SUMO2/3.

ZNF451, TDP2 had dramatically increased activity on non-denatured reconstituted TOP2βcc. To get insights into the mechanism by which ZNF451 is able to remodel TOP2cc to allow TDP2 access to the buried phosphotyrosyl bond, trypsin digest sensitivity of TOP2cc in the presence and absence of ZNF451 was measured. The data suggests that ZNF451 induces a conformational change in both TOP2αcc and TOPβcc.

Not surprisingly, ZNF451 was observed to regulate TOP2 sumoylation. When the effect of sumoylation on TDP2-catalyzed TOP2cc resolution was examined, it was found that sumoylation promoted only a minimal increase in TOP2cc hydrolysis by TDP2 over and above the ZNF451–TDP2 catalyzed reaction. Sumoylation of TOP2cc is therefore more likely aiding with the recruitment of TDP2 rather than directly affecting its 5'-phosphodiesterase activity.

Therefore, we propose a model for TDP2 mediated removal of TOP2cc (Figure D1). In our model, in addition to removal of proteasome degraded TOP2 adduct by TDP2 (or nucleases), there is an additional proteasome-independent pathway, which is entirely dependent on TDP2. ZNF451 mediated remodeling and sumoylation of TOP2cc would facilitate the recruitment of TDP2 and its access to the otherwise hidden phosphotyrosine bond.

The action of ZNF451 is likely regulated, as to not interfere with active TOP2 during the normal catalytic cycle, and mechanisms for its regulation have not yet been uncovered. Also, there is a possibility that ZNF451 action could affect reversibility of TOP2cc. Once bound to TOP2cc, poised for TDP2 cleavage, TOP2 is likely rendered unable to revert. Contrarily, ZNF451 could be targeting those TOP2cc that are already unable to revert. Moreover, the existence of this new pro-

teasome-independent pathway opens the door to the study of possible regulatory methods for pathway choice, that is, which TOP2cc are degraded by proteasome and which are removed by the novel pathway, whether the signal be sumoylation or not.

While ZNF451 has been identified as an E3 SUMO ligase responsible for SUMO2/3 conjugation of TOP2 in the context of the covalent complex, the E3 enzyme responsible for SUMO1 conjugation has not been addressed in this study. RANBP2 has been implicated in SUMO1 modification of TOP2α and could be a possible candidate. Very recently, work by *Sun and Nitiss* implied a role for sumoylation of TOP2cc in yeast by the Siz1 SUMO ligase (Sun & Nitiss, 2017). It would be interesting to test whether or not the homologous members of the PIAS family play a similar role in human cells.

5. TDP2, TOP2, and human diseases

The discovery of a TDP2-dependent pathway for the removal of full-length TOP2cc offers an additional therapeutic target route for potential TDP2 inhibitors. There is significant variation of TDP2 expression among cancer patients, limiting the success of TOP2 poisons as a treatment (Kont et al., 2016). This opens the door for individualized treatment of the patients with high TDP2 levels with TDP2 inhibitors in conjunction with TOP2 inhibitors. Additionally, *Schellenberg and col-*

leagues (2016) identified a TDP2 active site single nucleotide polymorphism (SNP) D350N that impairs TDP activity. TDP2 status could serve as a biomarker for personalized medicine.

Clinical use of TDP2 as a pharmacological target also stems from TDP2 knockout cells being highly sensitive to TOP2 poisons (Cortes-Ledesma et al., 2009). Additionally, as TDP2 serves as a backup form of repair in absence of TDP1 upon treatment with TOP1 inhibitors such as camptothecin, it might be useful for the treatment of certain lung cancers which are deficient for TDP1 (Gao et al., 2014). The combined use of TDP2 and TOP2 inhibitors could also be applied to patients with ATM or HR deficiencies, which occur frequently in cancers (Choi et al., 2016). TDP2 inhibitors may also further the study of the role of TDP2 in viral replication/integration and offer the possibility of generating novel antiviral compounds targeting it. A high throughput screening identified Toxoflavins and Dezaflavins as the first selective small molecule inhibitors of TDP2, but are of little pharmaceutical value due to poor *in vitro* pharmacokinetics profiles and low cell permeability, respectively (Raoof et al., 2013).

Major challenges of treatment with TOP2 poisons include toxicity, resistance, and secondary malignancies. A main goal of TOP2 cancer treatments is therefore maximization of clinical efficacy while minimizing toxicity and secondary malignancies (Nitiss, 2009a). TOP2 poisons generally have limited tumor selectivity and toxicity rooted in the need of TOP2 in normal cells, not only cancer cells. Part of the sensitivity to TOP2 targeting drugs depends on TOP2 protein levels. Most TOP2 targeting drugs kill cells by generating TOP2-mediated DNA damage. Cellular resistance to TOP2 poisons is generally related to decreased levels of TOP2 ex-

pression, and therefore generation of less TOP2-mediated DNA damage (Walker & Nitiss, 2002). On the other hand, elevated TOP2 levels render the cell hypersensitive to the poisons but resistant to inhibitors, as inhibitors and poisons are usually antagonistic. Catalytic inhibition of the enzyme is an alternative strategy to treatment with TOP2 poisons, although currently lack of potency is an issue, new inhibitors are being developed.

Because of its novel role in the cellular response to TOP2 damage, it would be useful to look into the possibility of the use of therapeutic ZNF451 inhibitors. Perhaps, if TDP2 and ZNF451 inhibitors were to be used in combination with etoposide, etoposide doses could be lessened, and therefore possibly decrease side effects of etoposide treatment. Additionally, in tumors where there are low TOP2 levels, it would be interesting to study the combination of TOP2, ZNF451, and TDP2 inhibitors.

6. Future work

V. CONCLUSIONS

V. CONCLUSIONS

1. TDP2 binds SUMO through a novel split-SIM independently from the previously described ^{280}I-V-D-V^{283} SIM.
2. SUMO1- and SUMO2/3-modified TOP2cc accumulate in response to etoposide in primary MEFs.
3. Proteasome inhibition does not increase accumulation of TOP2cc in response to etoposide, nor their SUMO2/3 modification, but it abolishes modification by SUMO1.
4. The absence of TDP2 does not affect accumulation of TOP2cc in response to etoposide, but it increases sumoylation specifically by the SUMO1 isoform.
5. TDP2 facilitates removal of undegraded SUMO2/3 modified TOP2cc *in vitro* and *in vivo*, and this is facilitated by TDP2-SUMO interactions mediated by the TDP2 split-SIM.
6. In conditions of proteasome inhibition, repair of TOP2-induced DSBs is completely dependent on TDP2.
7. ZNF451 is involved in the response to TOP2-induced DNA damage by both TDP2 dependent and independent pathways.

VI. MATERIALS AND METHODS

VI. Materials and Methods

1. Cell culture procedures

1.1 Cell lines and primary cell culture

1.2 Lentiviral production, titration, and infection

2. Cell and molecular biology procedures

2.1. γH2AX foci analysis and Immunofluorescence

2.2. Chromatin fractionation

2.3. TDP2 purification

2.4. BioID and protein identification by mass spectrometry

2.5. ICE assay

2.6. *In vitro* TDP2 activity on ICE-isolated TOP2-DNA crosslinks

2.7. *In vitro* 5'-TDP activity on oligonucleotides

2.8. Clonogenic survival assays

2.9. Site directed mutagenesis

2.10. Yeast two-hybrid

2.11. GFP pulldown

2.12. His-tag pulldown

3. Tables

3.1. Cell lines

3.2. Yeast strains

3.3. Antibodies

1. Cell culture procedures

1.1. Cell lines and primary cell culture

Cells in culture were maintained in HEPA class 100 incubators (Thermo) at 37 °C in 5% CO_2 unless otherwise indicated. All media was supplemented with 50 U μL^{-1} penicillin and 50 $\mu g\ mL^{-1}$ streptomycin.

Primary MEFs were isolated from embryos at day 13 p.c. and cultured at 3% O_2 in Dubelcco's Modified Eagle's Medium (DMEM) supplemented with 2 mM L-Glutamine, 15% Fetal Bovine Serum (FBS) and non-essential amino acids. All experiments were carried out between P1 and P4.

Transformed MEFs were maintained in DMEM supplemented with 2 mM L-Glutamine and 10% FBS. MEFs were transformed by retroviral delivery of T121, a fragment of the SV40 large T antigen that antagonizes the three Rb family members but not p53 (Saenz Robles et al., 1994). After several passages under puromycin selection, clones that efficiently grew were selected.

HEK293T and U2OS cells were maintained at 37°C, 5% CO_2 in DMEM supplemented with penicillin, streptomycin, 2 mM L-Glutamine and 10% FBS.

RPE-1 cells were maintained at 37°C, 5% CO_2 in F12 media with L-Glutamine (Sigma) supplemented with penicillin, streptomycin and 10% FBS.

1.2. Lentiviral production, titration, and infection

Lentiviral particles were either produced or purchased from the Viral Vector unit of the Spanish National Center for Cardiovascular Research (CNIC). To produce lentiviral particles in house, $6.9x10^6$ HEK293T cells were grown in 150 mm

plates and transfected by a calcium/phosphate protocol with a mixture composed of 38.4 μg of the lentiviral vector of interest, 25.6 μg of p8.91 (plasmid containing viral capsid genes) and 12.8 μg of pVSVG (plasmid containing viral envelope genes). Medium was changed 19 h after transfection, then particles were recovered 48 h later and filtered through a 0.45 μm polypropylene filter (10462100, Whatman: GE Healthcare). Viral particles were concentrated by centrifugation for 1.5 h at 22,000 rpm at 4°C in a Beckman-Coulter Optima L-100K Ultracentrifuge and resuspended in ice cold DMEM, aliquoted and stored at -80 °C.

For titration of shRNA-ZNF451, RPE-1 cells were infected with serial dilutions of lentiviral particles. After 72 h, qPCR was performed detecting lentiviral integration with oligonucleotides for the long terminal repeat (LTR). Values were normalized to Albumin (number of cells), and to the standard curve of oligonucleotides to correct for primer efficiency. Western blot confirming knockdown was performed in the cell type to be used for experiments.

Titer of GFP expressing lentivirus was calculated using BD FACSCalibur Flow Cytometer (342975, BD Biosciences) and measuring GFP expression in cells infected with serial dilutions of lentiviral particles.

Overexpression of TDP2 was carried out by lentiviral infection at MOI 2.5, and confirmed by western blot. For shRNA depletion, cells were infected with equal amounts, as determined by qPCR titer, of non-targeting and ZFP451 shRNA lentiviral particles followed by 10-day selection in 2μg mL^{-1} puromycin to obtain at least 80% knock-down efficiency.

2. Molecular and cell biology procedures

2.1. γH2AX foci analysis and Immunofluorescence

Primary MEFs were grown on coverslips for 7 days until confluency arrest, followed by 3 day serum starvation in DMEM supplemented with 0.5% FBS. Cells with shRNA depletion (and non-targeting controls) were not serum starved. Cells were pretreated with 20 μM MG132 or vehicle (DMSO) for 1.5 h then treated with 30 μM etoposide (MG132 free samples) or 200 μM etoposide and 20 μM MG132 for 30 minutes, then fixed in ice-cold methanol for 10 min at -20°C.

Immunofluorescence was carried out as described (Alvarez-Quilon et al., 2014). Briefly, cells were permeabilized (2 min in PBS-0.2% (v/v) Triton X-100), blocked (30 min in PBS-5% (w/v) BSA) and incubated with the primary antibody for 1 h in PBS-1% (w/v) BSA. Cells were then washed (three times in PBS-0.1% (v/v) TWEEN 20), incubated with the secondary antibody for 30 min in 1% (w/v) BSA -PBS, washed again as described above, counterstained with DAPI (Sigma) for 2 min, and mounted in Vectashield (Vector Labs). γH2AX foci were manually counted (blind) in 40 cells for each experimental condition with a Leica DM6000B microscope with the 100X oil objective. Statistical analysis with two-way ANOVA with Bonferroni post-test was performed.

2.2. Chromatin fractionation

Serum-starvation arrested RPE-1 cells were pretreated for 1.5 h with 20 μM MG132 or vehicle (DMSO), then 1 h with 100 μM etoposide or vehicle (DMSO), and processed as described (Ochi 2015). Briefly, cells were washed twice in ice-cold PBS, and pre-extracted twice for 3 min on ice in CSK buffer (100 mM NaCl,

300 mM sucrose, 3 mM $MgCl_2$, 0.7% (v/v) Triton X-100, 10 mM PIPES, pH 7.0). After pre-extraction, cells were washed 3 times in ice-cold PBS and harvested in SDS loading buffer. Samples were run in 4-20% precast polyacrylamide gels (Biorad) and transferred/incubated as described above.

2.3. TDP2 Purification

2.4. BioID

2.5. ICE assay

Confluency arrested primary MEFs were pretreated for 1.5 h with 20 μM MG132 or vehicle (DMSO) followed by 100 μM etoposide (Sigma E1383) or vehicle (DMSO) for 1 hour. They were either immediately lysed in 1% (w/v) sarkosyl (Sigma L7414) or washed twice with PBS and incubated at 37 °C in fresh media for the indicated times before lysis. Lysates were processed according to the *in vivo* complex of enzyme (ICE) assay (Nitiss et al., 2012). Briefly, sheared samples were

centrifuged with a CsCl (Applichem-Panreac, A1098) gradient at 57,000 r.p.m. for 20 h at 25 °C using 3.3 ml 13 x 33 mm polyallomer Optiseal tubes (Beckman Coulter) in a TLN100 rotor (Beckman Coulter) in an Optima MAX ultracentrifuge (Beckman Coulter).

For slot blotting, ICE samples containing 5 μg of DNA were transferred onto Odyssey Nitrocellulose Membranes (LI-COR Biosciences) using a Bio-Dot SF Microfiltration Apparatus (Biorad). For western blot of ICE, samples were resuspended in 12,000 units of Micrococcal Nuclease (NEB, M0247S), 1x micrococcal nuclease buffer (NEB, B0247S) and 100 μg mL^{-1} BSA (NEB, B9000S), then incubated at 37 °C for 6 h. Samples were run in 10% SDS-PAGE and transferred to Immobilon-FL Transfer Membranes (Millipore). Membranes were blocked for 1 h in Odyssey

Blocking Buffer (LI-COR Biosciences), then incubated for 2 h with primary antibodies in the same buffer with additional 0.1% (v/v) TWEEN 20, washed 3x with TBS-0.1%-TWEEN20, incubated with secondary antibodies for 1 h, and finally washed again. Once the membranes were dry, slots were analyzed and quantified in Odyssey CLx using ImageStudio Odyssey CLx Software.

2.6. *In vitro* TDP2 activity on ICE-isolated TOP2-DNA crosslinks

TOP2-DNA crosslinks were isolated as described above and resuspended in bi-distilled H_2O. Samples containing 20 µg of DNA were incubated in reaction buffer (50 mM Tris-HCl pH 7.5, 50 mM KCl, 1 mM DTT, 100 µg mL^{-1} BSA, 1mM $MgCl_2$) with the given concentration of TDP2 in a total volume of 300 µl for 1 h at 37°C. Reactions were stopped by the addition of 600 µL STOP buffer (50mM EDTA, 1% (w/v) Sarcosyl) and placed on ice. Samples were centrifuged a second time according to the ICE assay, and 5 µg of DNA was used in a slot blot. Statistical analysis was performed with F-test, exponential decay regression.

2.7. *In vitro* 5'-TDP activity on oligonucleotides

Assays of 5′–Tyrosyl DNA phosphodiesterase activity on synthetic 5′–phosphotyrosine DNA oligonucleotides were performed as previously described (Cortes-Ledesma et al., 2009). Substrates were generated by mixing the appropriate 40 pmoles of 5' phosphotyrosine and 20 pmoles of reverse complementary. They were mixed in a total volume of 30 µL, and annealed by heated to 95 °C for 10 min, and cooled down for 10 min at each of the following temperatures: 70°C, 45°C, 20° C, and 4°C.

Annealed DNA duplexes were labeled by incubation with Klenow polymerase (Takara) for 1 h at 37 °C in the presence of [α-32P]-dCTP and 50 μM ddTTP. Unincorporated [α-32P]- dCTP was removed by Illustra MicroSpin G-25 Columns (GE Healthcare). Reactions contained 50 nM substrate, 80 μM competitor single-stranded oligonucleotide and the indicated amount of recombinant protein in a total volume of 6 μL Reaction Buffer (50 mM Tris-Cl, pH 7.5, 50 mM KCl, 1 mM $MgCl_2$, 1 mM DTT, 100 μg ml^{-1} BSA).

Reactions were stopped by the addition of Formamide Loading Buffer and boiling for 5 min at 95 °C. Samples were resolved in 7 M Urea denaturing 20% polyacrylamide gel electrophoresis in 0.5x TBE buffer. Gels were analyzed by phosphorimaging in a Fujifilm FLA5100 device (GE Healthcare).

2.8. Clonogenic survival assays

Clonogenic survival assays were carried out by seeding T121 transformed MEFs in 100 mm dishes in duplicate for each experimental condition. To compensate for growth defects, 4,000 cells were seeded for *Tdp2*$^{+/+}$ cells and 20,000-50,000 cells for *Tdp2*$^{-/-}$. After 6 h, the indicated concentration of etoposide was added and cells were incubated for 10–12 days. Dishes were fixed and stained for manual colony counting in Crystal Violet solution (0.5% (w/v) Crystal Violet in 20% v) ethanol). The surviving fraction at each dose was calculated by dividing the average number of visible colonies in treated versus untreated dishes, relative to the number of seeded cells.

2.9. Site-directed Mutagenesis

Amino acid substitutions were performed by limited polymerase chain reaction amplification of plasmid DNA using KOD hot-start DNA polymerase and oligonucleotides containing the mutated codons, followed by digestion of remaining input plasmid DNA using the methylation sensitive enzyme DpnI (New England Biolabs).

2.10 .Yeast Two-Hybrid Assay (Y2H)

To check interactions between TDP2 and SUMO, a yeast two-hybrid assay (Y2H) was performed. A standard rapid yeast transformation protocol was used. A GAL4 based Y2H system was used, with TDP2 cloned into the bait vector pGBKT7, and SUMO1 and SUMO2 cloned into the prey pACT. The strain Y190 (see table 2 for genotype) was used. Growth on –leucine/-tryptophan plates indicated successful transformation of both plasmids while growth on –leucine/-tryptophan/-histidine plates represented interaction. 3-Amino-1,2,4-triazole (3-AT), a competitive inhibitor of the product of the HIS3 gene, was added to -histidine plates to remove background growth. 5x serial dilution drops were plated.

Non-conjugatable SUMO1 and 2 were a gift from Mario Garcia, in the pLEXA vector. They were cotransformed with TDP2 in the pACT vector, and the LexA system was used. Strain NMY51 was used (see table 2 for genotype).

2.11. GFP pulldown

Pulldown of GFP-tagged proteins was performed with GFP-Trap (Chromotek) following the manufacturer instructions.

2.12. His-tag pulldown

Cell name	Species	Origin
Primary MEFs	*Mus musculus*	Embryonic fibroblasts
Transformed MEFs	*Mus musculus*	SV40-transformed embryonic fibroblasts
HEK293T	*Homo sapiens*	Embryonic kidney transformed cell line
U2OS	*Homo sapiens*	Osteosarcoma cell line
RPE-1	*Homo sapiens*	Retinal pigmented epitelial cells
NIH 3T3	*Mus musculus*	Fibroblast
HeLa	*Homo sapiens*	Cervical cancer
A549	*Homo sapiens*	Adenocarcinomic human alveolar basal epithelial cells

Table M1: Cells used in this Thesis.

Primary Antibody	Working Dilution	Source	Species
GFP	1/3,000	Roche, 11814460001	Mouse
Histone H3	1/3,000	Abcam, ab1791	Rabbit
SUMO1	1/200, 1/500	DSHB	Mouse
SUMO2	1/500, 1/1,000	Santa Cruz, sc-32873	Rabbit
TDP2	1/1,000	Gift from Keith Caldecott	Rabbit
TOP2α	1/1,000, 1/3,000	Santa Cruz, sc-365916	Mouse
TOP2β	1/1,000	Santa Cruz, sc-13059	Rabbit
Tubulin	1/15,000	Sigma,T9026	Mouse
ZNF451	1/500, 1/1,000	SAB2102880, 108741	Rabbit
γH2AX	1/1,000	Millipore, 05-636	Mouse

Table M2: Primary antibodies used in this study

Secondary antibody	Working Dilution	Source
IRDye 680RD goat anti-mouse IgG (H+L)	1/10,000	LI-COR
IRDye 800RD goat anti-rabbit IgG (H+L)	1/10,000	LI-COR
Goat anti-mouse-AlexaFluor488	1/1,000	ThermoFisher
Goat anti-mouse-AlexaFluor594	1/1,000	ThermoFisher
Rabbit IgG/heavy and light chain cross absorbed Cy3	1/1,000	Bethyl Laboratories

Table M3: Secondary antibodies used in this study

Strain	Genotype
Y190	*MATa, ura3-52, his3-200, ade2-101, lys2-801, trp1-901, leu2-3, 112, gal4Δ, gal80Δ, cyh^{r}2, LYS2 : : GAL1$_{UAS}$-HIS3$_{TATA}$-HIS3, MEL1 URA3 : : GAL1$_{UAS}$-GAL1$_{TATA}$-lacZ*
NMY51	*MATa, his3Δ200, trp1–901, leu2–3 112, ade2, LYS2::(lexAop)4-HIS3, ura3::(lexAop)8-lacZ, ade2::(lexAop)8-ADE2 GAL4*

Table M4: Yeast used in this study

VII. BIBLIOGRAPHY

VII. BIBLIOGRAPHY

Adhikari, S., Karmahapatra, S. K., Karve, T. M., Bandyopadhyay, S., Woodrick, J., Manthena, P. V, Glasgow, E., Byers, S., Saha, T., Uren, A. (2012). Characterization of magnesium requirement of human 5'-tyrosyl DNA phosphodiesterase mediated reaction. *BMC Research Notes*, *5*(1), 134.

Abdurashidova, G., Sandoval, O., Danailov, M. B., Santamaria, L., Biamonti, G., Riva, S., & Falaschi, A. (2007). Functional interactions of DNA topoisomerases with a human replication origin. *EMBO J.*, *26*(4), 998–1009.

Alani, E., Thresher, R., Griffith, J.D., and Kolodner, R.D. (1992). Characterization of DNA-binding and strand-exchange stimulation properties of y-RPA, a yeast single-strand-DNA-binding protein. *Journal of Molecular Biology.* 227(1): 54-71.

Álvarez-Quilón, A., Serrano-Benítez, A., Lieberman, J. A., Quintero, C., Sánchez-Gutiérrez, D., Escudero, L. M., & Cortés-Ledesma, F. (2014). ATM specifically mediates repair of double-strand breaks with blocked DNA ends. *Nature Communications*, *5*, 3347.

Aparicio, T., Baer, R., Gottesman, M., & Gautier, J. (2016). MRN, CtIP, and BRCA1 mediate repair of topoisomerase II – DNA adducts. *Journal of Cell Biology*, *212*(4), 399–408.

Ashour, M. E., Atteya, R., & El-Khamisy, S. F. (2015). Topoisomerase-mediated chromosomal break repair: an emerging player in many games. *Nature Reviews Cancer*, *15*(3), 137–151.

Ayoubi, T. A., & Van De Ven, W. J. (1996). Regulation of gene expression by alternative promoters. *FASEB J*, 10(4):453-60

Azuma, Y., Arnaoutov, A., & Dasso, M. (2003). SUMO-2/3 regulates topoisomerase II in mitosis. *Journal Cell Biology*, *163*(3), 477–487. https://doi.org/10.1083/jcb.200304088

Azuma, Y., Arnaoutov, A., Anan, T., & Dasso, M. (2005). PIASy mediates SUMO-2 conjugation of Topoisomerase-II on mitotic chromosomes. *The EMBO Journal*, *24*(12), 2172–2182. https://doi.org/10.1038/sj.emboj.7600700

Bailey, D., & O'Hare, P. (2005). Comparison of the SUMO1 and ubiquitin conjugation pathways during the inhibition of proteasome activity with evidence of SUMO1 recycling. *The Biochemical Journal*, *392*, 271–281.

Ban, Y., Ho, C.-W., Lin, R.-K., Lyu, Y. L., & Liu, L. F. (2013). Activation of a novel ubiquitin-independent proteasome pathway when RNA polymerase II encounters a protein roadblock. *Molecular and Cell Biology*, *33*(20), 4008–16. https://doi.org/10.1128/MCB.00403-13

Bates, A. D., Berger, J. M., & Maxwell, A. (2011). The ancestral role of ATP hydrolysis in type II topoisomerases: prevention of DNA double-strand breaks. *Nucleic Acids Research*, *39*(15), 6327–6339.

Bernardi, R., & Pandolfi, P. P. (2007). Structure, dynamics and functions of promyelocytic leukaemia nuclear bodies. *Nature Reviews Molecular and Cell Biology*, *8*(Dec), 1007–1016.

Bhat, M. A., Philp, A. V., Glover, D. M., & Bellen, H. J. (1996). Chromatid Segregation at Anaphase Requires the barren Product, a Novel Chromosome-Associated Protein That Interacts with Topoisomerase II. *Cell*, *87*, 1103–1114.

Boddy, M. N., Howe, K., Etkin, L. D., Solomon, E., & Freemont, P. S., (1996). PIC 1, a novel ubiquitin-like protein which interacts with the PML component of a multiprotein complex that is disrupted in acute promyelocytic leukaemia. *Oncogene*, *15*(5), 971–982.

Branzei, D., Vanoli, F., & Foiani, M. (2008). SUMOylation regulates Rad18-mediated template switch. *Nature*, *456*(7224), 915–920.

Brill, S. J., DiNardo, S., Voelkel-Meiman, K., Sternglanz, R., (1987). Need for DNA topoisomerase activity as a swivel for DNA replication for transcription of ribosomal RNA. *Nature*. 326, 414-416

Cancer Research UK, <http://www.cancerresearchuk.org/>, accessed May 2017

Cappadocia, L., Pichler, A., & Lima, C. D. (2015). Structural basis for catalytic activation by the human ZNF451 SUMO E3 ligase. *Nature Structural Molecular Biology*, *22*(2), 134–139.

Champoux, J. J. (2001). DNA topoisomerases: structure, function, and mechanism. *Annual Reviews Biochemistry, 70*, 369–413.

Chapman-Smith, A., & Cronan, J. E. (1999). Molecular biology of biotin attachment to proteins. *The Journal of Nutrition*, *129*, 477S–484S.

Chen, M. & Beck, W. T. (1995). DNA Topoisomerase II Expression, Stability, and Phosphorylation in Two VM-26-Resistant Human Leukemic CEM Sublines. *Oncology Research* 7:103–111.

Chen, W., Qiu, J., & Shen, Y. (2012). Topoisomerase IIá, rather than IIâ, is a promising target in development of anti-cancer drugs. *Drug Discoveries & Therapeutics*, *6*(5), 230–237.

Choi, M., Kipps, T., & Kurzrock, R. (2016). ATM Mutations in Cancer: Therapeutic Implications. *Molecular Cancer Therapeutics*, *15*(8), 1781–1791.

Chou, D. M., Adamson, B., Dephoure, N. E., Tan, X., Nottke, A. C., Hurov, K. E., … Elledge, S. J. (2010). A chromatin localization screen reveals poly (ADP ribose)-regulated recruitment of the repressive polycomb and NuRD complexes to sites of DNA damage. *Proceedings of the National Academy of Sciences of the United States of America*, *107*(43), 18475–18480.

Ciccia, A., & Elledge, S. J. (2010). The DNA damage response: making it safe to play with knives. *Molecular Cell Cell*, *40*(2), 179–204.

Connelly, J. C., & Leach, D. R. F. (2004). Repair of DNA Covalently Linked to Protein. *Mol. Cell*, *13*, 307–316.

Cortés-Ledesma, F., El Khamisy, S. F., Zuma, M. C., Osborn, K., & Caldecott, K. W. (2009). A human 5'-tyrosyl DNA phosphodiesterase that repairs topoisomerase-mediated DNA damage. *Nature*, *461*(7264), 674–678.

Costes, S. V., Chiolo, I., Pluth, J. M., Barcellos-Hoff, M. H., & Jakob, B. (2010). Spatiotemporal characterization of ionizing radiation induced DNA damage foci and their relation to chromatin organization. *Mutation Research*, *704*(1–3), 78–87.

Cremona, C. A., Sarangi, P., Yang, Y., Hang, L. E., Rahman, S., & Zhao, X. (2012a). Extensive DNA Damage-Induced Sumoylation Contributes to Replication and Repair and Acts in Addition to the Mec1 Checkpoint. *Mol. Cell*, *45*(3), 422–432.

Cremona, C. A., Sarangi, P., & Zhao, X. (2012b). Sumoylation and the DNA Damage Response. *Biomolecules., 2,* 376–388.

Cui, X., Mcallister, R., Boregowda, R., Sohn, J. A., Ledesma, F. C., Caldecott, K. W., … Hu, J. (2015). Does Tyrosyl DNA Phosphodiesterase-2 Play a Role in Hepatitis B Virus Genome Repair? *PLoS One*. 1–15.

Cuvier, O., & Hirano, T. (2003). A role of topoisomerase II in linking DNA replication to chromosome condensation. *Journal of Cell Biology*, *160*(5), 645–655.

Dawlaty, M. M., Malureanu, L., Jeganathan, K. B., Kao, E., Sustmann, C., Tahk, S., Shuai, K., Grosschedt, R., Deursen, J. M. (2008). Resolution of Sister Centromeres Requires RanBP2-Mediated SUMOylation of Topoisomerase IIá. *Cell*, *133*(1), 103–115.

Depew, R. E., Liu, L. F., and Wang, J. C. (1978). Interaction between DNA and *Escherichia coli* protein omega. Formation of a complex between single-stranded DNA and omega protein. *Journal of Biological Chemistry.* 253, 511-518

Desterro, J. M., Rodriguez, M. S., & Hay, R. T. (1998). SUMO-1 modification of IêBá inhibits NF-êB activation. *Molecular Cell*, *2*(2), 233–239.

Desterro, J. M. P., Rodriguez, M. S., Kemp, G. D., & Hay, R. T. (1999). Identification of the Enzyme Required for Activation of the Small Ubiquitin-like Protein SUMO-1. *Journal of Biological Chemistry*, *274*(15), 10618–10624.

Deweese, J. E., & Osheroff, N. (2009). The DNA cleavage reaction of topoisomerase II: wolf in sheep's clothing. *Nucleic Acids Research*, *37*(3), 738–748.

Dikic, I., Wakatsuki, S., & Walters, K. J. (2009). Ubiquitin-binding domains - from structures to functions. *Nature Reviews Molecular Cell Biology*, *10*(10), 659–671.

Do, P. M., Varanasi, L., Fan, S., Li, C., Kubacka, I., Newman, V., … Martinez, L. A. (2012). Mutant p53 cooperates with ETS2 to promote etoposide resistance. *Genes and Development*, *26*(8), 830–845.

Drake, F. H., Hofmann, G. A., Bartus, H. F., Mattern, M. R., Crooke, S. T., & Mirabelli, C. K. (1989). Biochemical and Pharmacological Properties of p170 and p180 Forms of Topoisomerase II. *Biochemistry*, *28*, 8154–8160.

Drygin, Y. F. (1998). Natural covalent complexes of nucleic acids and proteins: Some comments on practice and theory on the path from well-known complexes to new ones. *Nucleic Acids Research*, *26*(21), 4791–4796.

Eckerle, S., Brune, V., Doring, C., Tiacci, E., Bohle, V., Sundstrom, C., … Hansmann, M. L. (2009). Gene expression profiling of isolated tumour cells from anaplastic large cell lymphomas: insights into its cellular origin, pathogenesis and relation to Hodgkin lymphoma. *Leukemia*, *23* (11), 2129–2138.

Eisenhardt, N., Chaugule, V. K., Koidl, S., Droescher, M., Dogan, E., Rettich, J., … Pichler, A. (2015). A new vertebrate SUMO enzyme family reveals insights into SUMO-chain assembly. *Nature Structural & Molecular Biology*, *22*(12), 959–967.

Friedl, A. A., Kiechle, M., Fellerhoff, B., & Eckardt-Schupp, F. (1998). Radiation-induced chromosome aberrations in Saccharomyces cerevisiae: Influence of DNA repair pathways. *Genetics*, *148*(3), 975–988.

Gao, R., Das, B. B., Chatterjee, R., Abaan, O. D., Agama, K., Matuo, R., … Pommier, Y. (2014). Epigenetic and genetic inactivation of tyrosyl-DNA-phosphodiesterase 1 (TDP1) in human lung cancer cells from the NCI-60 panel. *DNA Repair*, *13*(1), 1–9.

Gómez-Herreros, F., Romero-Granados, R., Zeng, Z., Álvarez-Quilón, A., Quintero, C., Ju, L., … Cortés-Ledesma, F. (2013). TDP2-Dependent Non-Homologous End-Joining Protects against

Topoisomerase II-Induced DNA Breaks and Genome Instability in Cells and In Vivo. *PLoS Genetics*, *9*(3).

Gómez-Herreros, F., Schuurs-Hoeijmakers, J. H. M., Mccormack, M., Greally, M. T., Rulten, S., Romero-Granados, R., … Caldecott, K. W. (2014). TDP2 protects transcription from abortive topoisomerase activity and is required for normal neural function. *Nat. Gen.*, *46*(5), 516–521.

Goodarzi, A. A., Yu, Y., Riballo, E., Douglas, P., Walker, S. A., Ye, R., … Lees-Miller, S. P. (2006). DNA-PK autophosphorylation facilitates Artemis endonuclease activity. *The EMBO Journal*, *25*(16), 3880–3889.

Grue, P., Gräßer, A., Sehested, M., Jensen, P. B., Uhse, A., Straub, T., Ness, W., Boege, F. (1998). Essential mitotic functions of DNA topoisomerase IIá are not adopted by topoisomerase IIâ in human H69 cells. *Journal of Biological Chemistry*, *273*(50), 33660–33666.

Guo, Z., Kanjanapangka, J., Liu, N., Liu, S., Liu, C., & Shen, B. (2013). Sequential post-translational modifications program FEN1 degradation during cell cycle progression Zhigang. *Molecular Biology Reports*, *47*(3), 444–456.

Hammel, M., Yu, Y., Mahaney, B. L., Cai, B., Ye, R., Phipps, B. M., … Tainer, J. A. (2010). Ku and DNA-dependent Protein Kinase Dynamic Conformations and Assembly Regulate DNA Binding and the Initial Non-homologous End Joining Complex. *J. Biol. Chem.*, *285*(2), 1414–1423.

Hannich, J. T., Lewis, A., Kroetz, M. B., Li, S. J., Heide, H., Emili, A., & Hochstrasser, M. (2005). Defining the SUMO-modified proteome by multiple approaches in Saccharomyces cerevisiae. *Journal of Biological Chemistry*, *280*(6), 4102–4110.

Hecker, C. M., Rabiller, M., Haglund, K., Bayer, P., & Dikic, I. (2006). Specification of SUMO1- and SUMO2-interacting motifs. *Journal of Biological Chemistry*, *281*(23), 16117–16127.

Hendriks, I. A., D'Souza, R. C. J., Yang, B., Verlaan-de Vries, M., Mann, M., & Vertegaal, A. C. O. (2014). Uncovering global SUMOylation signaling networks in a site-specific manner. *Nature Structural & Molecular Biology*, *21*(10), 927–936.

Hendriks, I. A., & Vertegaal, A. C. O. (2016). A comprehensive compilation of SUMO proteomics. *Nature Reviews Molecular Cell Biology*, *17*(9), 581–595.

Hershko, a, & Ciechanover, a. (1992). The ubiquitin system for protein degradation. *Annual Reviews of Biochemistry*, *61*, 761–807.

Hietakangas, V., Anckar, J., Blomster, H. A., Fujimoto, M., Palvimo, J. J., Nakai, A., & Sistonen, L. (2006). PDSM, a motif for phosphorylation-dependent SUMO modification. *Proceedings of the National Academy of Sciences of the United States of America*, *103*(1), 45–50.

Hirano, T. (2006). At the heart of the chromosome: SMC proteins in action *Nature Reviews Molecular Cell Biology*, 7(5): 311-322

Hoa, N. N., Shimizu, T., Zhou, Z. W., Wang, Z., Deshpande, R. A., Paull, T. T., Akter, S., Tsuda, M., Furuta, R., Tsusui, K., Takeda, S., Sasanuma, H. (2016). Mre11 Is Essential for the Removal of Lethal Topoisomerase 2 Covalent Cleavage Complexes. *Molecular Cell*, *64*(3), 580–592. h

Hornyak, P., Askwith, T., Walker, S., Komulainen, E., Paradowski, M., Pennicott, L. E., … Oliver, A. W. (2016). Mode of action of DNA-competitive small molecule inhibitors of tyrosyl DNA phosphodiesterase 2. *Biochemical Journal*, *473*(13), 1869–1879.

Hu, W., & Chen, Y. (2005). Small ubiquitin-like modifier (SUMO) recognition of a SUMO binding motif: A reversal of the bound orientation. *Journal of Biological Chemistry*, *280*(48), 40122–40129.

Huang, D. W., Sherman, B. T., & Lempicki, R. A. (2008). Systematic and integrative analysis of large gene lists using DAVID bioinformatics resources. *Nature Protocols*, *4*(1), 44–57.

Huang, D. W., Sherman, B. T., & Lempicki, R. A. (2009). Bioinformatics enrichment tools: Paths toward the comprehensive functional analysis of large gene lists. *Nucleic Acids Research*, *37* (1), 1–13.

Hudson, J. J. R., Chiang, S., Wells, O. S., Rookyard, C., & El-khamisy, S. F. (2012). single-strand break repair. *Nature Communications*, *3*, 713–733.

Hutchins, J. R. A., Toyoda, Y., Hegemann, B., Poser, I., Heriche, J. K., Sykora, M. M., … Peters, J. M. (2010). Systematic Analysis of Human Protein Complexes Identifies Chromosome Segregation Proteins. *Science*, *328*(5978), 593–599.

International Human Genome Sequencing Consortium. (2004). Finishing the euchromatic sequence of the human genome. *Nature*, *431*(7011), 931–45.

Ikeda, H., & Tomizawa, J. (1965). Transducing fragments in generalized transduction by phage P1. *Journal of Molecular Biology*, *14*(1), 85–109.

Isik, S., Sano, K., Tsutsui, K., Seki, M., Enomoto, T., Saitoh, H., & Tsutsui, K. (2003). The SUMO pathway is required for selective degradation of DNA topoisomerase IIâ induced by a catalytic inhibitor ICRF-193. *FEBS Letters*, *546*(2–3), 374–378.

Jackson, S. P., & Bartek, J. (2010). The DNA-damage response in human biology and disease. *Nature*, *461*(7267), 1071–1078.

Jackson, S. P., & Durocher, D. (2013). Review Regulation of DNA Damage Responses by Ubiquitin and SUMO. *Molecular Cell*, *49*(5), 795–807.

Jeppsson, K., Carlborg, K. K., Nakato, R., Berta, D. G., Lilienthal, I., Kanno, T., … Sjögren, C. (2014). The Chromosomal Association of the Smc5/6 Complex Depends on Cohesion and Predicts the Level of Sister Chromatid Entanglement. *PLoS Genetics*, *10*(10).

Johnson, E. S., & Blobel, G. (1997). Ubc9p is the conjugating enzyme for the ubiquitin-like protein Smt3p. *Journal of Biological Chemistry*, *272*(43), 26799–26802.

Johnson, E. S. (2004). Protein Modification by SUMO. *Annual Review of Biochemistry*, *73*(1), 355–382.

Joseph, J., Liu, S. T., Jablonski, S. A., Yen, T. J., & Dasso, M. (2004). The RanGAP1-RanBP2 Complex Is Essential for Microtubule-Kinetochore Interactions *In Vivo*. *Current Biology*. 14(7), 611-617.

Joshi, R. S., Piña, B., & Roca, J. (2012). Topoisomerase II is required for the production of long Pol II gene transcripts in yeast. *Nucleic Acids Research*, *40*(16), 7907–7915.

Ju, B.-G., Lunyak, V. V, Perissi, V., Garcia-Bassets, I., Rose, D. W., Glass, C. K., & Rosenfeld, M. G. (2011). A Topoisomerase IIâ-Mediated dsDNA Break Required for Regulated Transcription. *Science*, *312*(May), 1798–1802.

Kamitani, T., Nguyen, H. P., & Yeh, E. T. H. (1997). Preferential Modification of Nuclear Proteins by a Novel Ubiquitin-like Molecule. *Journal of Biological Chemistry*, *272*(22), 14001–14004.

Karvonen, U., Jääskeläinen, T., Rytinki, M., Kaikkonen, S., & Palvimo, J. J. (2008). ZNF451 Is a Novel PML Body- and SUMO-Associated Transcriptional Coregulator. *Journal of Molecular Biology*, *382*(3), 585–600.

Kerscher, O. (2007). SUMO junction-what's your function? New insights through SUMO-interacting motifs. *EMBO Reports*, *8*(6), 550–555.

Kerscher, O., Felberbaum, R., & Hochstrasser, M. (2006). Modification of Proteins by Ubiquitin and Ubiquitin-Like Proteins. *Annual Review of Cell and Developmental Biology*, *22*(1), 159–180.

King, I. F., Yandava, C. N., Mabb, A. M., Hsiao, J. S., Huang, H., Pearson, B. L., … Zylka, M. J. (2014). Topoisomerases facilitate transcription of long genes linked to autism. *Nature*, *501* (7465), 58–62.

Kingma, P. S., & Osheroff, N. (1997). Apurinic sites are position-specific topoisomerase II poisons. *Journal of Biological Chemistry*, *272*(2), 1148–1155.

Koidl, S., Eisenhardt, N., Fatouros, C., Droescher, M., Chaugule, V. K., & Pichler, A. (2016). The SUMO2/3 specific E3 ligase ZNF451-1 regulates PML stability. *International Journal of Biochemistry and Cell Biology*, *79*, 478–487.

Königer, C., Wingert, I., Marsmann, M., Rösler, C., Beck, J., & Nassal, M. (2014). Involvement of the host DNA-repair enzyme TDP2 in formation of the covalently closed circular DNA persistence reservoir of hepatitis B viruses. *Proceedings of the National Academy of Sciences of the United States of America*, E4244–E4253.

Kont, Y. S., Dutta, A., Mallisetty, A., Mathew, J., Minas, T., Kraus, C., … Adhikari, S. (2016). Depletion of tyrosyl DNA phosphodiesterase 2 activity enhances etoposide-mediated double-strand break formation and cell killing. *DNA Repair*, *43*, 38–47.

Koster, D. A., Croquette, V., Dekker, C., Shuman, S., & Dekker, N. H. (2005). Friction and torque govern the relaxation of DNA supercoils by eukaryotic topoisomerase IB. *Nature*, *434*, 671–674.

Königer, C., Wingert, I., Marsmann, M., Rösler, C., Beck, J., & Nassal, M. (2014). Involvement of the host DNA-repair enzyme TDP2 in formation of the covalently closed circular DNA persistence reservoir of hepatitis B viruses. *Proceedings of the National Academy of Sciences of the United States of America*, E4244–E4253

Kont, Y. S., Dutta, A., Mallisetty, A., Mathew, J., Minas, T., Kraus, C., … Adhikari, S. (2016). Depletion of tyrosyl DNA phosphodiesterase 2 activity enhances etoposide-mediated double-strand break formation and cell killing. *DNA Repair*, *43*, 38–47.

Kumagai, A., & Dunphy, W. G. (2000). Claspin, a novel protein required for the activation of Chk1 during a DNA replication checkpoint response in Xenopus egg extracts. *Molecular Cell*, *6*(4), 839–849.

Lee, K. C., Bramley, R. L., Cowell, I. G., Jackson, G. H., & Austin, C. A. (2016). Proteasomal inhibition potentiates drugs targeting DNA topoisomerase II. *Biochemical Pharmacology*, *103*, 29–39.

Lee, M. P., Brown, S. D., Chen, A., & Hsieh, T. (1993). DNA topoisomerase I is essential in Drosophila melanogaster. *Proceedings of the National Academy of Sciences of the United States of America*, *90*(July), 6656–6660.

Lee, M. T., & Bachant, J. (2009). SUMO Modification of DNA topoisomerase II: Trying to get a CENse of it all. *DNA Repair*, *8*(4), 557–568.

Lees-Miller, S. P., & Meek, K. (2003). Repair of DNA double strand breaks by non-homologous end joining. *Biochimie*, *85*(11), 1161–1173.

Li, C., Fan, S., Owonikoko, T. K., Khuri, F. R., Sun, S.-Y., & Li, R. (2011). Oncogenic role of EAPII in lung cancer development and its activation of the MAPK-ERK pathway. *Oncogene*, *30* (September 2010), 3802–3812.

Li, C., Sun, S. Y., Khuri, F. R., & Li, R. (2011). Pleiotropic functions of EAPII/TTRAP/TDP2: Cancer development, chemoresistance and beyond. *Cell Cycle*, *10*(19), 3274–3283.

Li, R., Pei, H., & Papas, T. (1999). The p42 variant of ETS1 protein rescues defective Fas-induced apoptosis in colon carcinoma cells. *Proceedings of the National Academy of Sciences of the United States of America*, *96*(7), 3876–81.

Li, T., & Liu, L. F. (2001). Tumor Cell Death Induced by Topoisomerase-Targeting Drugs. *Annual Reviews Pharmacological Toxicology*, 53–77.

Linka, M., Porter, A. C. G., Volkov, A., Mielke, C., Boege, F., & Christensen, M. O. (2007). C-Terminal regions of topoisomerase IIá and IIâ determine isoform-specific functioning of the enzymes in vivo. *Nucleic Acids Research*, *35*(11), 3810–3822.

Lisby, M., Barlow, J. H., Burgess, R. C., & Rothstein, R. (2004). Choreography of the DNA Damage Response: Spatiotemporal Relationships among Checkpoint and Repair Proteins. *Cell*, *118*, 699–713.

Liu, L. F. & Wang, J. C. (1979). Interaction between DNA and Escherichia coli DNA topoisomerase I. Formation of complexes between the protein and superhelical and nonsuperhelical duplex. *Journal of Biological Chemistry,* 254, 11082-11088

Liu, X., Shao, Z., Jiang, W., Lee, B. J., & Zha, S. (2017). PAXX promotes KU accumulation at DNA breaks and is essential for end-joining in XLF-deficient mice. *Nature Communications*, *8*, 13816.

Lovett, B. D., Strumberg, D., Blair, I. A., Pang, S., Burden, D. A., Megonigal, M. D., … Felix, C. A. (2001). Etoposide metabolites enhance DNA topoisomerase II cleavage near leukemia-associated MLL translocation breakpoints. *Biochemistry*, *40*(5), 1159–1170.

Madabhushi, R., Gao, F., Pfenning, A. R., Cho, S., Madabhushi, R., Gao, F., … Rueda, R. (2015). Activity-Induced DNA Breaks Govern the Expression of Neuronal Early-Response Genes Article Activity-Induced DNA Breaks Govern the Expression of Neuronal Early-Response Genes. *CELL*, *161*(7), 1592–1605.

Maeshima, K., & Laemmli, U. K. (2003). A Two-Step Scaffolding Model for Mitotic Chromosome Assembly. *Developmental Cell*, *4*, 467–480.

Marchand, C., Abdelmalak, M., Kankanala, J., Huang, S. Y., Kiselev, E., Fesen, K., … Pommier, Y. (2016). Deazaflavin Inhibitors of Tyrosyl-DNA Phosphodiesterase 2 (TDP2) Specific for the Human Enzyme and Active against Cellular TDP2. *ACS Chemical Biology*, *11*(7), 1925–1933.

Mattsson, K., Pokrovskaja, K., Kiss, C., Klein, G., & Szekely, L. (2001). Proteins associated with the promyelocytic leukemia gene product (PML)-containing nuclear body move to the nucleolus upon inhibition of proteasome-dependent protein degradation. *Proceedings of the National Academy of Sciences of the United States of America*, *98*(3), 1012–7.

Mahajan, R., Delphin, C., Guan, T., Gerace, L., & Melchior, F. (1997). A small ubiquitin-related polypeptide involved in targeting RanGAP1 to nuclear pore complex protein RanBP2. *Cell*, *88* (1), 97–107.

Mahajan, R., Gerace, L., Melchior, F., Delphin, C., & Guan, T. (1998). Molecular characterization of the SUMO-1 modification of RanGAP1 and its role in nuclear envelope association. *Journal of Cell Biology*, *140*(2), 259–70.

Makharashvili, N., Tubbs, A. T., Yang, S., Wang, H., Zhou, Y., Deshpande, R. A., … Paull, T. T. (2015). Catalytic and non-catalytic roles of the CtIP endonuclease in double-strand break end resection. *Molecular Cell*, *54*(6), 1022–1033.

Mao, Y., Desai, S. D., & Liu, L. F. (2000a). SUMO-1 conjugation to human DNA topoisomerase II isozymes. *Journal of Biological Chemistry*, *275*(34), 26066–26073.

Mao, Y., Sun, M., Desai, S. D., & Liu, L. F. (2000b). SUMO-1 conjugation to topoisomerase I: A possible repair response to topoisomerase-mediated DNA damage. *Proceedings of the National Academy of Sciences of the United States of America, 97*(8), 4046–51.

Mao, Y., Desai, S. D., Ting, C. Y., Hwang, J., & Liu, L. F. (2001). 26 S Proteasome-mediated Degradation of Topoisomerase II Cleavable Complexes. *Journal of Biological Chemistry*, *276*(44), 40652–40658.

Marechal, A., & Zou, L. (2017). DNA Damage Sensing by the ATM and ATR Kinases. C*old Spring Harbor Perspectives in Biology*, *5*, 1–18.

Mari, P.-O., Florea, B. I., Persengiev, S. P., Verkaik, N. S., Bruggenwirth, H. T., Modesti, M., … van Gent, D. C. (2006). Dynamic assembly of end-joining complexes requires interaction between Ku70/80 and XRCC4. *Proceedings of the National Academy of Sciences of the United States of America*, *103*(49), 18597–18602.

Matunis, M. J., Coutavas, E., & Blobel, G. (1996). A novel ubiquitin-like modification modulates the partitioning of the Ran-GTPase-activating protein RanGAP1 between the cytosol and the nuclear pore complex. *Journal of Cell Biology*, *135*(6), 1457–1470.

McClendon, A. K., Rodriguez, A. C., & Osheroff, N. (2005). Human Topoisomerase IIα Rapidly Relaxes Positively Supercoiled DNA. *Journal of Biological Chemistry*, *280*(47), 39337–39345.

Mi, H., Huang, X., Muruganujan, A., Tang, H., Mills, C., Kang, D., & Thomas, P. D. (2017). PANTHER version 11: Expanded annotation data from Gene Ontology and Reactome pathways, and data analysis tool enhancements. *Nucleic Acids Research*, *45*(D1), D183–D189.

Morris, J. R., Boutell, C., Keppler, M., Densham, R., Weekes, D., Alamshah, A., Butler, L., Galanty, Y., Pangon, L., Kiuchi, T., Ng, T., … Solomon, E. (2009). The SUMO modification pathway is involved in the BRCA1 response to genotoxic stress. *Nature*, *462*(7275), 886–90.

Nayak, A., & Müller, S. (2014). SUMO-specific proteases/isopeptidases: SENPs and beyond. *Genome Biology*, *15*(7), 422.

Nitiss, J. L. (2009a). Targeting DNA topoisomerase II in cancer chemotherapy. *Nature Reviews Cancer*, *9*(5), 338–350.

Nitiss, J. L. (2009b). DNA topoisomerase II and its growing repertoire of biological functions. *Nature Reviews Cancer*, *9*(5), 327–337.

Nitiss, J. L., Soans, E., Rogojina, A., Seth, A., & Mishina, M. (2012). Topoisomerase assays. *Current Protocols in Pharmacology.*

Ochi, T., Blackford, A. N., Coates, J., Jhujh, S., Mehmood, S., Tamura, N., … Jackson, S. P. (2015). PAXX, a paralog of XRCC4 and XLF, interacts with Ku to promote DNA double-strand break repair. *Science*, *347*(6218), 185–188.

Ouyang, J., Shi, Y., Valin, A., Xuan, Y., & Gill, G. (2009). Direct Binding of CoREST1 to SUMO-2/3 Contributes to Gene-Specific Repression by the LSD1/CoREST1/HDAC Complex. *Molecular Cell*, *34*(2), 145–154.

Paull, T. T., & Deshpande, R. A. (2014). The Mre11/Rad50/Nbs1 Complex: recent insights into catalytic activities and ATP-driven conformational changes. *Experimental Cell Research*, *329*(1), 139–147.

Pei, H., Yordy, J. S., Leng, Q., Zhao, Q., Watson, D. K., & Li, R. (2003). EAPII interacts with ETS1 and modulates its transcriptional function. *Oncogene*, *22*, 2699–2709.

Pichler, A., Gast, A., Seeler, J. S., Dejean, A., & Melchior, F. (2002). The nucleoporin RanBP2 has SUMO1 E3 ligase activity. *Cell*, *108*(1), 109–120.

Polo, S., & Jackson, S. (2011). Dynamics of DNA damage response proteins at DNA breaks: a focus on protein modifications. *Genes & Development*, *25*(5), 409–433.

Pommier, Y., Sun, Y., Huang, S.-Y. N., & Nitiss, J. L. (2016). Roles of eukaryotic topoisomerases in transcription, replication and genomic stability. *Nature Reviews. Molecular Cell Biology*, *17* (11), 703–721.

Postow, L., Ghenoiu, C., Woo, E. M., Krutchinsky, A. N., Brian, T., Postow, L., … Funabiki, H. (2015). Ku8O removal from DNA through double strand break-induced ubiquitylation. *Journal Cell Biology*, *182*(3), 467–479.

Pouliot, J. J., Yao, K. C., Robertson, C. A., Nash, H. A., (1999). Yeast Gene for a Tyr-DNA Phosphodiesterase that Repairs Topoisomerase I Complexes. *Science*, *286*(5439), 552-555.

Povirk, L. F. (2012). Processing of Damaged DNA Ends for Double-Strand Break Repair in Mammalian Cells. *ISRN Molecular Biology*, *2012*, 1–16.

Psakhye, I., & Jentsch, S. (2012). Protein group modification and synergy in the SUMO pathway as exemplified in DNA repair. *Cell*, *151*(4), 807–820.

Pyeon, D., Newton, M. A., Lambert, P. F., Den Boon, J. A., Sengupta, S., Marsit, C. J., … Ahlquist, P. (2007). Fundamental differences in cell cycle deregulation in human papillomavirus-positive and human papillomavirus-negative head/neck and cervical cancers. *Cancer Research*, *67*(10), 4605–4619.

Pype, S., Declercq, W., Ibrahimi, A., Michiels, C., Van Rietschoten, J. G. I., Dewulf, N., … Remacle, J. E. (2000). TTRAP, a novel protein that associates with CD40, tumor necrosis factor (TNF) receptor-75 and TNF receptor-associated factors (TRAFs), and that inhibits nuclear factor-B activation. *Journal of Biological Chemistry*, *275*(24), 18586–18593.

Rao, T., Gao, R., Takada, S., Abo, M. Al, Chen, X., Walters, K. J., Pommier, Y., Aihara, H. (2016). Novel TDP2-ubiquitin interactions and their importance for the repair of topoisomerase II-mediated DNA damage. *Nucleic Acids Research*, *44*(10), 10201–10215.

Raoof, A., Depledge, P., Hamilton, N. M., Hamilton, N. S., Hitchin, J. R., Hopkins, G. V, … Ogilvie, D. J. (2013). Toxoflavins and Deazaflavins as the First Reported Selective Small Molecule Inhibitors of Tyrosyl-DNA Phosphodiesterase II. *Journal of Medicinal Chemistry*, *56*(16), 6352–6370.

Robinson, M. J., Martinli, B. A., Gootzv, T. D., Mcguirkll, P. R., Moynihanll, M., Sutcliffev, J. A., & Osheroff, N. (1991). Effects of Quinolone Derivatives on Eukaryotic Topoisomerase II. *Journal of Biological Chemistry*, *266*(22), 14585–14592.

Roca, J., Berger, J. M., Harrison, S. C., & Wang, J. C. (1996). DNA transport by a type II topoisomerase: Direct evidence for a two-gate mechanism. *Proceedings of the National Academy of Sciences of the United States of America*, *93*(April), 4057–4062.

Rodrigues-Lima, F., Josephs, M., Katan, M., & Cassinat, B. (2001). Sequence Analysis Identifies TTRAP, a Protein That Associates with CD40 and TNF Receptor-Associated Factors, as a Member of a Superfamily of Divalent Cation-Dependent Phosphodiesterases. *Biochemical and Biophysical Research Communications*, *285*(5), 1274–1279.

Rogakou, E. P., Boon, C., Redon, C., & Bonner, W. M. (1999). Megabase Chromatin Domains Involved in DNA Double-Strand Breaks In Vivo. *The Journal of Cell Biology*, *146*(5), 905–915.

Roos, W. P., & Kaina, B. (2013). DNA damage-induced cell death: From specific DNA lesions to the DNA damage response and apoptosis. *Cancer Letters*, *332*(2), 237–248.

Rosa, I. D., Goffart, S., Wurm, M., Wiek, C., Essmann, F., Sobek, S., … Christensen, M. O. (2009). Adaptation of topoisomerase I paralogs to nuclear and mitochondrial DNA. *Nucleic Acids Research*, *37*(19), 6414–6428. https://doi.org/10.1093/nar/gkp708

Rothkamm, K., Krüger, I., Thompson, L. H., & Lobrich, M. (2003). Pathways of DNA Double-Strand Break Repair during the Mammalian Cell Cycle. *Molecular and Cellular Biology*, *23* (16), 5706–5715.

Roux, K. J., Kim, D. I., Raida, M., & Burke, B. (2012). A promiscuous biotin ligase fusion protein identifies proximal and interacting proteins in mammalian cells. *Journal of Cell Biology, 196* (6), 801–810.

Roy, S., de Melo, A. J., Xu, Y., Tadi, S. K., Négrel, A., Hendrickson, E., … Meek, K. (2015). XRCC4/XLF Interaction Is Variably Required for DNA Repair and Is Not Required for Ligase IV Stimulation. *Molecular and Cellular Biology*, *35*(17), 3017–3028.

Ryu, H., Furuta, M., Kirkpatrick, D., Gygi, S. P., & Azuma, Y. (2010). PIASy-dependent SUMOylation regulates DNA topoisomerase IIá activity. *Journal of Cell Biology*, *191*(4), 783–784.

Sabates-Bellver, J., Van der Flier, L. G., de Palo, M., Cattaneo, E., Maake, C., Rehrauer, H., … Marra, G. (2007). Transcriptome Profile of Human Colorectal Adenomas. *Molecular Cancer Research*, *5*(12), 1263–1275.

Sahin, U., Ferhi, O., Jeanne, M., Benhenda, S., Berthier, C., Jollivet, F., Niwa-Kawakita, M., Faklaris, O., Setterblad, N., de Thé, H., Lallemand-Breitenbach, V. (2014a). Oxidative stress-induced assembly of PML nuclear bodies controls sumoylation of partner proteins. *Journal of Cell Biology*, *204*(6), 931–945.

Sáenz Robles, M. T., Symonds, H., Chen, J., & Van Dyke, T. (1994). Induction versus progression of brain tumor development: differential functions for the pRB- and p53-targeting domains of simian virus 40 T antigen. *Molecular and Cellular Biology*, *14*(4), 2686–2698.

Sahin, U., de Thé, H., Lallemand-Breitenbach, V. (2014b). PML nuclear bodies: Assembly and oxidative stress-sensitive sumoylation. *Nucleus*, *5*(6), 499–507.

Saitoh, H., & Hinchey, J. (2000). Functional heterogeneity of small ubiquitin-related protein modifiers SUMO-1 versus SUMO-2/3. *Journal of Biological Chemistry,* 275, 6252–6258

Sancar, A., Lindsey-Boltz, L. A., Unsal-Kacmaz, K., & Linn, S. (2004). Molecular mechanisms of mammalian DNA repair and the DNA damage checkpoints. *Annual Reviews of Biochemistry*, *73*, 39–85.

Schellenberg, M. J., Appel, C. D., Adhikari, S., Robertson, P. D., Ramsden, D. A., & Williams, R. S. (2012). Mechanism of 5′ Topoisomerase II DNA adduct repair by mammalian Tyrosyl DNA phosphodiesterase 2 (Tdp2). *Nature Structural Molecular Biology, 19*(4), 1363–1371.

Schellenberg, M. J., Perera, L., Strom, C. N., Waters, C. A., Monian, B., Appel, C. D., … Williams, R. S. (2016). Reversal of DNA damage induced Topoisomerase 2 DNA – protein crosslinks by Tdp2. *Nucleic Acids Research*, *44*(8), 3829–3844.

Schmidt, B. H., Osheroff, N., Berger, J. M., (2012). Structure of topoisomerase II-DNA-nucleotide complex reveals a new control mechanism for ATPase activity. *Nature Structural Molecular Biology*, 19, 1147-1154

Schalbetter, S. A., Mansoubi, S., Chambers, A. L., Downs, J. A., & Baxter, J. (2015). Fork rotation and DNA precatenation are restricted during DNA replication to prevent chromosomal instability. *Proceedings of the National Academy of Sciences of the United States of America*, *112* (33), E4565–E4570.

Shen, Z., Pardington-Purtymun, P. E., Comeaux, J. C., Moyzis, R. K., & Chen, D. J. (1996). UBL1, a human ubiquitin-like protein associating with human RAD51/RAD52 proteins. *Genomics*, *36*, 271–279.

Seol, Y., & Neuman, K. C. (2016). The dynamic interplay between DNA topoisomerases and DNA topology. *Biophysical Reviews*, *8*, 101–111.

Shiotani, B., & Zou, L. (2009). Single-Stranded DNA Orchestrates an ATM-to-ATR Switch at DNA Breaks. *Molecular Cell*, *33*(5), 547–558.

Song, J., Durrin, L. K., Wilkinson, T. a, Krontiris, T. G., & Chen, Y. (2004). Identification of a SUMO-binding motif that recognizes SUMO-modified proteins. *Proceedings of the National Academy of Sciences of the United States of America*, *101*(40), 14373–14378.

Sun, Y., & Nitiss, J., A SUMO-ubiquitin mediated proteasome pathway in repair of DNA damage induced by topoisomerase II inhibitors. Abstract in *FASEB J.,* April 2017; 31(1) Supplement lb57

Szklarczyk, D., Franceschini, A., Wyder, S., Forslund, K., Heller, D., Huerta-Cepas, J., Simonovic, M., Roth, A., Santos, A., Tsafou, K. P., Kuhn, M., Bork, P., Jensen, L. J., Von Mering, C. (2015). STRING v10: Protein-protein interaction networks, integrated over the tree of life. *Nucleic Acids Research*, *43*(D1), D447–D452.

Takahashi, Y., Yong-Gonzalez, V., Kikuchi, Y., & Strunnikov, A. (2006). SIZ1/SIZ2 control of chromosome transmission fidelity is mediated by the sumoylation of topoisomerase II. *Genetics*, *172*(2), 783–794.

Takashima, H., Boerkoel, C. F., John, J., Saifi, G. M., Salih, M. A. M., Armstrong, D., … Lupski, J. R. (2002). Mutation of TDP1, encoding a topoisomerase I–dependent DNA damage repair enzyme, in spinocerebellar ataxia with axonal neuropathy. *Nature Genetics*, *32*(2), 267–272.

Tatham, M. H., Kim, S., Yu, B., Jaffray, E., Song, J., Zheng, J., … Chen, Y. (2003). Role of an N-terminal site of Ubc9 in SUMO-1,-2, and-3 binding and conjugation. *Biochemistry*, *42*(33), 9959–9969.

Tewey, K. M., Chen, G. L., Nelson, E. M., & Liu, L. F. (1984). Intercalative antitumor drugs interfere with the breakage-reunion reaction of mammalian DNA Topoisomerase II. *Journal of Biological Chemistry*, *259*(14), 9182–9187.

Toyoda, E., Kagaya, S., Cowell, I. G., Kurosawa, A., Kamoshita, K., Nishikawa, K., … Adachi, N. (2008). NK314, a topoisomerase II inhibitor that specifically targets the á isoform. *Journal of Biological Chemistry*, *283*(35), 23711–23720.

Tsutsui, K., Tsutsui, K., Sano, K., Kikuchi, A., & Tokunaga, A. (2001). Involvement of DNA Topoisomerase IIâ in Neuronal Differentiation. *Journal Biological Chemistry*, *276*(8), 5769–5778.

Tyanova, S., Temu, T., & Cox, J. (2016). The MaxQuant computational platform for mass spectrometry-based shotgun proteomics. *Nature Protocols*, *11*(12), 2301–2319.

Uematsu, N., Weterings, E., Yano, K. I., Morotomi-Yano, K., Jakob, B., Taucher-Scholz, G., … Chen, D. J. (2007). Autophosphorylation of DNA-PKCS regulates its dynamics at DNA double -strand breaks. *Journal of Cell Biology*, *177*(2), 219–229.

Ulrich, H. D. (2005). Mutual interactions between the SUMO and ubiquitin systems: A plea of no contest. *Trends in Cell Biology*, *15*(10), 525–532.

Ulrich, H. D. (2012a). Ubiquitin, SUMO, and Phosphate: How a Trio of Posttranslational Modifiers Governs Protein Fate. *Molecular Cell*, (47), 335–337.

Ulrich, H. D. (2012b). Ubiquitin and SUMO in DNA repair at a glance. *Journal Cell Science*, *125*(2), 249–254.

Umar, A., Buermeyer, A. B., Simon, J. A., Thomas, D. C., Clark, A. B., Liskay, R. M., & Kunkel, T. A. (1996). Requirement for PCNA in DNA mismatch repair at a step preceding DNA resynthesis. *Cell*, *87*(1), 65–73.

Uusküla-Reimand, L., Hou, H., Samavarchi-Tehrani, P., Rudan, M. V., Liang, M., Medina-Rivera, A., … Wilson, M. D. (2016). Topoisomerase II beta interacts with cohesin and CTCF at topological domain borders. *Genome Biology*, *17*(1), 1–22.

Vilotti, S., Biagioli, M., Foti, R., Dal Ferro, M., Lavina, Z. S., Collavin, L., … Gustincich, S. (2012). The PML nuclear bodies-associated protein TTRAP regulates ribosome biogenesis in nucleolar cavities upon proteasome inhibition. *Cell Death and Differentiation*, *19*(3), 488–500.

Virgen-slane, R., Rozovics, J. M., Fitzgerald, K. D., Ngo, T., Chou, W., van der Heden van Noort, G. J., … Semler, B. L. (2012). An RNA virus hijacks an incognito function of a DNA repair enzyme. *Proceedings of the National Academy of Sciences of the United States of America*, *109* (36), 14634–14639.

Vologodskii, A. (2016). Disentangling DNA molecules. *Physics of Life Reviews*, *18*, 118–134.

Vogt B., Hofmann K., (2012) Ubiquitin Family Modifiers and the Proteasome, *Springer,* (Dohmen, R. J. & Scheffner, M., eds) 249-261

Vos, S. M., Tretter, E. M., Schmidt, B. H., & Berger, J. M. (2011). All tangled up: how cells direct , manage and exploit topoisomerase function. *Nature Reviews Molecular Cell Biology*, *12*(12), 827–841.

Walker, J. V., & Nitiss, J. L. (2002). DNA Topoisomerase II as a Target for Cancer Chemotherapy. *Cancer Investigation*, *20*(4), 570–589.

Wang, J. C. (1971). Interaction between DNA and an Escherichia coli protein omega. *Journal Molecular Biology*, *55*(3), 523–533.

Wang, J. C., Caron, P. R., & Kim, R. A. (1990). The role of DNA topoisomerases in recombination and genome stability: A double-edged sword? *Cell*, *62*(3), 403–406.

Wang, J. C., & Liu, L. F. (1979). DNA Topoisomerases: Enzymes which catalyze the concerted breaking and rejoining of DNA backbone bonds. In "Molecular Genetics" Part III (Taylor, J. H., ed) Academic Press, New York, 65-88

Wang, Y., Knudsen, B. R., Bjergbaek, L., Westergaard, O., & Andersen, A. H. (1999). Stimulated Activity of Human Topoisomerases IIá and IIâ on RNA-containing Substrates. *Journal of Biological Chemistry*, *274*(32), 22839–22846.

Watson, J. D., & Crick, F. H. (1953). Genetical implications of the structure of deoxyribonucleic acid. *Nature* 171, 964-967.

Werner, A., Flotho, A., & Melchior, F. (2012). The RanBP2/RanGAP1 *SUMO1/Ubc9 Complex Is a Multisubunit SUMO E3 Ligase. *Molecular Cell*, *46*(3), 287–298.

Wotton, D., & Merrill, J. C. (2007). Pc2 and SUMOylation. *Biochemical Society Transactions*, *35*(Pt 6), 1401–1404.

Wu, H., Liu, L. F., Wang, J. C., & Liu, L. F. (1988). Transcription Generates Positively and Negatively Supercoiled Domains in the Template. *Cell*, *53*, 433–440.

Woessner, R. D., Mattern, M. R., Mirabelli, C. K., Johnson, R. K., & Drake, F. H. (1991). Proliferation- and cell cycle-dependent differences in expression of the 170 kilodalton and 180 kilodalton forms of topoisomerase II in NIH-3T3 cells. *Cell Growth and Differentiation*, *2*(4), 209–214.

Wu, C. C., Li, T. K., Farh, L., Lin, L. Y., Lin, T. S.,Yu, Y. J., Yen, T. J., Chiang, C. W., Chan, N. L., (2011). Structural basis of type II topoisomerase inhibition by the anticancer drug etoposide. *Science*, 333, 459-462.

Xu, G. lan, Pan, Y. kun, Wang, B. yin, Huang, L., Tian, L., Xue, J. lun, … Jia, W. (2008). TTRAP is a novel PML nuclear bodies-associated protein. *Biochemical and Biophysical Research Communications*, *375*(3), 395–398.

Xu, H., Zhang, P., Liu, L., & Lee, M.Y. (2001). A novel PCNA-binding motif identified by the panning of a random peptide display library. *Biochemistry,* 40, 4512–4520

Yang, X., Prescott, E. D., Burden, S., J., Wang, J. C., (2000). DNA topoisomerase IIβ and neural development. *Science*. 287(5450), 131-134.

Yoshida, M. M., Ting, L., Gygi, S. P., & Azuma, Y. (2016a). SUMOylation of DNA topoisomerase IIá regulates histone H3 kinase Haspin and H3 phosphorylation in mitosis. *Journal Cell Biology*, *213*(6), 665–678.

Yoshida, M. M., & Azuma, Y. (2016b). Mechanisms behind Topoisomerase II SUMOylation in chromosome segregation. *Cell Cycle*, *15*(23), 1–2.

Yunus, A. A., & Lima, C. D. (2009). Structure of the Siz/PIAS SUMO E3 Ligase Siz1 and Determinants Required for SUMO Modification of PCNA. *Molecular Cell*, *35*(5), 669–682.

Zhang, A., Lyu, Y. L., Lin, C.-P., Zhou, N., Azarova, A. M., Wood, L. M., & Liu, L. F. (2006). A Protease Pathway for the Repair of Topoisomerase II-DNA Covalent Complexes. *Journal of Biological Chemistry*, *281*(47), 35997–36003.

Zhang, J. qi, Wang, J. jing, Li, W. juan, Huang, L., Tian, L., Xue, J. lun, … Jia, W. (2009). Cellular protein TTRAP interacts with HIV-1 integrase to facilitate viral integration. *Biochemical and Biophysical Research Communications*, *387*(2), 256–260.

Zhao, Q., Xie, Y., Zheng, Y., Jiang, S., Liu, W., Mu, W., … Ren, J. (2014). GPS-SUMO: A tool for the prediction of sumoylation sites and SUMO-interaction motifs. *Nucleic Acids Research*, *42* (W1), 325–330.

Zhou, C. H., Xue, J. G., & Chen, J. Z. (2013). Overexpression of TTRAP inhibits cell growth and induces apoptosis in osteosarcoma cells. *Biochemistry and Molecular Biology Reports*, *46*(2), 113–118.

Zucchelli, S., Vilotti, S., Calligaris, R., Lavina, Z. S., Biagioli, M., Foti, R., … Gustincich, S. (2009). Aggresome-forming TTRAP mediates pro- apoptotic properties of Parkinson's disease- associated DJ-1 missense mutations. *Cell Death and Differentiation*, *16*(3), 428–438.